

**Investigating proglacial groundwater systems in the Quilcayhuanca and  
Yanamarey Pampas, Cordillera Blanca, Peru**

Laura Maharaj

Department of Earth and Planetary Sciences

McGill University

Montréal, Québec, Canada

July 2011

A thesis submitted to McGill University in partial fulfillment of the requirements of the degree  
of Master of Science

© Laura Maharaj 2011

## Abstract

High-elevation Andean water storage is extremely important for water resources for the arid western coast of South America. Pampas (a subset of páramos) are a freshwater reservoir in the Cordillera Blanca, Peru. These organic-rich clay systems buffer stream and river runoff to the Rio Santa and provide water to surrounding communities. More than 50% of dry season discharge from pampas is groundwater derived, however little is known about their geomorphology and subsurface sedimentology. Watertable measurements, streambed temperature sensors, and ground penetrating radar (GPR) were used to characterize the subsurface and develop a formational model for the Yanamarey and Quilcayhuanca pampas, Cordillera Blanca, Peru.

The water table in July 2009 was found on average to be 0.35 m and 0.57 m below the land surface at Quilcayhuanca and Yanamarey respectively. In the Yanamarey Pampa, streambed temperature sensors showed that upstream, water flows from the stream into the ground and further downstream, water flows upwards recharging the stream. From watertable measurements, a watertable map was produced that showed steeper watertable gradients further up valley. GPR was an effective tool for imaging the subsurface to a depth of 8 meters in the high permittivity material and delineated four stratigraphic units at both sites. In sequence the units are; dry sandy peat soils with pebbles at the surface, water saturated soil with sand and pebbles, linear stratified clay and glacial outwash intermixed with colluviums deposits. The identification of the subsurface sedimentary units allowed for the creation of formation models of both sites. The valley walls of Quilcayhuanca are steeper than Yanamarey, which caused more landslides and consequently more extensive colluvial deposits throughout the Quilcayhuanca valley subsurface. These connected colluvial deposits are likely the primary zone for groundwater flow and storage.

## Résumé

Les réservoirs hydrologiques des hautes Andes constituent une partie importante des ressources d'eau de la région aride de la côte ouest de l'Amérique du Sud. Les Pampas, un sous-ensemble des pãramos, représentent un des réservoirs d'eau fraîche de la Cordillère Blanche du Pérou. Ces systèmes riches en argile et en matière organique modulent le ruissellement des rivières et des cours d'eau, et offrent de l'eau fraîche aux communautés voisines. Plus de 50 % du volume d'eau provenant des Pampas durant la saison sèche sont d'origine souterraine, cependant peu d'études se sont penchées sur la géomorphologie et la sédimentologie de ces systèmes. Des relevés du niveau de la nappe, des mesures de température dans le lit de la rivière, et des profils obtenus à l'aide de radars à pénétration du sol (RPS) ont été utilisés pour décrire le sous-sol et développer un modèle pour expliquer le fonctionnement des pampas de Yanamarey et de Quilcayhuancas de la Cordillère Blanche.

Le niveau de la nappe se situe en moyenne à 0,35 m et 0,57 m de profondeur à Quilcayhuanca et Yanamarey respectivement. Dans le Pampa du Yanamarey, les capteurs de température du lit du cours d'eau mettent en évidence un flux d'eau positif de la rivière vers le sol dans la partie supérieure des pampas, ce flux s'inversant dans sa partie inférieure. La carte du niveau de la nappe, réalisées à partir des mesures effectuées sur le terrain, montrent que les gradients du niveau d'eau sont plus forts en amont du système. L'outil RPS s'est montré utile pour produire des images du sous-sol jusqu'à une profondeur de huit mètres dans le matériau à haute permittivité, distinguant quatre unités stratigraphiques. Du sol aux profondeurs nous trouvons: de la tourbe sèche avec des galets superficiels; du sol saturé en eau avec du sable et des galets; de l'argile stratifiée linéairement et finalement divers dépôts glaciaires et paraglaciaires. L'identification de la géologie souterraine a permis la création du modèle pour chacun des deux sites. Les flancs de la vallée de Quilcayhuanca sont plus pentus que ceux du Yanamarey, ce qui induit plus de glissement de terrain et par conséquent, plus de dépôts paraglaciaires dans le sous-sol de la vallée du Quilcayhuanca. Ces dépôts et leurs interconnexions forment vraisemblablement le passage privilégié de l'eau souterraine et forment possiblement les zones de stockage primaires de ces systèmes.

## **Preface**

The following thesis presents original research by the author at the Department of Earth and Planetary Sciences, McGill University during the 2009-2011 academic years. It is submitted in a traditional thesis format, and is ultimately intended to form a manuscript to be submitted to a peer-reviewed journal.

Data acquisition, analysis and interpretation were advised by Professor Jeffrey M. McKenzie, who acted as principal research supervisor along with Professor Sarah Hall, the additional committee member. The acquisition of the light detection and radar data took place in 2008 and was supervised by Professor Bryan Mark at The Ohio State University. Fieldwork took place during July 2009 and July 2010 in the Cordillera Blanca, Peru. Data were collected in the Cordillera Blanca, Peru, and analysis and interpretation were done by the author at McGill University, Montréal, Québec, Canada. ESRI ArcGIS was used by Sara Knox to identify pampas throughout the Cordillera Blanca.

## Acknowledgements

I would like to express my heartfelt gratitude to the entire Department of Earth and Planetary Sciences (EPS). This department has been my second family during my years at McGill University. At such a large university, it can be hard to find your place, but the friendly faces of the faculty, staff and students of EPS made that task easy by creating a wonderful social and academic environment. I count myself lucky to have been able to be a part of the EPS community.

I extend my gratitude to Jeffrey M. McKenzie, my principal supervisor, who gave me the freedom to take risks and expand my project into new, uncertain, directions. Although, no one travels as much as Jeff does, he still managed to always make himself readily available. He has been a constant source of inspiration and dedicated his time and energy to ensure that I reached my goals. I could not have asked for a better advisor.

Many thanks go out to my vibrant research group, namely Michel Baraer, Stephanie Palmer, Bernardo Brixel, Rob Carver and Elizabeth Walsh along with my many other office mates of the first floor in Frank Dawson Adams. You have all been my rock, and I could not have completed my thesis without your advice, support, and most of all your cheerfulness, which made this office a place I loved walking into each day.

EPS would not function if it weren't for our dynamic administrative office trio of Anne Kosowski, Kristy Thornton and Angela Di Ninno. You ladies have been there to answer all of my questions throughout the years, and I will be at a loss of where to turn for advice once I have graduated. Brigitte Dionne, I also thank you for your patience with my countless computer questions.

Throughout my fieldwork I had the help of many individuals from various institutions. Firstly, thank you to Fiona Darbyshire and Eric Rosa from L'Université du Québec à Montréal for all their help with the rental and use of their ground penetrating radar equipment. Secondly, great appreciation to Bryan Mark, KyungIn Huh, Jeffrey La Frenierre, Alyssa Singer and Shawn Stone from Ohio State University and Jeffrey Bury and Adam French from University of

California Santa Cruz, for making my two field seasons in Peru a great success. Lastly a special thanks to the B&B Mi Casa Staff in Huaraz, Peru for your continued support of our work in Peru.

Outside of my academics, I would like to acknowledge the vibrant city of Montreal. Even with its never ending winters, rain filled springs and melting hot summers, I will miss this city. The lively culture and free spirited people have made it a magnificent place in which to live, laugh and learn.

To my parents, thank you, I love you, and I am going to come home, now. I Promise.

## Table of Contents

<i>Abstract</i> .....	ii
<i>Résumé</i> .....	iii
<i>Preface</i> .....	iv
<i>Acknowledgements</i> .....	v
<i>Table of contents</i> .....	vii
<i>List of figures</i> .....	ix
<i>List of appendices</i> .....	x
<b>Chapter 1 – Introduction</b> .....	11
<b>Chapter 2 – Study Area</b> .....	12
2.1 <i>The Cordillera Blanca</i> .....	12
2.2 <i>The Quilcayhuanca and Yanamarey Pampas</i> .....	14
<b>Chapter 3 – Methods</b> .....	15
3.1 <i>Water table measurements and LiDAR</i> .....	15
3.2 <i>Vertical streambed temperature profiles</i> .....	15
3.3 <i>Ground penetrating radar</i> .....	18
<b>Chapter 4 – Results and Discussion</b> .....	19
4.1 <i>Pampa area</i> .....	19
4.2 <i>Water table measurements</i> .....	19
4.3 <i>Vertical streambed temperature profiles</i> .....	20
4.4 <i>Ground penetrating radar</i> .....	23
4.41 <i>Quilcayhuanca GPR results</i> .....	24
4.42 <i>Yanamarey GPR results</i> .....	24
<b>Chapter 5 – Pampa Formation</b> .....	29
5.1 <i>General pampa formation</i> .....	29
5.12 <i>Quilcayhuanca pampa formation</i> .....	29
5.13 <i>Yanamarey pampa formation</i> .....	33

5.2 Differences in the Northern and Southern Pampas .....	35
<b>Chapter 6 – Conclusions .....</b>	<b>36</b>
<b>References .....</b>	<b>38</b>
<b>Appendix 1 – Quilcayhuanca GPR results .....</b>	<b>42</b>
<b>Appendix 2 – Yanamarey GPR results .....</b>	<b>43</b>
<b>Appendix 3 – Required streambed velocity parameters and temperature data .....</b>	<b>44</b>



## List of Figures

<i>Figure 1) Quilcayhuanca and Yanamarey Pampa locations, Cordillera Blanca, Peru .....</i>	<i>13</i>
<i>Figure 2) Wooden dowels embedded with iButtons in the stream .....</i>	<i>16</i>
<i>Figure 3) Quilcayhuanca and Yanamarey watertable and GPR location maps .....</i>	<i>17</i>
<i>Figure 4) One year streambed velocity graphs .....</i>	<i>21</i>
<i>Figure 5) 10 Day streambed velocity graphs .....</i>	<i>22</i>
<i>Figure 6) Quilcayhuanca CO-GPR Profile 7 .....</i>	<i>25</i>
<i>Figure 7) Quilcayhuanca stratigraphic unit model .....</i>	<i>26</i>
<i>Figure 8) Yanamarey CO-GPR Profile 98-6 .....</i>	<i>27</i>
<i>Figure 9) Yanamarey stratigraphic unit model .....</i>	<i>28</i>
<i>Figure 10) Quilcayhaunca pampa formation model .....</i>	<i>30</i>
<i>Figure 11) Llanganuco Valley .....</i>	<i>32</i>
<i>Figure 12) Yanamarey pampa formation model .....</i>	<i>34</i>

## List of Appendices

Appendix 1 – Quilcayhuanca GPR results .....	42
Appendix 2 – Yanamarey GPR results .....	43
Appendix 3 – Required streambed velocity parameters and temperature data .....	44

## Chapter 1 – Introduction

High elevation mountain glaciers, páramos, groundwater and river networks are critical components of the high Andean water resources, which provide water to the arid west coast of South America. These systems are important for regulating water to downstream local communities and hydropower plants, and providing water for domestic and agricultural uses (Célleri and Feyen, 2009). As Andean glaciers are rapidly retreating, these water resources, in particular water-regulating páramos, are under intense scrutiny. Without proper management, water resources to more than the 10 million people in the Andean highlands may be at risk (Buytaert et al., 2006).

Páramo is a neotropical alpine ecosystem that covers more than 75,000 km<sup>2</sup> of the northern Andes of Venezuela, Ecuador, Colombia, Costa Rica, and Peru (Buytaert et al., 2006). They are located at high elevations (between approximately 3000 – 5000 m.a.s.l) and are characterized by low temperatures and a relatively humidity of greater than 80% (Flamingo Resource Centre, nd). Páramos have a high water holding capacity due to clay assemblages and accumulation of high organic matter, making them a major store of water in the Andean highlands (Célleri and Feyen, 2009).

In the Cordillera Blanca, Peru, pampas (also called ‘dry puna’) are a unique subset of páramos that are found in long, topographically flat, high-elevation valleys. Soils in these pampas are poorly developed and sparse vegetation (partly the result of overgrazing by livestock) consists of small moss plants, very few trees, grassy prairie and grass steppe, which is commonly known as pampa grass (Mark and Seltzer, 2003). A common feature of pampas is the presence of glacially fed streams that flow across the pampa and discharge into the Rio Santa. Groundwater storage in the pampas buffers streamflow, and is an important component of the hydrologic cycle, providing water for domestic and agricultural use for downstream communities (Baraer et al., 2009).

The current accelerated glacial recession has resulted in great concern for regional water availability and the fate of these glacially sourced streams in particular (Mark and McKenzie, 2007; Mark et al., 2010, Bury et al., 2010). Based on chemical mass balance

modeling, it is estimated that more than 50% of dry season discharge from many of the pampas is derived as groundwater stored in pampas, as opposed to glacial meltwater (Baraer et al., 2009).

To determine stratigraphy and groundwater aquifers, ground penetrating radar (GPR) has been used to extensively map shallow subsurface hydrogeologic systems. GPR is sensitive to variations in both fine (centimeters) and large (tens of meters) scale depositional stratigraphy, which has significant impacts on groundwater flow. It can detect hydrological constraints, ranging from geological structure to material properties, and outline zones of homogeneity for hydrogeological parameters. GPR is a fast, efficient, economical and non-invasive measurement tool that can be employed to address numerous hydrogeological and geomorphological questions (Annan, 2005).

While there has been research to quantify the contributions of pampas to valley and regional hydrologic systems, very little is known about their sedimentology and formational history. Understanding the geology and geomorphology of these systems is important as they control patterns of groundwater flow recharge and residence times (Robinson et al., 2008). However, as a result of the remote location of the Cordillera Blanca pampas, investigating the subsurface sedimentology and hydrogeological parameters is difficult. We present research looking at the stratigraphy, shallow hydrogeology, and formation of pampas in the Cordillera Blanca. Combinations of techniques are employed, including GPR, to develop a conceptual model of how these systems formed.

## **Chapter 2 – Study Area**

### 2.1 The Cordillera Blanca

The Cordillera Blanca, Peru, is the most extensively glaciated mountain range in the tropics, with a total glaciated area of 631 km<sup>2</sup> (Suarez et al., 2008). It is located between 8.5° - 10°S and 76.5° - 77.5°W, along an 120 km transect on the northwest-southeast strike of the Andes (Mark and Seltzer, 2005) (Figure 1). The mountain range is approximately 10 million years old and sits on the magmatic Andean arc formed by the subduction of the Nazca plate

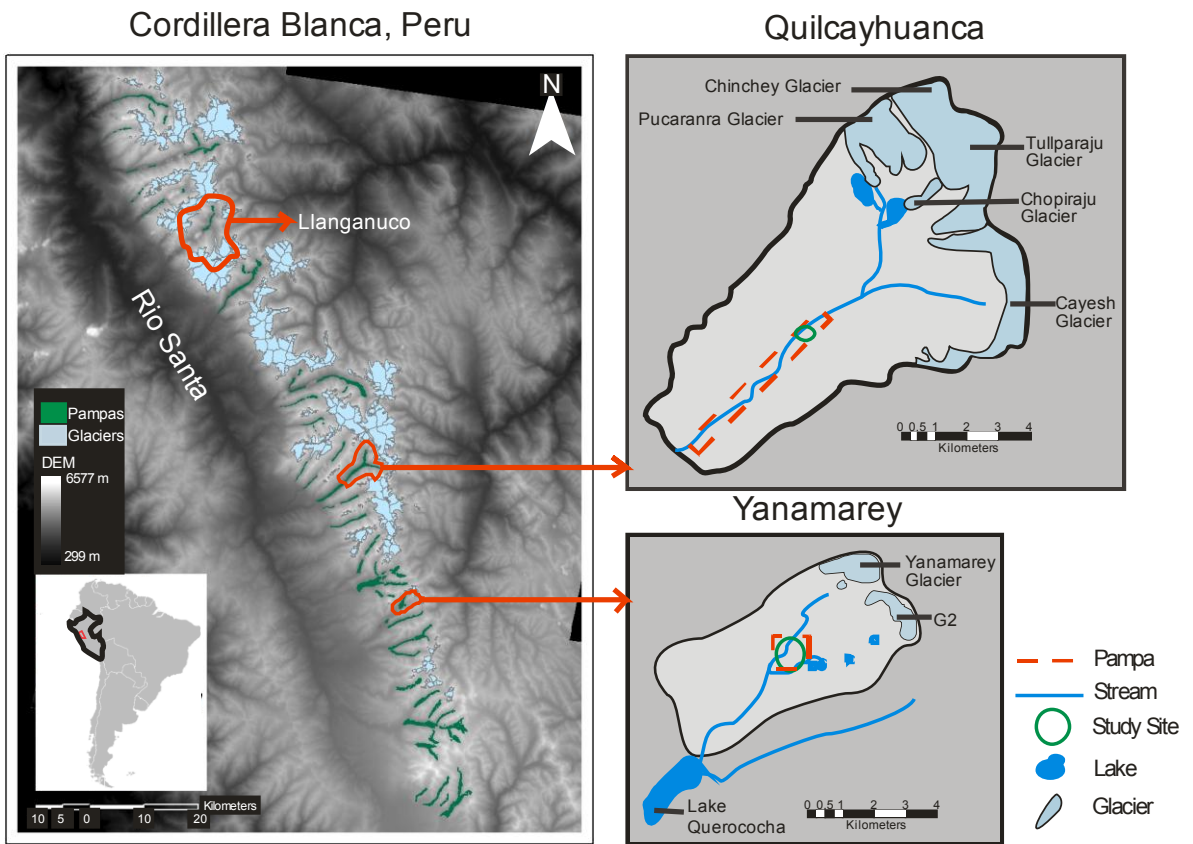
Figure 1)

The Quilcayhuanca (9.4° S, 77.3° W) and Yanamarey (9.6° S, 77.2° W) Pampas are located southwest of their source glaciers and have little vegetation and poor soil development. The streams in the pampas are shallow, with depths less than 1 m, and have streambeds composed of well-rounded rocks, with riverbanks comprised of fine clays and silts.

A) Quilcayhuanca Pampa is in a thin, long valley, surrounded by steep valley walls, and is representative of pampas in the northern Cordillera Blanca.

B) Yanamarey Pampa is in a wide valley, with shallow sloping walls, and is representative of pampas in the southern Cordillera Blanca.

Figure 1)



under the South American plate (McNulty et al., 1998). The bedrock on the western side of the Cordillera Blanca is composed of metamorphosed sedimentary rocks (quartzite and hornfels) (Wilson et al., 1967) and is 80% to 90% batholith with the remainder being isolated areas of tonalite and diorite (McNulty et al., 1998).

The diurnal air temperature has a range up to 14°C, however the average monthly air temperature has an annual range of only 1°C on average (Mark and Seltzer, 2005). There is strong precipitation variation throughout the region, where more than 90% of annual precipitation occurs between October and April and almost no precipitation falls in the dry season (May to September) (Juen et al., 2007). The maximum river discharge occurs at the beginning of the dry season (October to November), as the precipitation from the wet season becomes runoff and the glacier melting reaches its annual maximum (Mark and Seltzer, 2003).

## 2.2 The Quilcayhuanca and Yanamarey Pampas

The Yanamarey and Quilcayhuanca pampas were selected based on their representativeness of pampas throughout the Cordillera Blanca. Both study sites are located southwest of their respective source glaciers and are similar with little vegetation and poor soil development. The streams in the pampas are shallow, with depths less than 1 m, and streambeds usually composed of a mixture of silts and well-rounded rocks, with bank cuts showing deposits of fine clays and silts.

The Quilcayhuanca Pampa (9.4° S, 77.3° W) is representative of pampas in the northern region of the Cordillera Blanca. The pampa is long and narrow (approximately 1.5 km<sup>2</sup>) with near vertical steep surrounding valley walls. The Pucaranra, Chinchey, Tullparaju, Chopiraju and Cayesh glaciers, at elevations between 5500 and 6500 m.a.s.l., discharge into the Quilcayhuanca stream, which flows across the pampa.

The Yanamarey Pampa (9.6° S, 77.2° W) is representative of pampas in the southern end of the Cordillera Blanca. The pampa is significantly shorter in length and wider (approximately 1.0 km<sup>2</sup>) and has less steep valley walls than Quilcayhuanca. The Yanamarey and G2 glaciers, between 4600 and 5300 m.a.s.l., discharge into two glacially fed streams that flow down the pampa into Lake Querococha.

## Chapter 3 – Methods

### 3.1 Water table measurements and LiDAR

At both sites a water table map was created to assist in understanding the topographic drivers of groundwater flow through these systems. The depth to the water table was measured by augering an open hole and letting the water level within the hole equilibrate. At Quilcayhuanca, an engineer's level was used for local elevation surveys of the land surface where the auger holes were located. The Yanamarey Pampa was surveyed in 2008 with an airborne light detections and ranging (LIDAR), and auger holes were geolocated by GPS.

### 3.2 Vertical streambed temperature profiles

The interaction between groundwater and surface water was characterized using heat as a tracer to determine vertical streambed seepage rates (Lautz, 2010). Heat tracing utilizes the regular, diurnal fluctuations in temperature that occur in the stream water column. The propagation of these diurnal signals into the streambed sediments is controlled by both conduction and advection due to porewater flow. The degree to which the signal propagates into the bed is directly related to the porewater velocity and physical properties of the sediment.

Wooden dowels were drilled with 2.5 cm holes to a depth of approximately 2 cm and embedded with iButton temperature sensors held in place by a thin layer of silicone caulk and one wrap of duct tape (Figure 2a). While caulk has a different thermal conductivity than the streambed sediments, the equilibration time for the iButtons, with or without silicone caulk, is much faster than iButton sampling rates. The dowels were inserted vertically into the stream sediments, with one temperature logger located in the stream and the others at different depths (Figure 2b). On July 14<sup>th</sup> 2006, one dowel with five iButtons (A,B,C,D,E) temperature sensors was installed in the northern Yanamarey stream, which recorded data for an entire year, at four hour intervals. From July 8<sup>th</sup> – 17<sup>th</sup> 2007, four dowels were installed along the northern Yanamarey stream with four temperature loggers that recorded temperature for ten days, at intervals of fifteen minutes (Figure 3). The vertical flux of water is calculated by



Figure 2)

- A) Two wooden dowels embedded with iButton temperature sensors.
- B) Dowel inserted vertically into the stream sediments.

Figure 2)



A)



B)

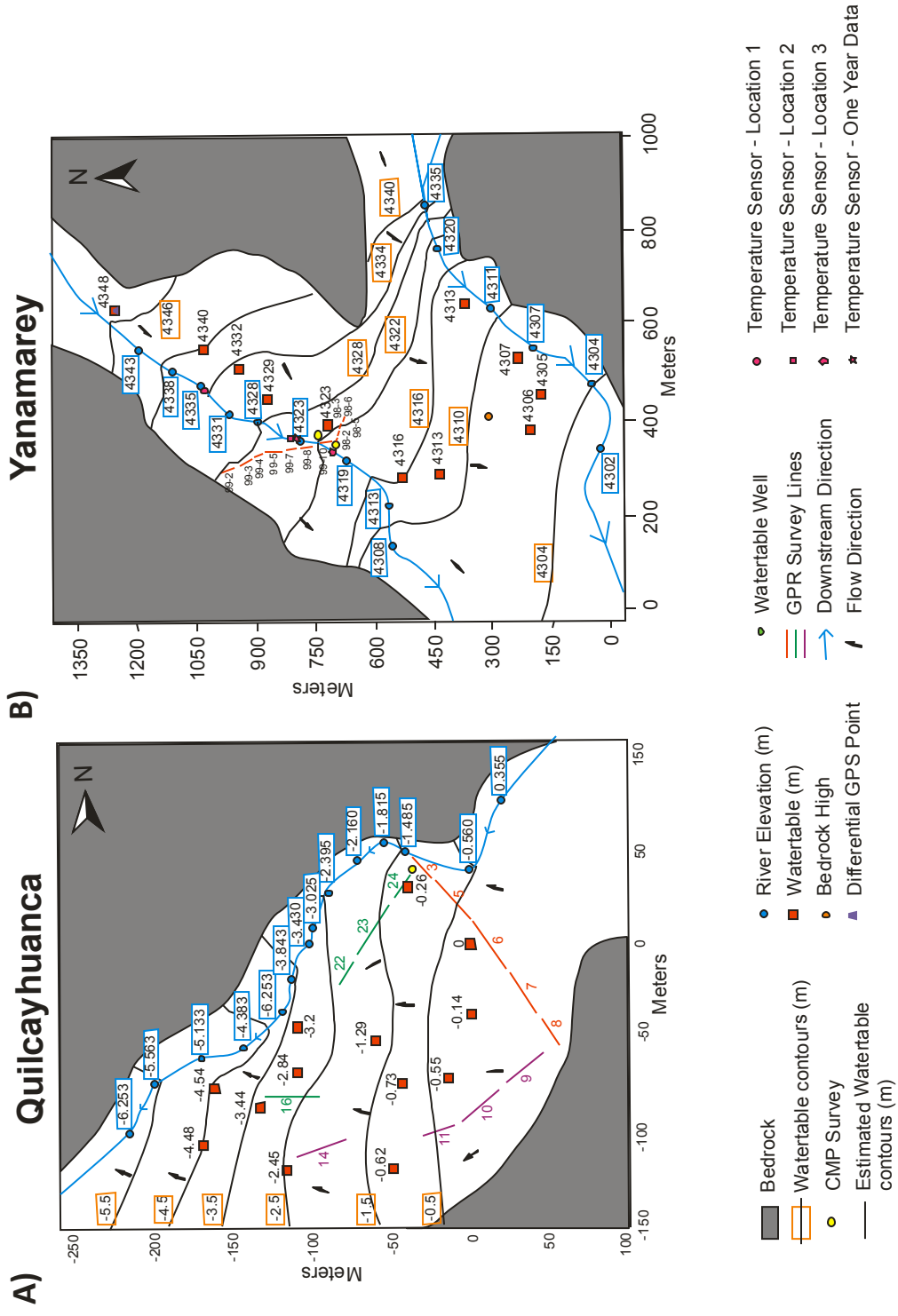
Figure 3)

Common offset (CO) and Common Mid Point (CMP) GPR surveys were completed in the Quilcayhuanca and Yanamarey Pampas along with watertable and elevation measurements.

A) Quilcayhuanca: Twenty-five CO GPR transects (400 m distance) were taken in several directions to cover potential spatial heterogeneities CMP surveys were done to determine the electromagnetic velocity. The elevation of the pampa is between 3915 – 3930 m.a.s.l.

B) Yanamarey: Eleven CO GPR transects were taken in a northeast direction from the valley wall towards the center of the pampa. A total linear distance of 375 m was covered and two in addition to CMP surveys.

Figure 3)



quantify the daily dissipation of the daily maximum and minimum temperatures into the streambed using the analytical solution presented by Hatch et al., (2006).

### 3.3 Ground penetrating radar

GPR generates high frequency (MHz to GHz) electromagnetic (EM) waves from a transmitting antenna, which penetrate into the subsurface. The EM waves reflect off an interface and are measured at the surface by the receiving antenna as a function of time. The travel time is the time for the wave to travel down to an interface and back up to the surface, and it is used to determine the in situ propagation velocity of the subsurface material (Baker and Jol, 2007). The velocity of the EM wave is primarily controlled by relative permittivity, a geophysical property strongly dependent on water content and is defined as the ability of a material to store and then permit the passage of EM energy when an EM field is imposed on the material. Reflections occur where moisture content changes, at major sediment interfaces, and with changes in bulk density and organic matter content (Warner et al., 1990).

Common offset (CO) and common midpoint (CMP) GPR reflection surveys were run at the Yanamarey and Quilcayhuanca pampas with a Sensors and Software PulseEKKO GPR system. The CO survey was used to create profiles of the subsurface and the CMP survey was used to determine the mean propagation velocity of the radar waves to the major reflections in the subsurface (Van Overmeeren, 1998). The system uses a 400 volt transmitter with 50 MHz transmitting and receiving antennas. The antenna spacing was 3 m with 0.50 m horizontal spacing between traces.

In each pampa, survey lines were sited and CO GPR transects were collected along transects. Twenty-five CO GPR transects in Quilcayhuanca and eleven in Yanamarey produced usable data. Small streams, marsh areas and large pampa grass vegetation prevented continuous transects along the GPR survey lines. In Quilcayhuanca transects were taken in several sections to cover the maximum area over the pampa. Five transects were taken in the southeast direction, four transects in the west-southwest direction, four in the north-northeast direction and one in the northeast direction over the topographic high in the centre of the study site. The total linear distance covered with the GPR in the Quilcayhuanca area was

approximately 400 m. In Yanamarey, data acquisition time was limited due to inclement weather and all transects were taken in a northeast direction perpendicular to the direction of groundwater flow in the pampa. A total linear distance of approximately 375 m was covered and additionally, two CMP GPR surveys were taken in Yanamarey to determine the EM velocity.

## **Chapter 4 – Results and Discussion**

### 4.1 Pampa area

A semi-automated method was used to delineate the pampas based on topography and their location within the mountain range. ESRI ArcGIS was used to analyze a slope layer model derived from the DEM. Areas with an elevation greater than 3500 m.a.s.l, with a topographic slope less than or equal to 10° and surrounded by steep slopes and glacierized valleys were identified as pampas. Determining the location of pampas was further refined by examining ASTER data and excluding regions where no vegetation was present. Using this method, the total area of the pampas in the Cordillera Blanca is 63.6 km<sup>2</sup>. This can be seen in figure one.

### 4.2 Water table measurements

The depth to the water table from the land surface, and the topography of the water table were surveyed at Quilcayhuanca and Yanamarey. The water table was found on average to be 0.35 m and 0.57 m below the land surface at Quilcayhuanca and Yanamarey respectively. The water table in the Quilcayhuanca Pampa generally follows the topography of the landsurface, with a down valley gradient and towards the river. The water table gradient increases closer to the river, and the largest gradient is at the furthest downstream measurement point. The depth of the water table varies between 0.1 and 0.5 m below the surface and the water table is closest to the surface upstream, away from the river. The Yanamarey Pampa is roughly divided into a northern half and a southern half by a slight (< 1m high) topographic divide. The southern side is approximately 0.5 to 1.0 m lower in elevation than the northern half. The water table on the southern side is closer to the land surface and has extensive waterlogged soils, whereas the northern side of the pampa is higher and is dryer

at the land surface. In the northern side, the depth to the water table varies between 0.30 and 0.85 m. The water table gradient is highest upstream on the southern side of the pampa. The northern side of the pampa, and the middle of the valley further downstream have a less steep water table gradient.

#### 4.3 Vertical streambed temperature profiles

Vertical streambed temperature profiles were used to determine vertical groundwater flow velocities between the northern Yanamarey stream and the streambed sediments. The Hatch analytical solution (2006) uses the change in amplitude of the temperature signal in the subsurface with depth. This method required several parameters including the maximum and minimum daily temperature values, period, depth, effective thermal conductivity, effective porosity, total porosity and the volumetric heat capacity of the water and sediments. The parameters used in the calculations and the collected data are in Appendix 3.

Three of the five temperature sensors for the one year data recorded viable data (A – in the stream, C – 15cm depth and E – 35cm depth). The range of velocities for the 15 cm depth is – 2 m/day to -7 m/day. The negative value implies upward flow. For 35 cm depth, the velocity ranges from 2 m/day to -2 m/day (Figure 4a). The majority (390 out of 426) of the velocity values are less than zero indicating upward porewater flow (groundwater discharge). The average velocity for sensors A (stream) to C (15 cm) is -3.81 m/day with a standard deviation of 1.6 (Figure 4b). The average velocity for sensors A (stream) to E (35 cm) is -0.30 with a standard deviation of 1.3. The average velocity of both depths is -2.0 m/day. Ten of the sixteen temperature sensors for the ten day sensor installations produced viable data. At Location 1 all four sensors (B1 – B4) recorded data (Figure 5a). The average velocity for the Location 1 dowel was 0.230 m/day. The vertical porewater velocity from the B4 (stream) to B3 (5 cm) was 0.391 m/day with a standard deviation of 0.68, to B2 (15 cm) was 0.12 m/day with a standard deviation of 0.10 and to B1 (25 cm) was 0.39 m/day with a standard deviation of 0.13. Between the temperature sensors B3 (5 cm) to B2 (15 cm) the vertical porewater velocity was 0.04 m/day with a standard deviation of 0.33, B3 (5cm) to B1 (25 cm) had a velocity of 0.41 m/day with a standard deviation of 0.19 and B2 (15 cm) to B1 (25 cm) had a velocity of 0.910 m/day

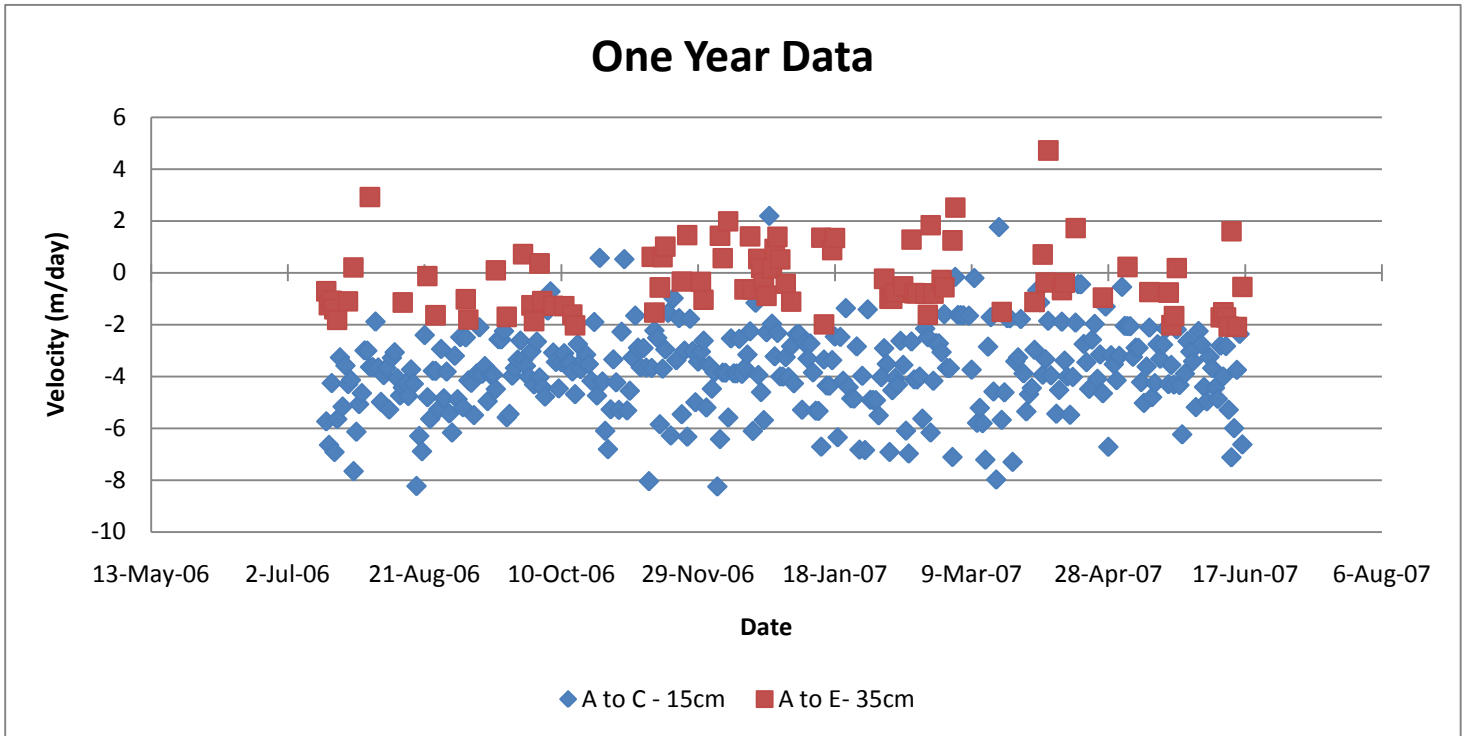
Figure 4) One Year streambed velocity graphs measured July 14<sup>th</sup> 2006 – July 14<sup>th</sup> 2007

- A) One Year streambed velocity graphs
- B) One Year streambed velocity graphs – middle velocities



Figure 4)

A)



B)

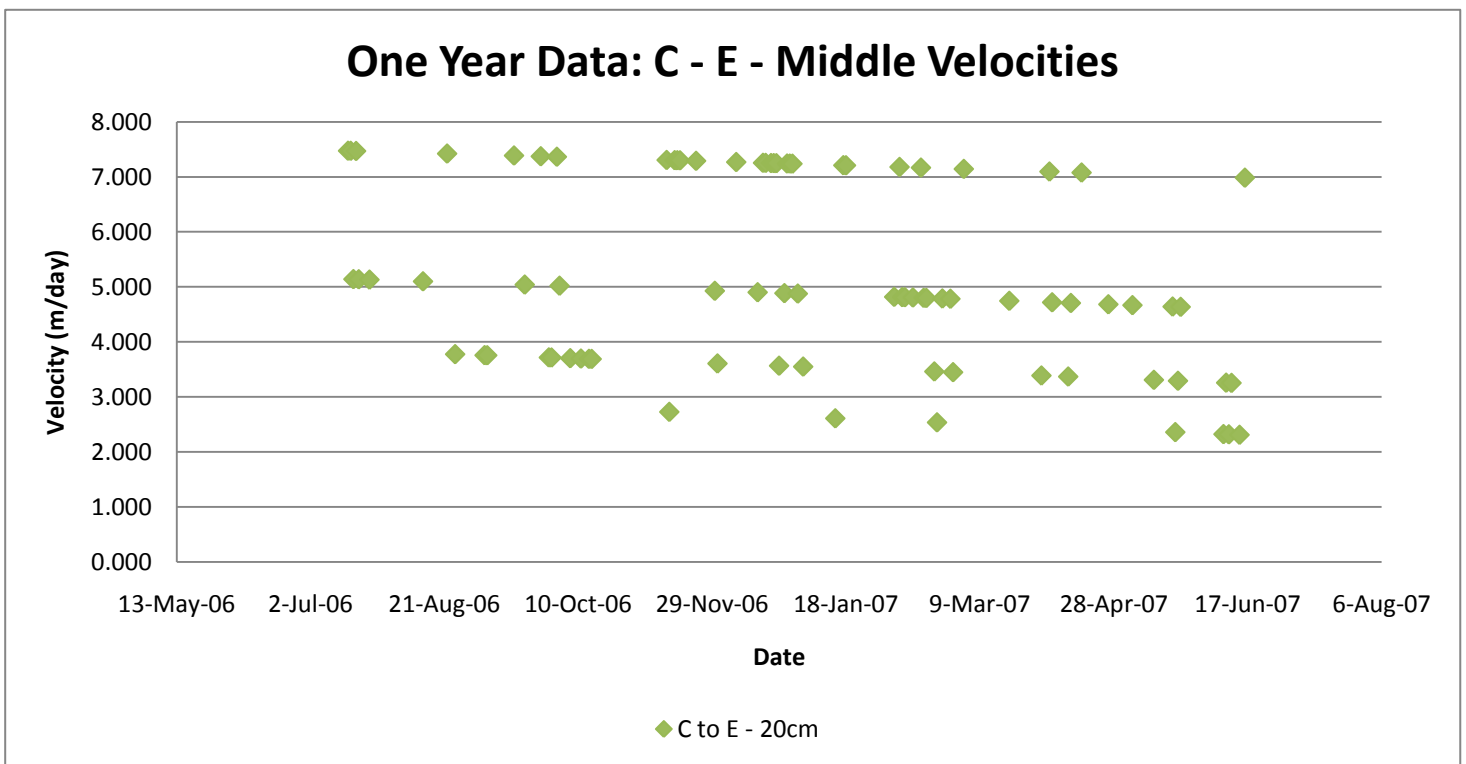
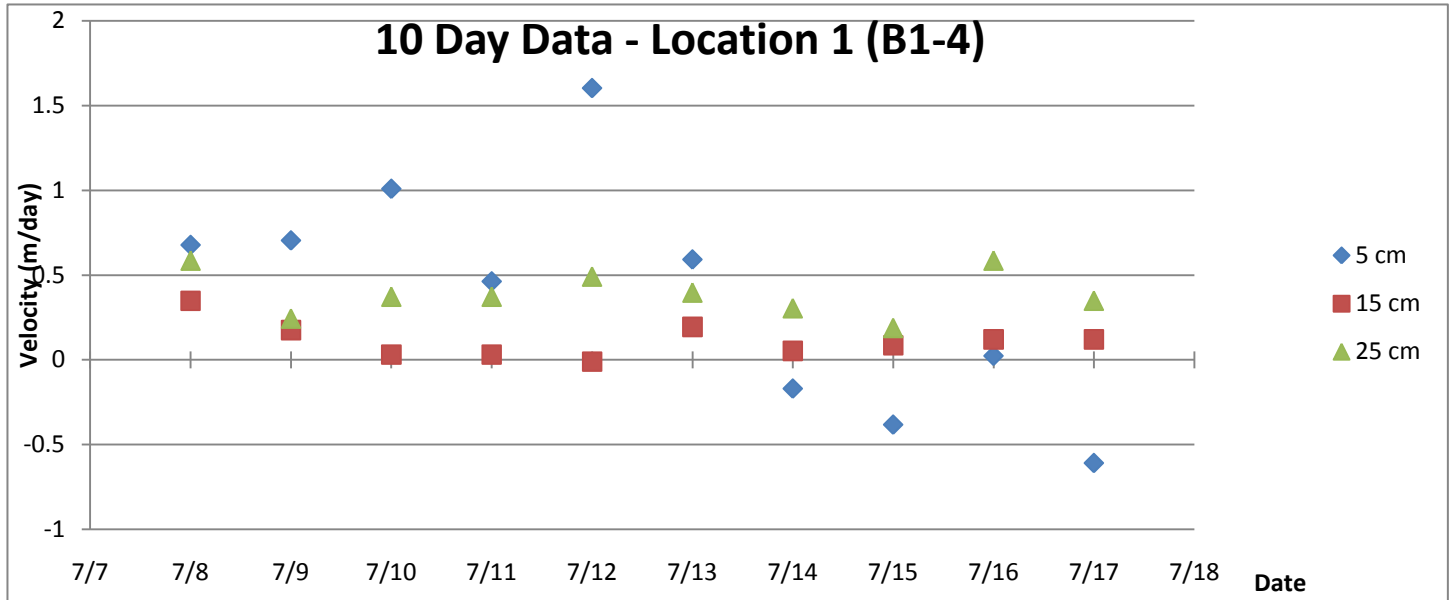


Figure 5) 10 Day streambed velocity graphs measured July 8<sup>th</sup> – 17<sup>th</sup>, 2007

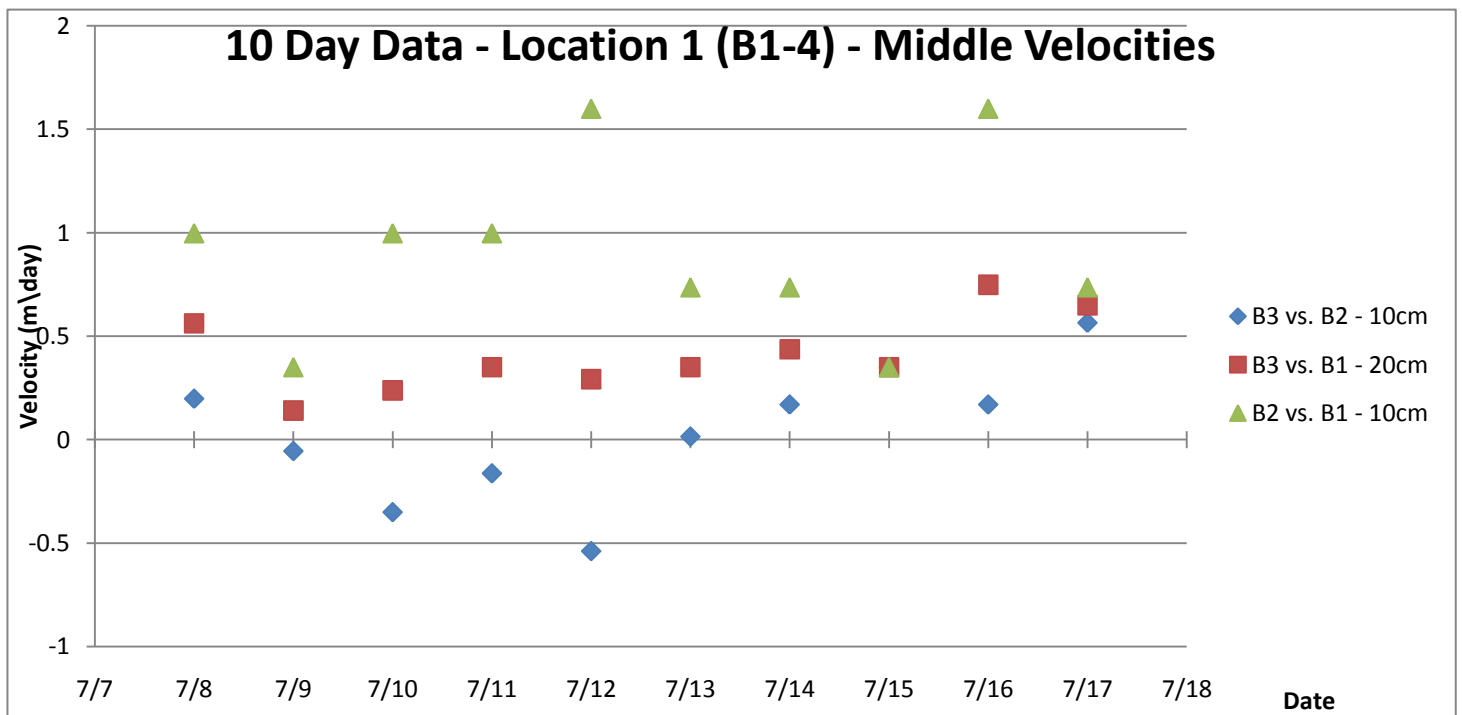
- A) 10 Day streambed velocity graphs – location 1
- B) 10 Day streambed velocity graphs – location 1 – middle velocities
- C) 10 Day streambed velocity graphs – location 2
- D) 10 Day streambed velocity graphs – location 3

Figure 5)

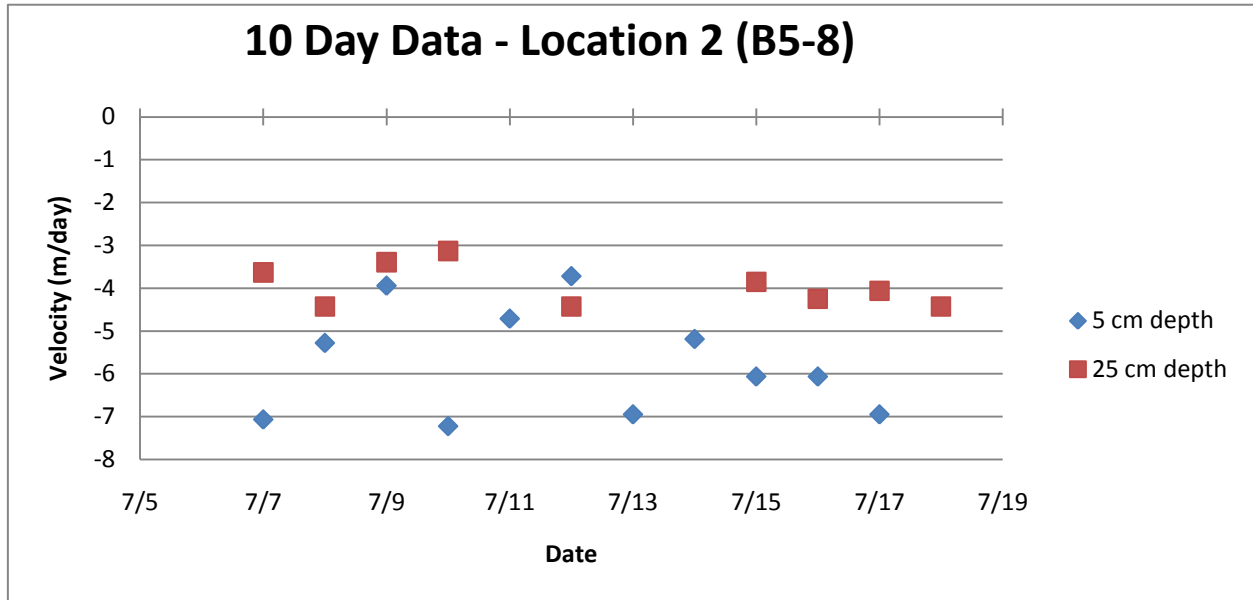
A)



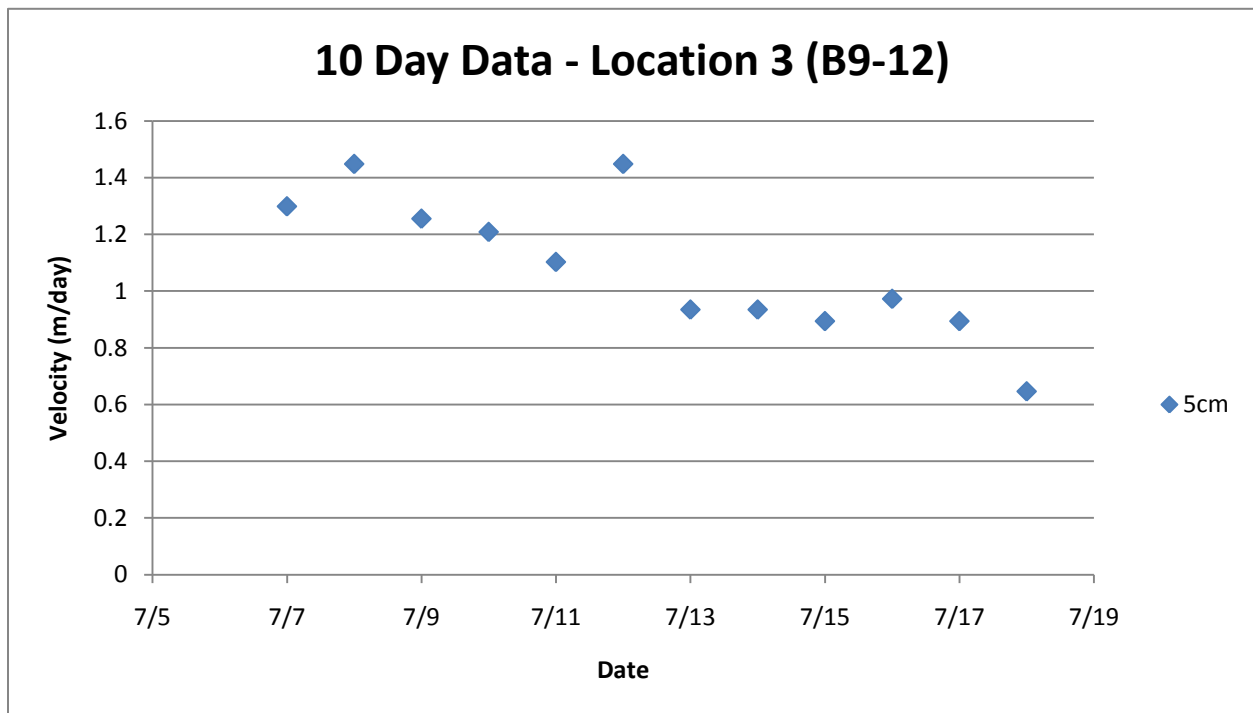
B)



C)



D)



with a standard deviation of 0.43 (Figure 5b). The average vertical porewater velocity between the sensors was 0.45 m/day.

Location 2 has values ranging from 3 m/day to 7 m/day upwards for the B7 (5 cm) and B5 (25 cm) depths the average velocity was -4.85 m/day (Figure 5c). The vertical porewater velocity between the B8 (stream) to B7 (5 cm) was -5.74 m/day with a standard deviation of 1.27, to B5 (25cm) the velocity was -3.96 m/day with a standard deviation of 0.49.

Location 3 had two temperature sensor malfunction, and only the B12 (stream) and B11 (5 cm) recorded data (Figure 5d). The results showed an average velocity of 1.09 m/day and a standard deviation of 0.25.

The results can be interpreted as indicating that on the upgradient or eastern side of the pampa the stream is recharging groundwater and at the downgradient or western side of the pampa groundwater is discharging to the stream. Effectively the surface and shallow groundwater are interacting similar to what would might be expect for a large bend in a meandering mountain river, similar to what is hypothesized by Lautz and Siegel (2006) in the Wind River Range, Wyoming.

#### 4.4 Ground penetrating radar

The GPR data was processed using RELFEX 2D-QUICK software. The EM velocity was analyzed using a hyperbola-adaption and CMP analysis. The CMP velocity analysis used the zero offset technique, whereby the true distance was used for calibration along with the corresponding reflections. Minimal processing steps were taken to interpret the data. A 'dewow' filter was applied to remove very low frequency components that would otherwise obscure the profile image. A simple background removal was used to eliminate temporally consistent noise from the whole profile and help to make signals visible. An automatic static correction was applied to eliminate the time delay between trigger and recording. An automatic gain control (AGC) was added in order to compensate for possible damping or geometric spreading losses. AGC facilitates the creation of equally distributed amplitudes on the time axis. Lastly, an automatic interpolation was applied over the profiles in the x- and y-

direction in the point mode plot setting. Elevation corrections were not required, as the changes in topography of the two sites was negligible over the transect lines (Sandmeier, 2007).

#### 4.41 Quilcayhuanca GPR results

The CO GPR reflection profiles for Quilcayhuanca penetrated to an average depth of 8 m (Figure 6). Four subsurface sedimentary units were identified that correlated to deposits observed in river cuts and shallow soil cores (Figure 7). The first was dry organic-rich soils (EM velocity 0.13 m/ns), located at the land surface and extending to a depth of approximately 0.3 m. The dry organic-rich soils is found in the shallow soil cores and best observed in the wigglemode GPR profiles by the low amplitude discontinuous reflections. The dry organic-rich soils gradually changes to the second unit of a fining upwards sequence of water-saturated sandy, organic-rich soils with coarse sediment (16 – 64 mm) (EM velocity 0.085 m/ns, determined from the CMP GPR surveys), which extends to between 0.3 – 3.0 m below the land surface. This unit has the lowest amplitude on the point mode GPR profile

Clay (EM velocity 0.06 m/ns) was the third identified unit and had an average thickness of 3 m throughout the pampa, and is characterized by linearly continuous high amplitude reflections. The fourth unit observed from the GPR surveys is coarse-grained gravels from colluvium deposits intermixed with glacial outwash till. The GPR reflection profiles show high-amplitude irregular reflections, especially in the wigglemode GPR profile. The most recent colluvial deposits are fanned out on the floor of the pampa valley and older colluvial deposits cut into the pampa and dip toward the center of the valley. Transects 7 and 8 were taken in a direction from the pampa valley floor up over the colluviums and show interlaced colluvial deposits with the soil and clay deposits.

#### 4.42 Yanamarey GPR Results

The CO GPR reflection profiles for the Yanamarey Pampa penetrated to an average depth of 6 m (Figure 8). Three subsurface sedimentary units were identified (Figure 9). The top two units were the same as found in Quilcayhuanca, dry organic-rich soils at the land surface, extending to a depth of approximately 0.5 m and a water-saturated fining-upwards sequence of

Figure 6)

The Quilcayhuanca CO-GPR Profile 7 was taken over a distance of 28 m and penetrated to a depth of approximately 8.0 m. The elevation over the survey area was approximately 3915 m.a.s.l. Three plotmode views are presented:

A) A true depth profile, which delineates the three stratigraphic units and the watertable. They are plotted with velocities obtained from CMP surveys and Baker et al., 2007.

B) The point mode GPR profile shows continuous groundwater surface reflections and the laterally continuous clay layer.

C) The wigglemode GPR profile, which highlights the strongest reflections.

Figure 6)

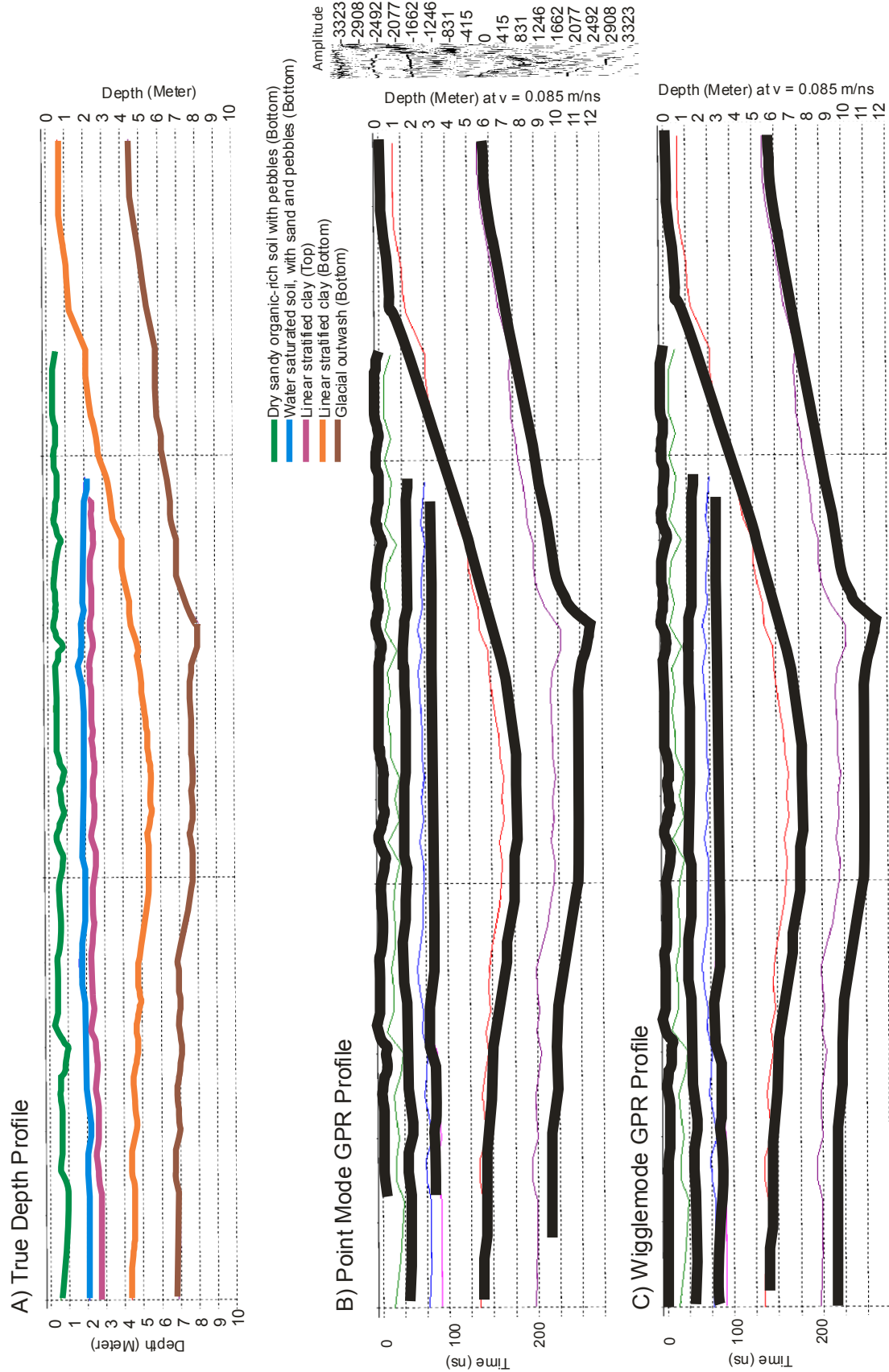




Figure 7)

The Quilcayhuanca stratigraphic unit model. Material < 8m depth is based on GPR observations and material >8m depth is based on general observations and stratigraphic principals.

Figure 7)

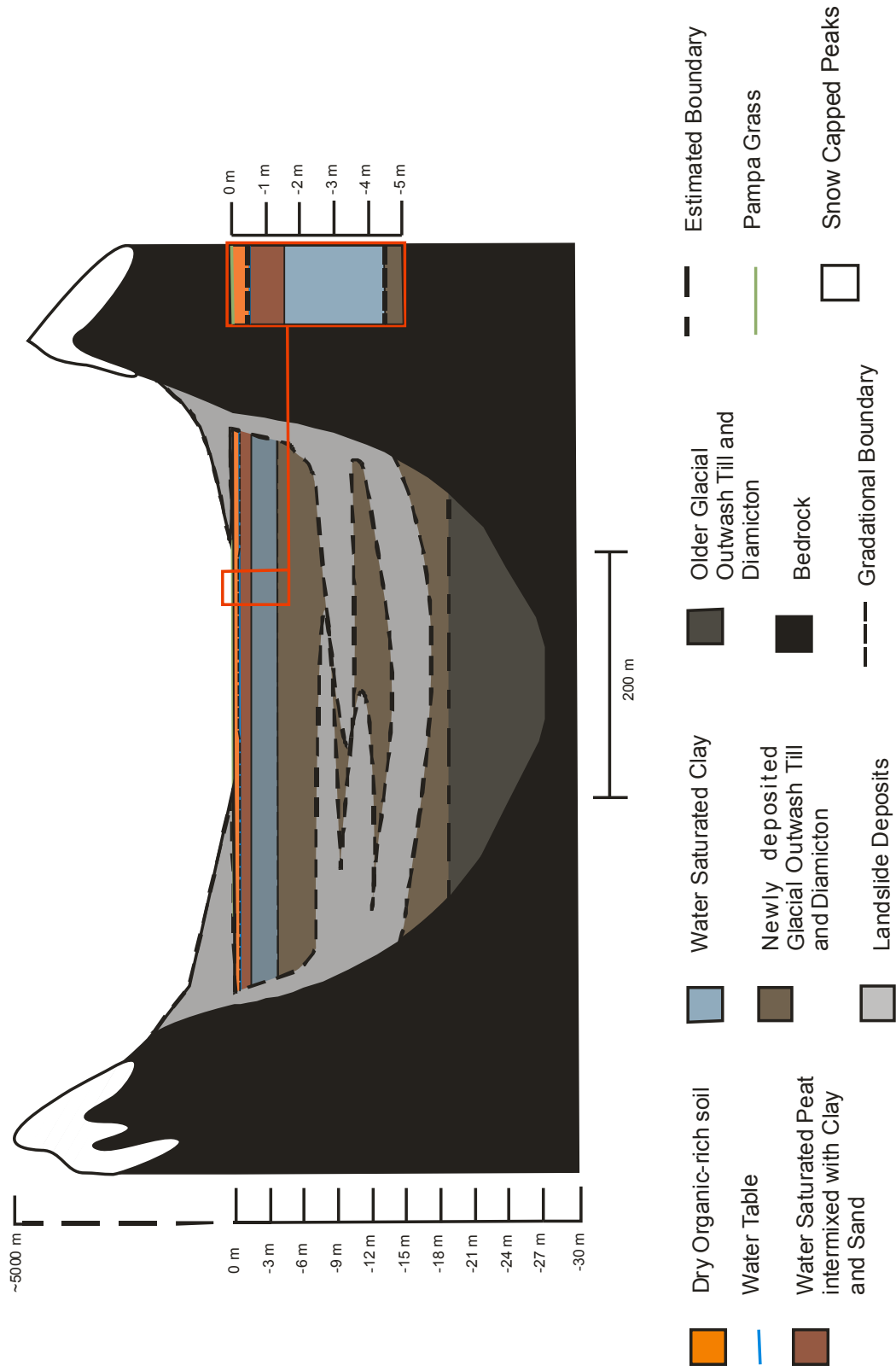


Figure 8)

The Yanamarey CO GPR profile 98-6 was taken over a distance of 28 m and penetrated to a depth of approximately 6.5 m. The elevation over the survey area was approximately 4324 m.a.s.l. Three plotmode views are presented:

A) A true depth profile, which delineates the three stratigraphic units and the watertable. They are plotted with velocities obtained from CMP surveys and Baker et al., 2007.

B) The point mode GPR profile shows continuous groundwater surface reflections and the laterally continuous clay layer.

C) The wigglemode GPR profile, which highlights the strongest reflections.

Figure 8)

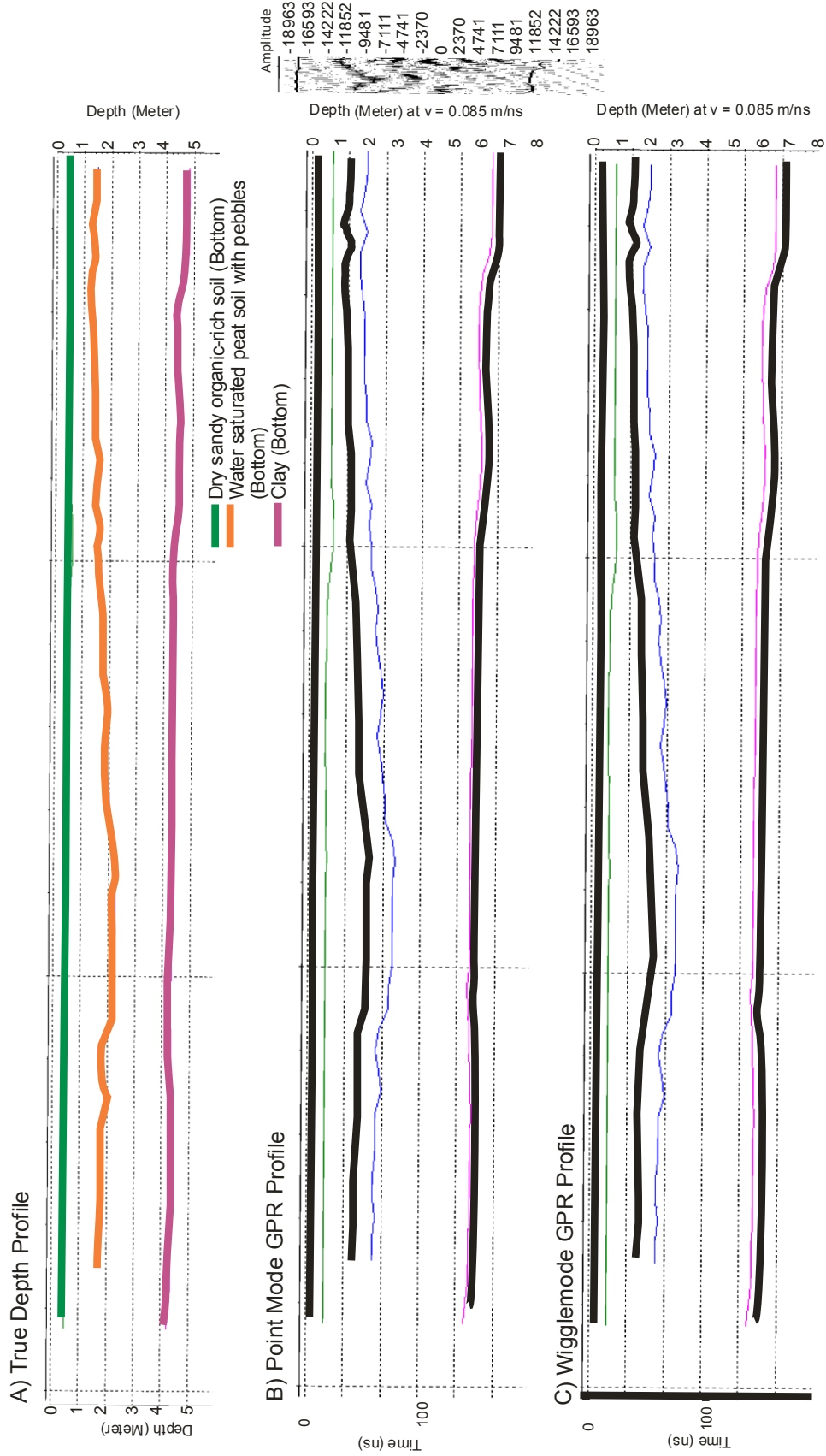
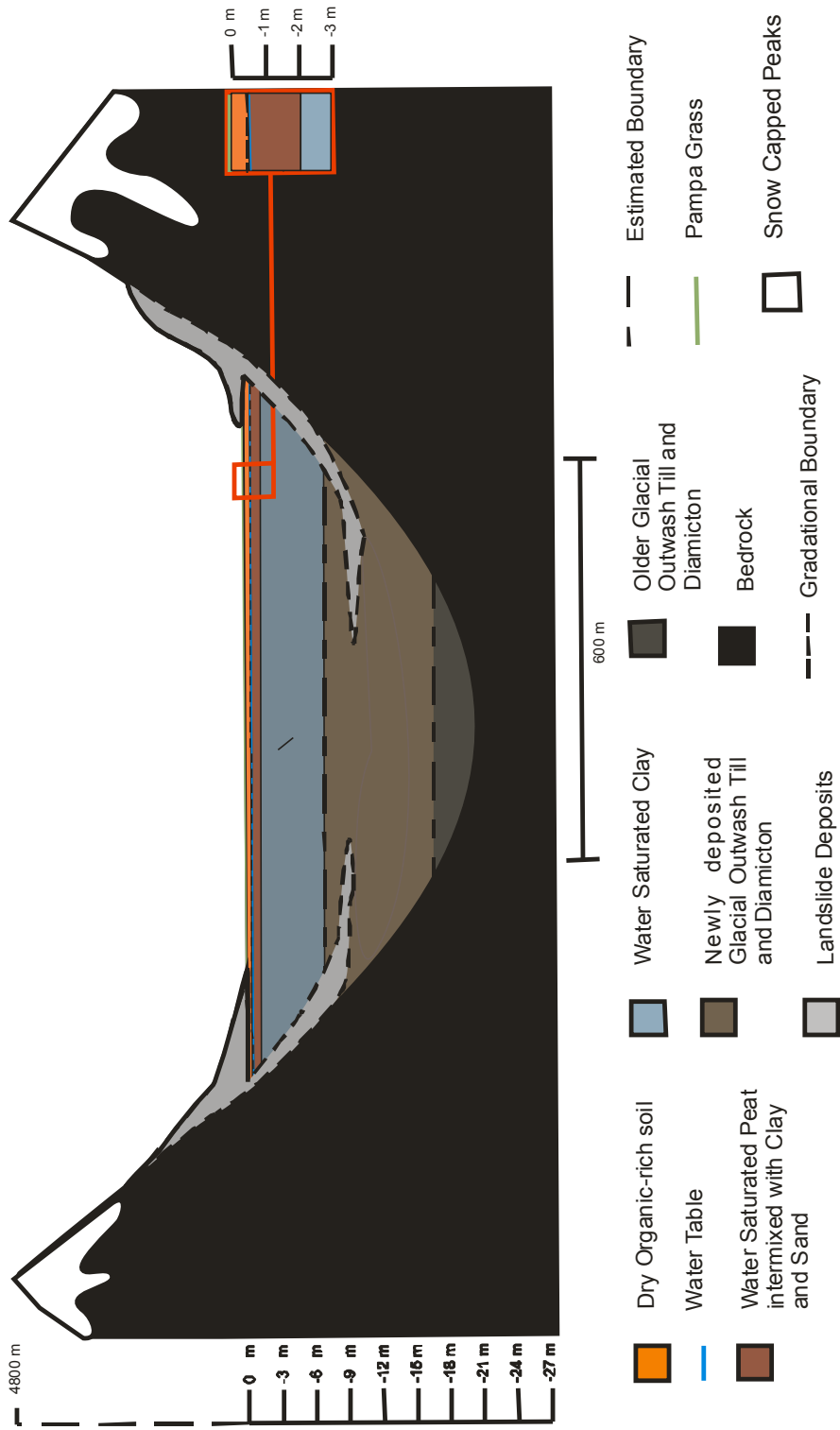


Figure 9)

The Yanamarey stratigraphic unit model. Material < 8m depth is based on GPR observations and material >8m depth is based on general observations and stratigraphic principals.

Figure 9)



sandy organic-rich soils with coarse sediment (16 – 64 mm) down to a depth of 2.0 m below the land surface. The boundary between these units is similar in gradational style to that observed in Quilcayhuanca and they are seen in the wigglemode GPR profile by the sub-horizontal semi-continuous reflections. The third unit was clay; it was identified in the GPR profiles by linearly continuous high amplitude reflections. The clay is thicker in Yanamarey than in Quilcayhuanca and due to the high signal attenuation of clay, the bottom termination of this unit was not observed. Therefore, the minimum clay thickness is 1 m.

## **Chapter 5 – Pampa Formation**

### 5.1 General pampa formation

During the late Pleistocene to Holocene, there have been several glacier advances and retreats in the Cordillera Blanca. The last glacial cycle had two separate major advances, the first from 29 ka to 20.5 ka and that of the last glacial maximum at 16.5 ka (Farber et al., 2005). In addition to these major advances there were several smaller intermittent glacial advances and retreats, which shaped the valleys of the Cordillera Blanca and are responsible for the depositional deposits observed in the pampa valleys.

In the Cordillera Blanca the eastern and western sides of the mountain range have different valley morphology. The long topographically flat pampa valleys are not observed on the eastern side of the range, but instead there are steeper valleys, many with the characteristic 'v' bottom shape indicative of fluvial erosion. These differences likely reflect differences in precipitation and temperature gradients across the range, set up orographically driven precipitation from the east (Smith et al., 2005).

### 5.12 Quilcayhuanca pampa formation

#### *Braided Streams and Glacial Outwash Deposits (Figure 10A)*

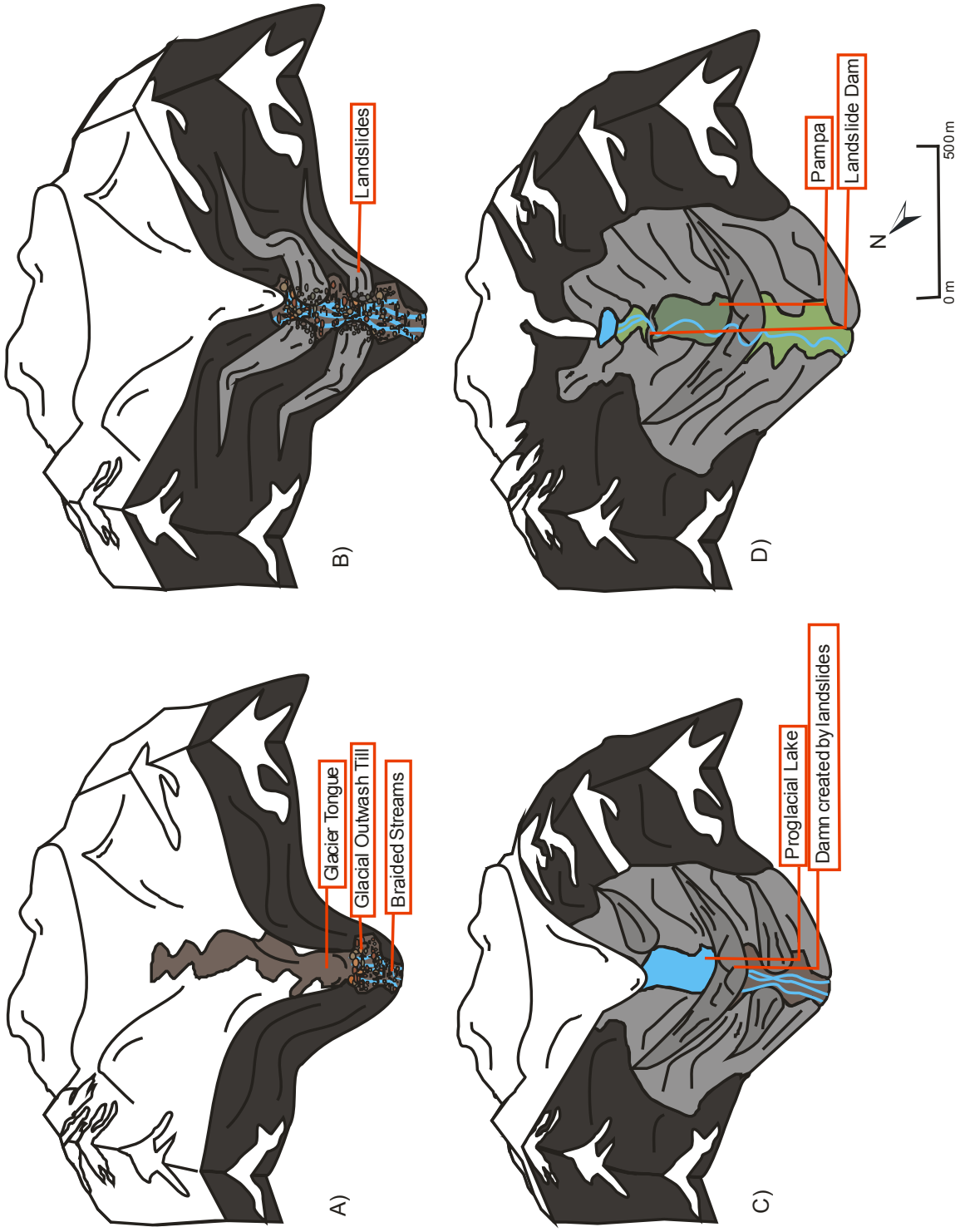
Repeated glacial advances eroded steep sided u-shaped valleys in Quicayhuanca. Shallow unstable braided streams formed and continuously shifted positions in response to the highly variable flows and sediment load from glacial meltwaters (Ashley, 1985). During low

Figure 10)

Based on the GPR survey results and field observations, a pampa formation model is hypothesized. As the glaciers retreated from the Quilcayhuanca Pampa, glacial melt water formed braided streams and glacial outwash materials that were deposited on the valley floor (A). More landslides occurred in Quilcayhuanca (B). These landslides and moraines dammed lakes, and coarser glacial outwash materials were deposited at the mouth of the glacier, whereas finer sediments were carried out in the epilimnion of the lakes (C). The deposition of these finer sediments are observed today as laminated clays with intermixed fine to coarse sediments. These deposits form poorly drained surface causing the watertable to remain close to the land surface and enhance the development of organic-rich peat soils (D).



Figure 10)



energy periods, less dense debris was carried and deposited downstream and more dense sediment was deposited in shallower waters around the ice margins at the mouth of the glacier. For the high energy periods, braided streams carried coarser materials further downstream and deposited it on the valley floor. These glacio-fluvial deposits are likely underlain by ground-moraine deposited as the glacier retreated, sitting upon bedrock on the valley bottom. Additionally there may be end moraines deposited cross valley at times when the glacier stopped retreating.

#### *Landslides (Figure 10B)*

The steep valley walls were, and still are, prone to frequent landslides which deposited gravels and unsorted debris onto the valley floor. Based on slope analysis of modern landslide deposits (seen in the Quilcayhuanca and Llanganuco valleys) the volume of landslides deposited is  $8,000,000 \text{ m}^3 - 20,000,000 \text{ m}^3$ , over an area of  $150,000 \text{ m}^2$  to  $250,000 \text{ m}^2$ . The volume estimation is based on the length, width and height of current landslide deposits. The coarse-grained gravels from colluvium and glacial outwash material was simultaneously being deposited. Based on the GPR data there are laterally extensive landslide deposits that cut into the most recent glacial deposits in the subsurface. Additionally, some valleys in the Cordillera Blanca have modern landslide deposits, such as the landslide at the base of the Northern Wall of the the Llanganuco Valley between the Llanganuco and Laguna Llanganuco lakes, that were triggered by the 1970 earthquake. More recent debris flow deposits can be attributed to gravity and slope movement (Figure 11) (Vilímek et al., 2000).

#### *Proglacial Lakes (Figure 10C)*

Throughout pampas in the northern Cordillera Blanca, landslides and end-moraines created transient dams behind which valley lakes can form. This lake forming processes is still occurring in some of the pampas, such as the Llanganuco Valley. Glacial outwash materials were continuously being deposited into these lakes, deposited as lacustrine sediment. The degree to which a glacier influences sedimentation in a lake depends in part on its proximity to the lake; finer sediments were carried out in the epilimnion of the lake and eventually deposited over

Figure 11)

Modern day landslide deposits in the Llanganuco Valley. These deposits dam Laguna Llanganuco and Llanganuco.

Figure 11)



the larger glacial outwash material during periods of low water activity (Smith, 1985). The deposition of these finer sediments is observed today as laminated clays. There are also fine to coarse sediments intermixed with the clay, due to the seasonal variation of runoff into the lake, progradation of lake deltas, and the differential glacial melt rates.

#### *Pampa (Figure 10D)*

The layers of clay and silt infilled the lake and formed a poorly drained surface, which allowed precipitation and glacial melt water to accumulate. This buildup of water, in addition to the flat topography, led to the formation of perennially water-logged soils and organic-rich soils. Today, pampa grass has grown over the organic-rich soils and two glacially fed streams are located in the pampa and down the valley.

#### 5.13 Yanamarey pampa formation

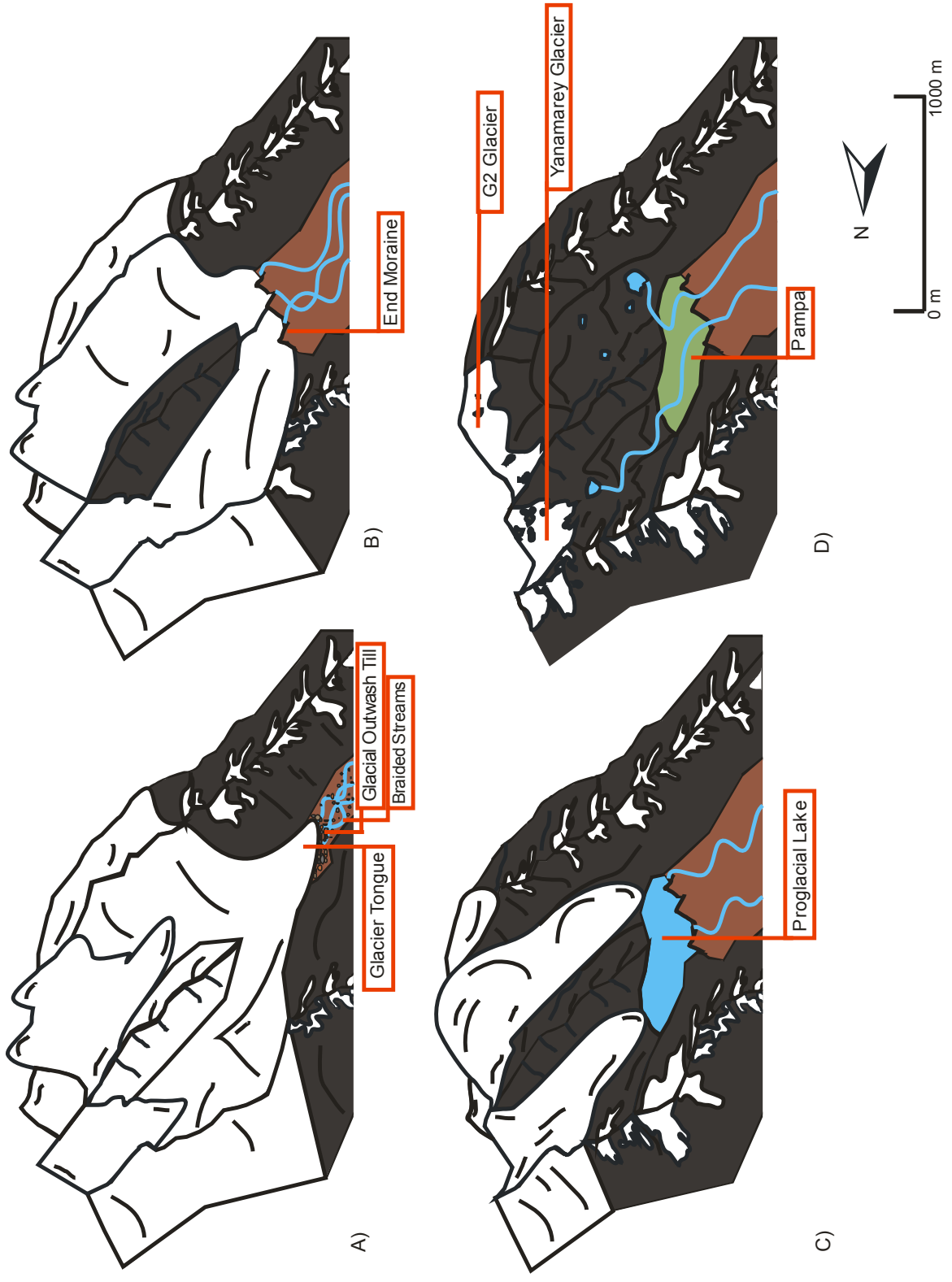
The Yanamarey pampa is divided by a central ridge which extends down from the bedrock. The ridge is likely lengthened from lateral moraines that formed along the axis where the Yanamarey and G2 glaciers would have merged. The northern side of the pampa is at a slightly higher elevation and has a steeper topographic gradient than the southern side. The glacial melt water and precipitation in this region caused considerable erosion and resulted in a deeper incision of the northern stream. The southern side of the pampa is extremely flat and developed a small stream where the water table remained very close to the surface.

The same five units observed in Quilcayhuanca are also present in Yanamarey. However there are some difference in the formation of the Yanamarey pampa and pampas in the south, Cordillera Blanca. Similar material was deposited on the valley floor by glacial metwaters and braided streams (Figure 12A). An end moraine formed at the western end of the pampas (Figure 12B), which dammed a proglacial lake and as the glacier continued retreating up the valley it split back into the two respective glaciers (Figure 12C). End moraines damming proglacial lakes, instead of landslides, are a common feature of pampas throughout the southern Cordillera Blanca, since valley walls are less steep than the north and thus less prone

Figure 12)

Based on the GPR survey results and field observations, a pampa formation model is hypothesized. As the glaciers retreated from the Yanamarey Pampas, glacial melt water formed braided streams and glacial outwash materials that were deposited on the valley floor (A). Glaciers created end moraines (B). These moraines and less frequent landslides dammed lakes, and coarser glacial outwash materials were deposited at the mouth of the glacier, whereas finer sediments were carried out in the epilimnion of the lakes (C). The deposition of these finer sediments are observed today as laminated clays with intermixed fine to coarse sediments. These deposits form poorly drained surface causing the watertable to remain close to the land surface and enhance the development of organic-rich peat soils (D).

Figure 12)



to landslides. The deposits in the lake are similar to Quilcayhuanca, seen from shallow soil cores and CO GPR profiles, and eventually through the same processes formed the present day clays.

Subsequently the pampa grass grew throughout the pampa and two glacially fed streams are still present today (Figure 12D). The ridge likely either reflects a slight bedrock high or a medial moraine that formed along the axis where the the Yanamarey and G2 glaciers would have merged and the slightly higher elevation and steeper topographic gradient on the northern side resulted in a deeper incision of the northern stream.

## 5.2 Differences in Northern and Southern Pampas

The Northern and Southern Pampas, though similar in formation and topography, show come distinct differences. The northern valleys are steeper, more u-shaped, and topographic range from the pampas to the Rio Santa increases moving northwards, giving the northern range more 'hanging valleys' than in the south. The southern valley is less steep and therefore the glaciers would be able to flow out onto the Rio Santa valley floor resulting in more marshy-wetlands.

The less steep valleys in the south also result in fewer landslides and less extensive colluvial deposits in the subsurface of the valley floor. The colluvial deposits on the valley walls are likely groundwater recharge zones, fed by runoff. Within the pampa, the connected colluvial deposits and glacial outwash should be primary zones for groundwater flow and storage.

Pampas in the northern valleys have a smaller area and are more isolated, whereas in the southern valleys the pampas are longer, thinner and extended down the valleys. The glacierized area surrounding the pampas is greater in the north and decreases in the southern valleys and consequently the melt water production decrease from north to south (Baraer et al., 2009)



## Chapter 6 – Conclusions

Investigating the subsurface sedimentology and geomorphology of Cordillera Blanca pampas is crucial in determining the hydrogeological parameters of these vital water storage systems. GPR was successful in studying the high permittivity pampa sediments of the Yanamarey and Quilcayhuanca pampas. Four distinct stratigraphic units were delineated in addition to the water table location. The effectively impermeable upper clay layers appear to hydrologically isolate the top three units of the pampas from the underlying extensive more permeable glacial outwash and colluvial deposits. These units highlight the dominant depositional mechanisms responsible for the formation of pampas from glacier recession. Based on the GPR survey results and field observations, models of pampa formation are proposed.

As the glaciers retreated from the Quilcayhuanca and Yanamarey Pampas, glacial melt water formed braided streams and glacial outwash materials that were deposited on the valley floor. Landslides and moraines formed dams behind which lakes formed, within which lacustrine sediments were deposited. Once the lakes drained, the glaciolacustrine sediments were poorly drained, causing the water table to remain close to the land surface and enhance the development of the organic-rich soils presently found throughout the pampas. The connected subsurface colluvial and glacial outwash deposits are assumed to be the primary zone for the storage and movement of groundwater.

Based on the shape and scale of the valley walls (in particular in the northern pampas) and the size of the visible landslide deposits, it is conservatively estimated that the thickness of the colluvial deposits should be at least 15 m. The estimated area of the pampas, based primarily on topography, is 63.3 km<sup>2</sup>. Assuming a porosity of 0.1 (Freeze and Cherry, 1979), the coarsely estimated total volume of groundwater stored in the pampas is ~0.1 km<sup>3</sup>. For comparison, the total volume of glacial ice across the Cordillera Blanca (on both the East and West sides of the range) is approximately 19.0 km<sup>3</sup>. Therefore, while the glaciers are obviously a much larger store of water than groundwater, the amount of stored groundwater is not insignificant and is an important component of the larger hydrologic system. This is

confirmed by research from Baraer et al., (2009) who estimate that more than 50% of dry season discharge from many of the pampas is groundwater derived.

The research presented in this thesis has focused primarily on water storage in low-topography mountain pampas; there are other settings in the Rio Santa watershed that may also have similar hydrologic functionality. For example, near Laguna Conocha, at the head waters of the Rio Santa, there is a large flat plain that may behave similarly to the mountain reservoirs. Using the same 10° topographic cutoff as was used to delineate the pampas, this region has an area of 32.6 km<sup>2</sup>.

GPR has many applications in the field of hydrogeology. The GPR wave properties are highly sensitive to the presence of water, as well as those factors that control water movement in the subsurface. This study showed that GPR is a viable and useful technique for evaluating subsurface stratigraphy in areas of water saturated high organic content soils and clays. Depths of 8 m were attained with 50 MHz antennas and further studies should be carried out in similar hydrogeologic settings to facilitate hydrogeological investigations. Unfortunately, GPR cannot be used to investigate these systems during the wet season, as the signal would be attenuated by the higher water content. Further investigations can be completed on the water table during the wet season with the use of monitoring wells.

The high Andean paramos and pampas are an extremely important for water resources for people in the surrounding communities. In the Cordillera Blanca, Peru, pampas are the wetland that act as a groundwater reservoir and control the patterns of groundwater flow and residence times. These systems behave in specific ways, based on their geomorphology, and can be easily investigated with the use of geophysics. Similar studies can be implemented to investigate paramos and other wetland environments in the Andes to assess the role of the systems and importance of groundwater in the overall water budget.

## References

- Annan, A.P., (2005), GPR methods for hydrogeological studies, Sensors and Software Inc., Hydrogeolophysics, 185-213.
- Ashley, G.M., J. Shaw, N.D Smith, (1985), Glacial sedimentary environments. Soc. Econ. Paleontol. Mineral., Short Course 16.
- Baker, G.S., and H.M. Jol, (2007), Stratigraphic Analyses Using GPR. The Geological Society of America, Inc. Boulder, Colorado, USA.
- Baraer M., J.M McKenzie, B.G Mark, J. Bury, S. Knox, (2009), Characterizing contributions of glacier melt and ground water during the dry season in the Cordillera Blanca, Peru. Adv Geosci 22:41–49.
- Bury, J., B.G. Mark, J.M. McKenzie, A. French, M. Baraer, K.I. Huh, M.A. Zapata Luyo, R.J. Gómez López, (2010), Glacier recession and human vulnerability in the Yanamarey watershed of the Cordillera Blanca, Peru. Climatic Change, 1-20.
- Buytaert, W., J., Deckers and G. Wyseure, (2006), Description and classification of nonallophanic Andosols in south Ecuadorian alpine grasslands (páramo). Geomorphology 73:207–221.
- Célleri, R. and Feyen, J., (2009), The Hydrology of Tropical Andean Ecosystems: Importance, KnowledgeStatus, and Perspectives, Mt. Res. Dev., 29: 350–355.
- Farber, D.L., G.S. Hancock, R.C. Finkel and D.T. Rodbell, (2005), The age and extent of tropical alpine glaciation in the Cordillera Blanca, Peru, J. Quat. Sci. 20 (7–8): 759–776.

Farouki, O.T., (1986), Thermal Properties of Soils, Series on Rock and Soil Mechanics, Volume 11, Trans Tech, Clausthal-Zellerfeld, Germany.

Flamingo Resource Centre, High Andean Wetlands fragile strategic ecosystems for millions of people, High Andean Wetlands Regional Strategy, <[http://www.flamingoresources.org/docs/literature/andean\\_wetlands.pdf](http://www.flamingoresources.org/docs/literature/andean_wetlands.pdf)>, (accessed May 2, 2011).

Freeze, R.A., Cherry J.A., (1979), Groundwater Englewood Cliffs, NJ: Prentice-Hall

Hatch, C.E., A.T. Fisher, J.S. Revenaugh, J. Constantz and C. Ruehl, (2006), Quantifying surface water-groundwater interactions using time series analysis of streambed thermal records: method development, Water Resources Research 42.

Juen, I., G. Kaser, C. Georges, (2007), Modelling observed and future runoff from a glacierized tropical catchment (Cordillera Blanca, Peru), Global and Planetary Change, 59(1-4): 37-48.

Lautz, L.K., (2010), Impacts of non-ideal field conditions on vertical water velocity estimates from streambed temperature time series, Water Resources Research 46: W01509.

Lautz, L. K., and D. I. Siegel, (2006), Modeling surface and ground water mixing in the hyporheic zone using MODFLOW and MT3D, Advances in Water Resources, 29: 1618-1633.

Mark, B. G., J. Bury, J.M. McKenzie, A. French, and M. Baraer, (2010), Climate Change and Tropical Andean Glacier Recession: Evaluating the Hydrologic Changes and Livelihood Vulnerability in the Cordillera Blanca, Annals of the Association of American Geographers.

Mark, B. G., J. M. McKenzie, (2007), Tracing Increasing Tropical Andean Glacier Melt with stable

Isotopes in Water: Callejon de Huaylas, Peru, *Environmental Science and Technology*, 41(20): 6955-6960.

Mark, B. G., and G. O. Seltzer, (2005), Evaluation of recent glacier recession in the Cordillera Blanca, Peru (AD 1962-1999): spatial distribution of mass loss and climatic forcing, *Quaternary Science Reviews*, 24: 2265-2280.

Mark, B. G., and G. O. Seltzer, (2003), Tropical glacier meltwater contribution to stream discharge: a case study in the Cordillera Blanca, Peru, *Journal of Glaciology*, 49(165), 271-281.

McNulty, B. A., D. L. Farber, G. S. Wallace, R. Lopez, O. Palacios, (1998), Role of plate kinematics and plate-slip-vector partitioning in continental magmatic arcs: Evidence from the Cordillera Blanca, Peru, *Geology*, 26(9): 827-830.

Robinson, Z., I. Fairchild, A. Russell, (2008), Hydrogeological implications of glacial landscape evolution at Skeiðarársandur, SE Iceland, *Geomorphology* 97: 218-236.

Sandmeier, K.J., (2007), REFLEX 2-D Manual., Scientific Software, Germany.

Smith, J.A., G.O. Seltzer, D.L. Farber, D.T. Rodbell, R.C. Finkel, (2005), Early Local Last Glacial Maximum in the Tropical Andes, *Science* 308: 678–681.

Suarez, W., P. Chevalier, B. Pouyaud, P. Lopez, (2008), Modelling the water balance in the glacierized Paron Lake basin (White Cordillera, Peru), *Hydrological Sciences Journal- Journal Des Sciences Hydrologiques*, 53(1): 266-277.

Van Overmeeren, R.A., (1998), Radar facies of unconsolidated sediments in The Netherlands: A

radar stratigraphy interpretation method for hydrogeology, *Journal of Applied Geophysics*, 40, 1–18.

Warner, B.G., D.C., Nobes, B.D., Theimer, (1990), An application of ground-penetrating radar to peat stratigraphy of Ellice Swamp, Southwest Ontario. *Canadian Journal of Earth Sciences* 27: 932–938.

White, S. and F. Maldonado, (1991), The use and conservation of natural resources in the Andes of southern Ecuador. *Mt IRes. Dev.*11: 37-55.

Wilson, J., L. Reyes and J. Garayar, (1967), Geología de los cuadrangulos de Mollebamba, Tayabamba, Huaylas, Pomebamba, Carhuaz u Huari. *Serv. Geol.Minería Bol.* 16: 95.

Vilímek, V., M.L. Zapata, J. Stemberk,(2000), Slope movements in Callejón de Huaylas, Peru. *Acta Universitatis Carolinae, Geographica* 35, Supplementum, 39–51.

Appendix 1 – Quilcayhuanca GPR results. The location of these profiles can be seen in Figure 2.

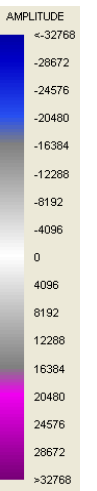
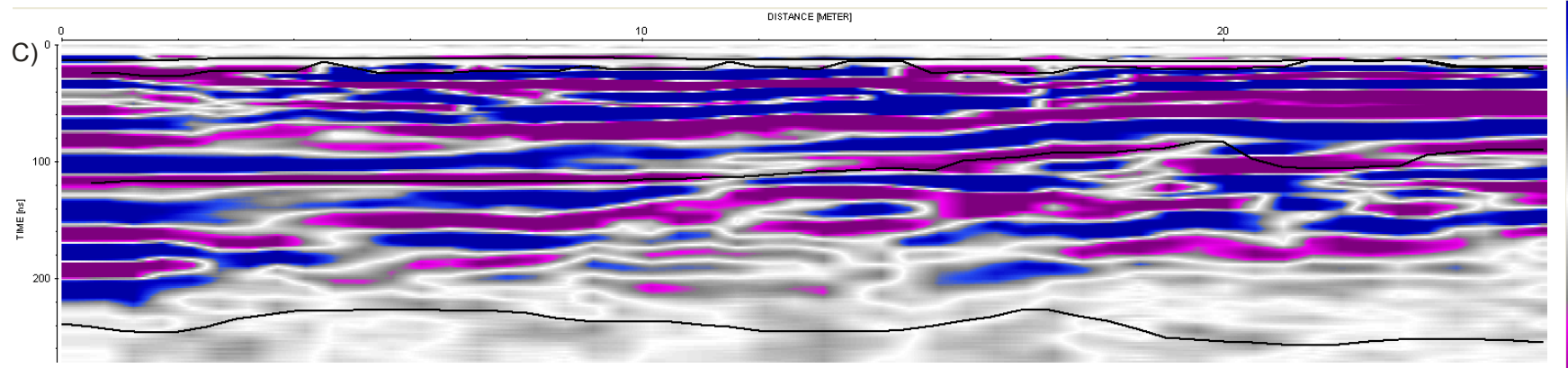
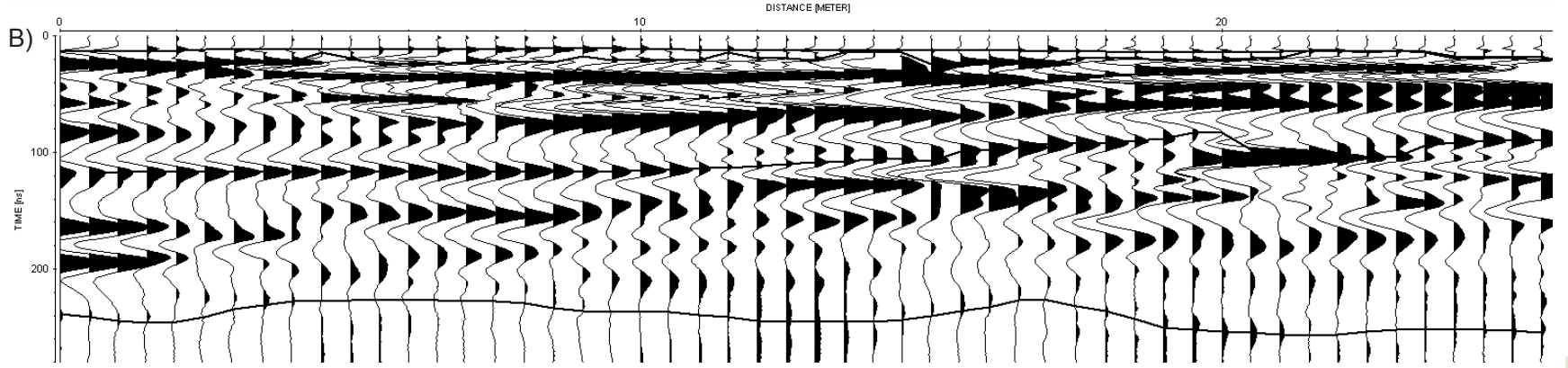
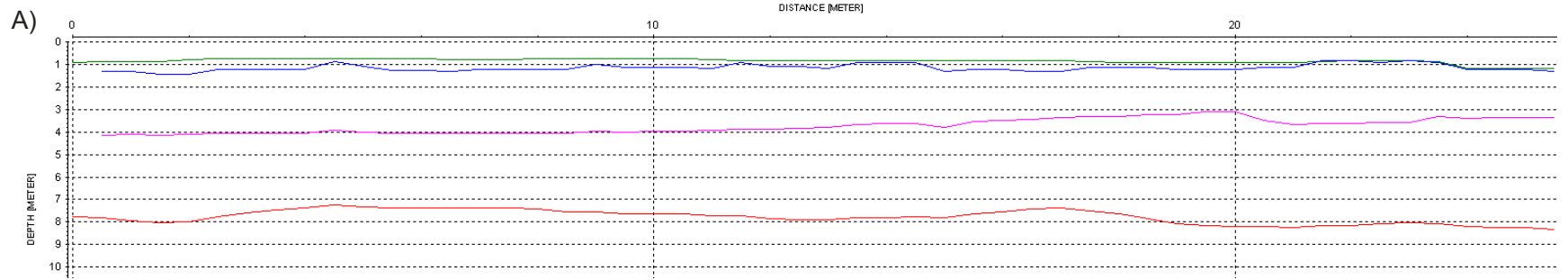
A) A true depth profile, which delineates the three stratigraphic units and the perched watertable. They are plotted with velocities obtained from CMP surveys and Baker et al., 2007.

B) The wigglemode GPR profile, which highlights the strongest reflections.

C) The point mode GPR profile shows continuous groundwater surface reflections and the laterally continuous clay layer.

Quilcayhuanca - Q3

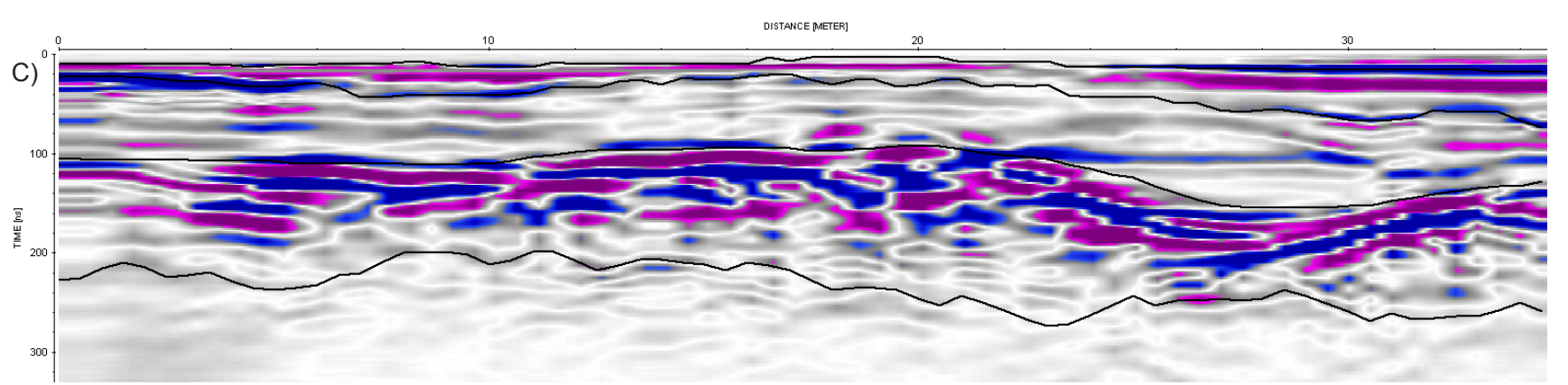
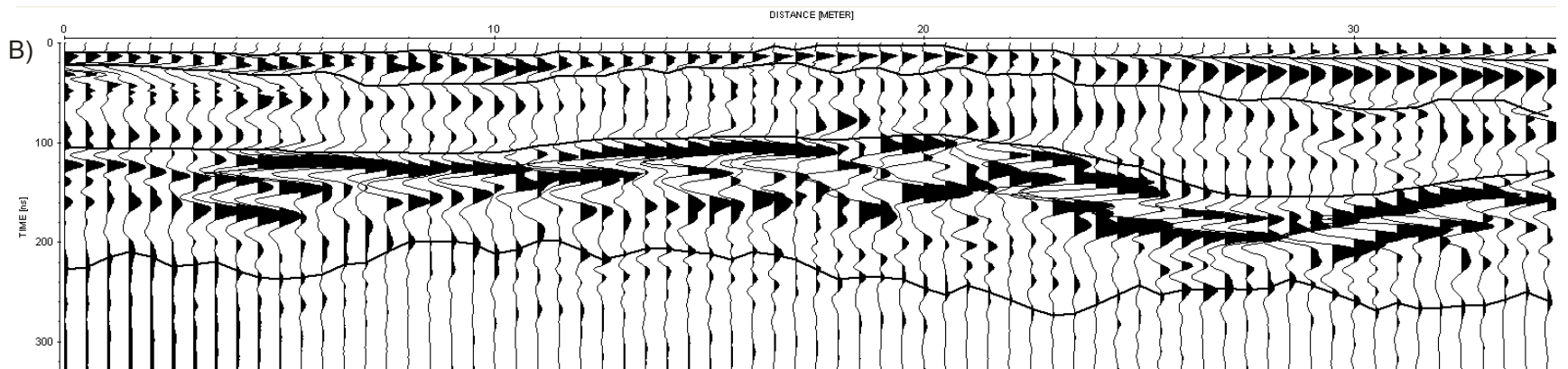
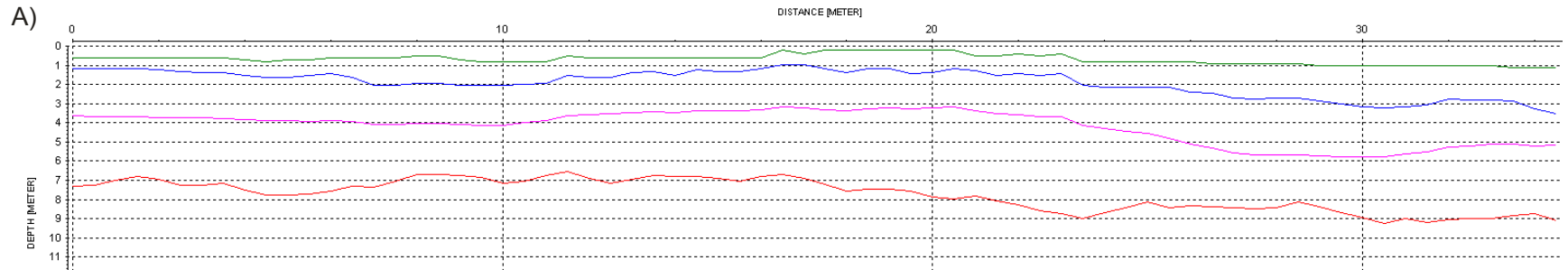
- Dry sandy soil with pebbles (Bottom)
- Water saturated soil, with sand and pebbles (Bottom)
- Linear stratified clay (Bottom)
- Glacial Outwash (Bottom)





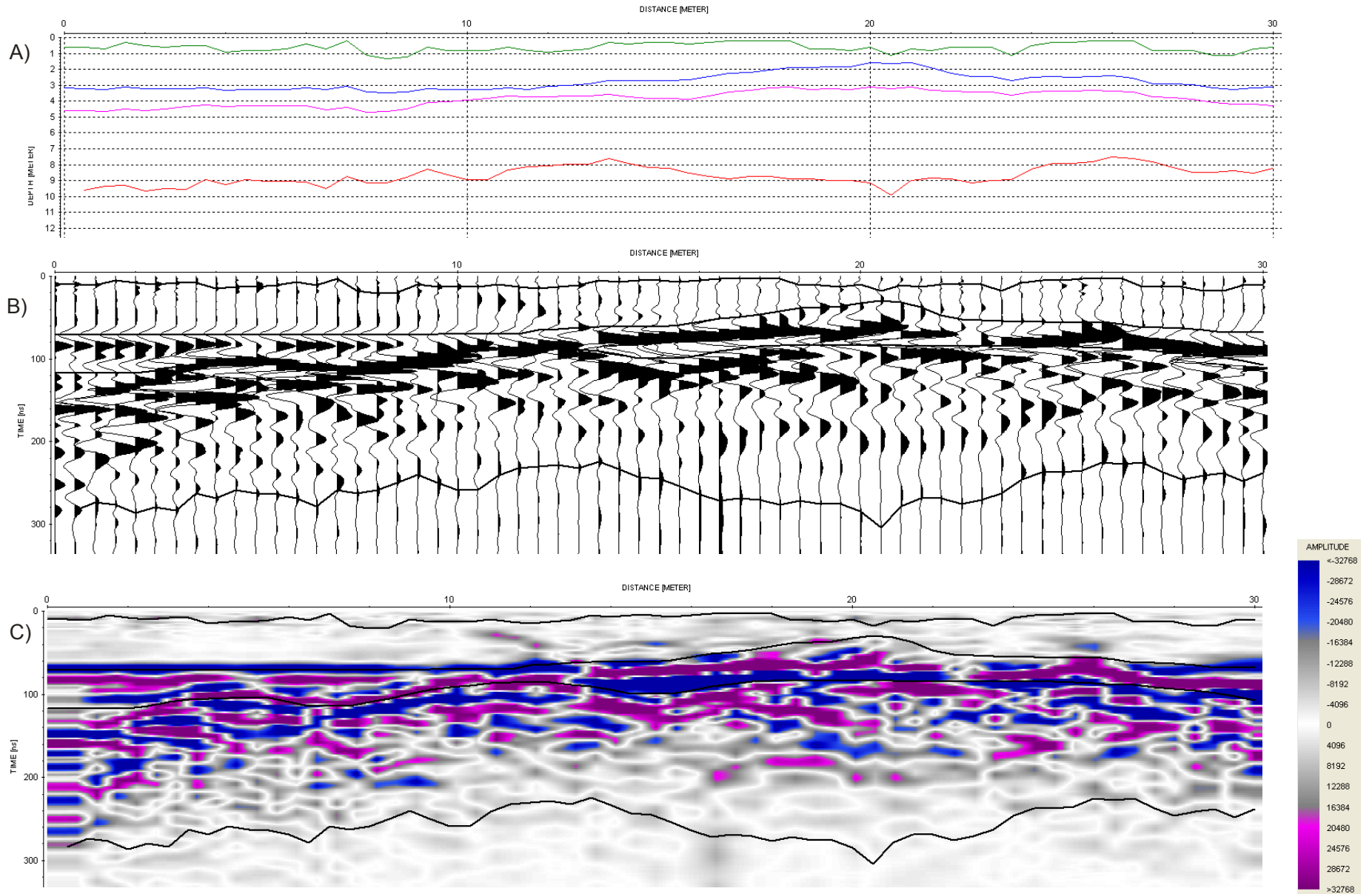
- Dry sandy soil with pebbles (Bottom)
- Water saturated soil, with sand and pebbles (Bottom)
- Linear stratified clay (Bottom)
- Glacial Outwash (Bottom)

Quilcayhuanca - Q5



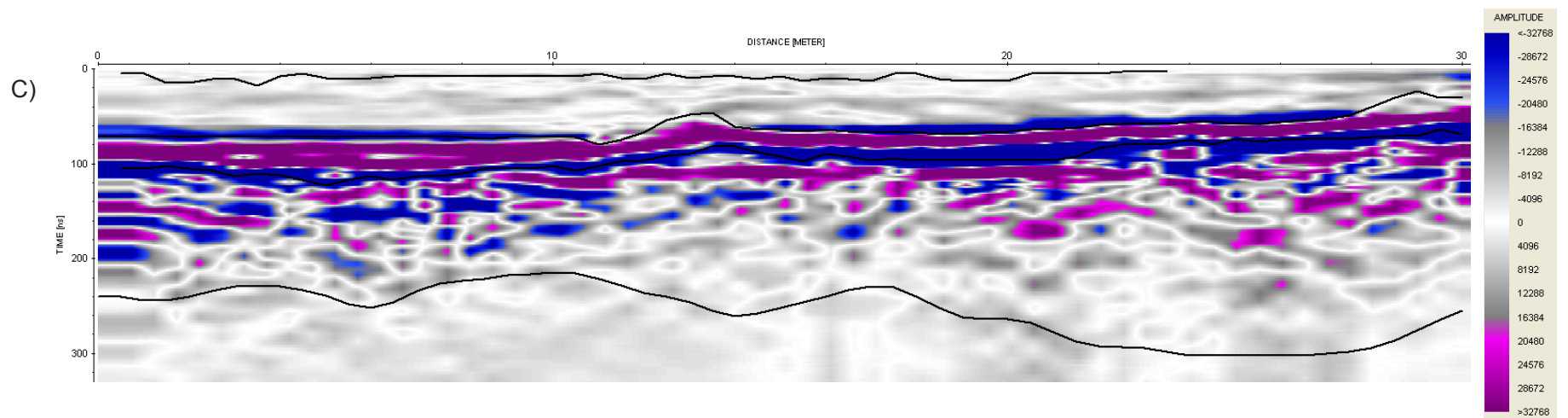
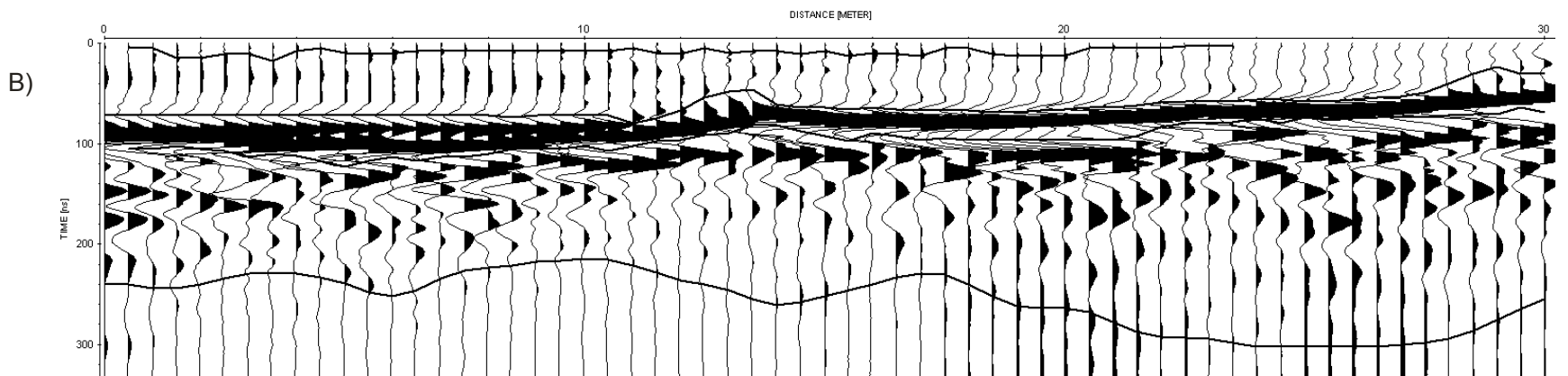
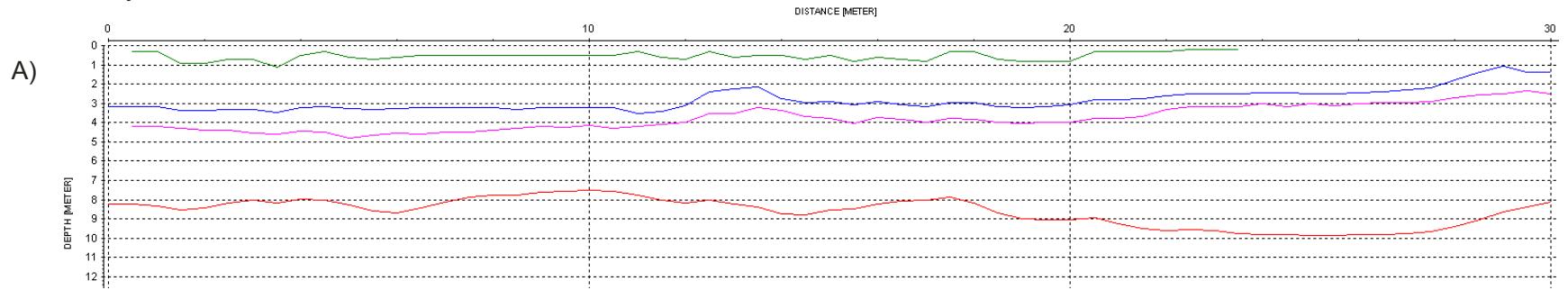
- Dry sandy soil with pebbles (Bottom)
- Water saturated soil, with sand and pebbles (Bottom)
- Linear stratified clay (Bottom)
- Glacial Outwash (Bottom)

Quilcayhuanca - Q6



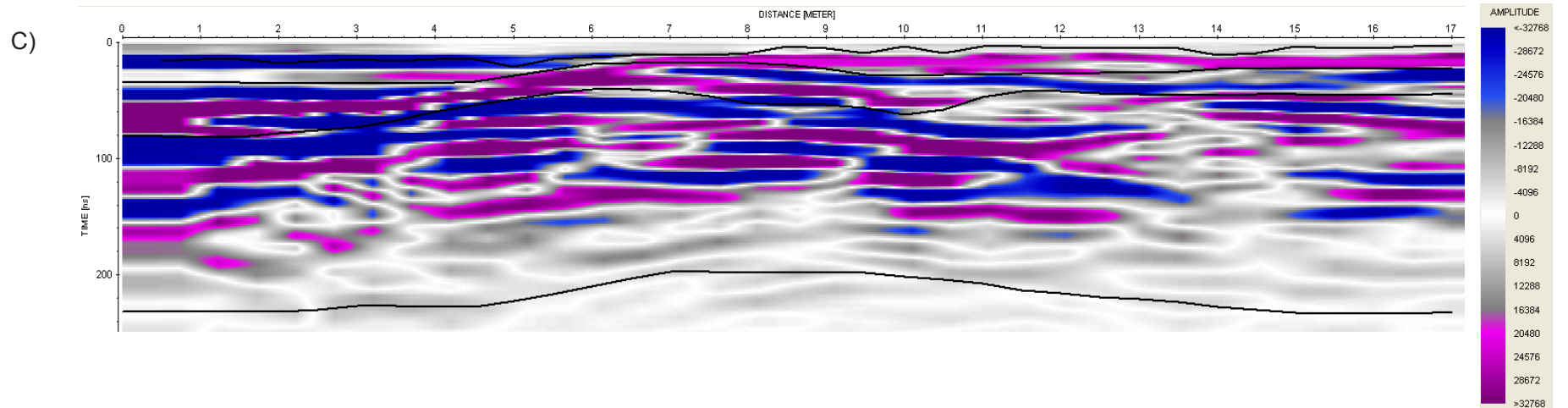
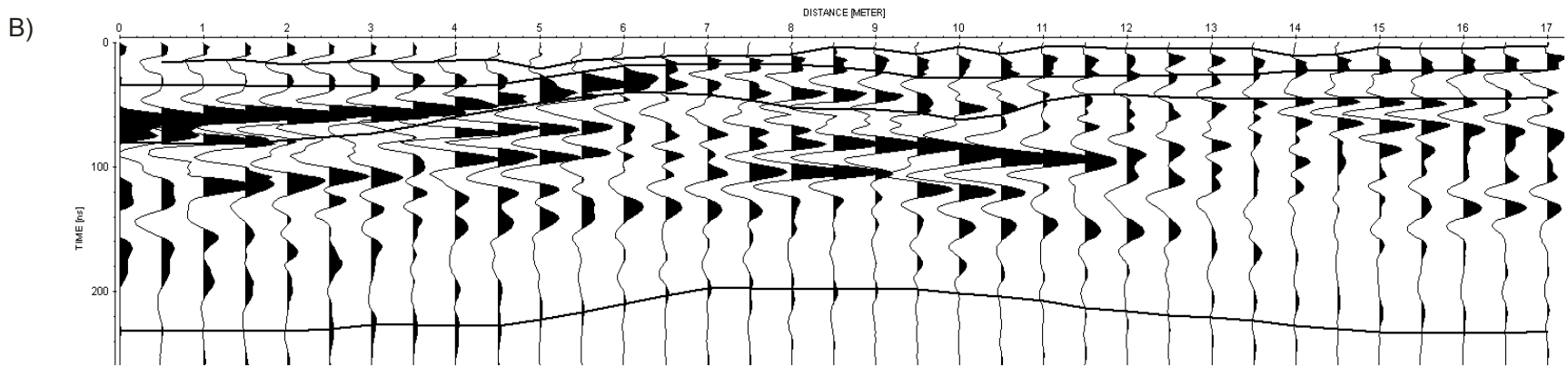
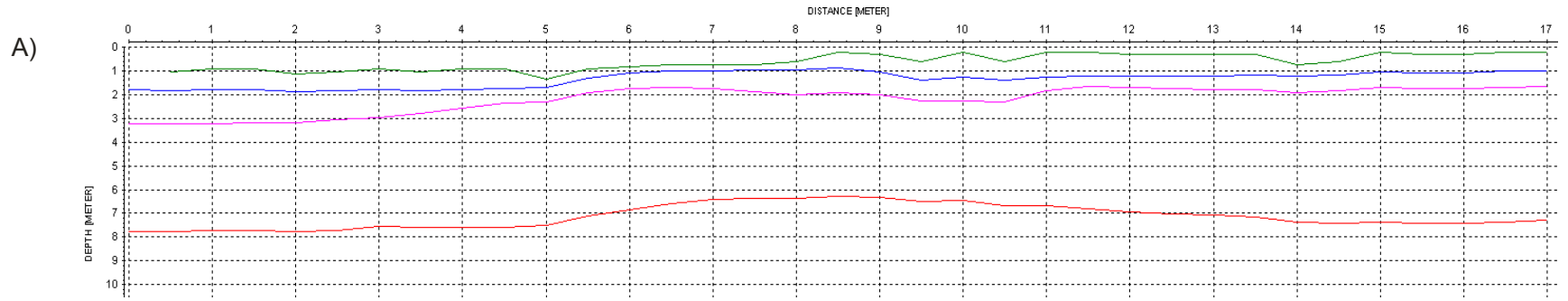
- Dry sandy soil with pebbles (Bottom)
- Water saturated soil, with sand and pebbles (Bottom)
- Linear stratified clay (Bottom)
- Glacial Outwash (Bottom)

Quilcayhuanca - Q7



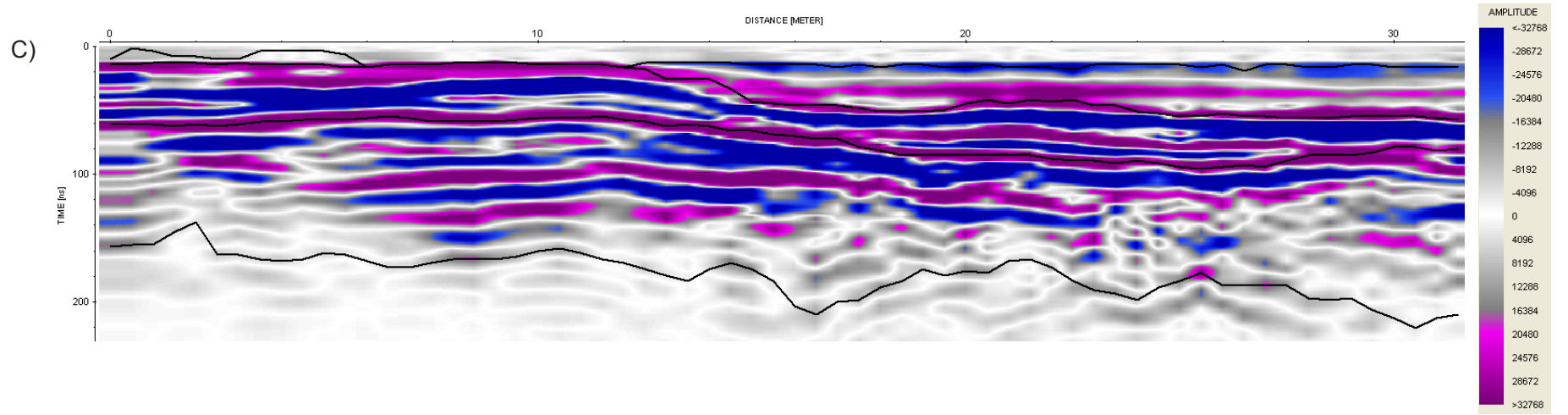
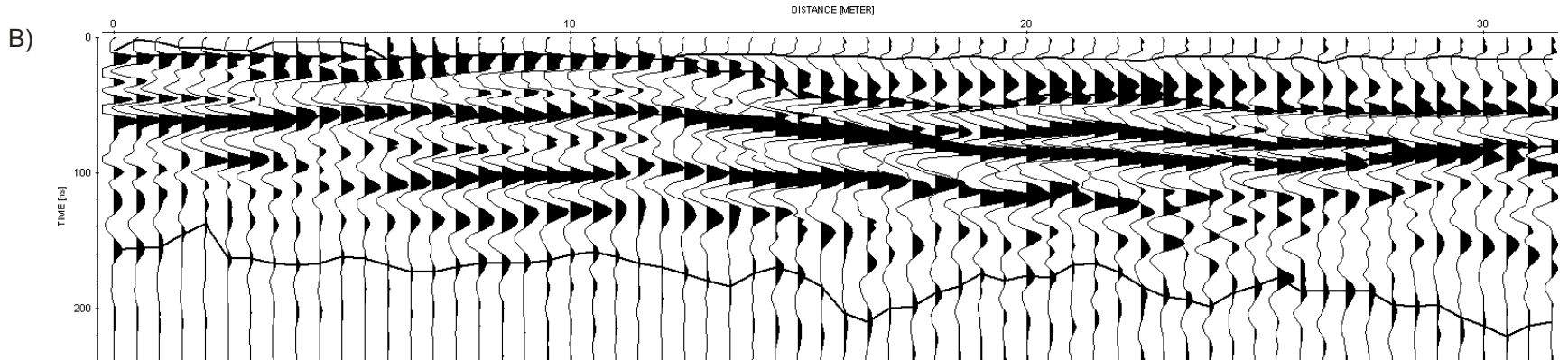
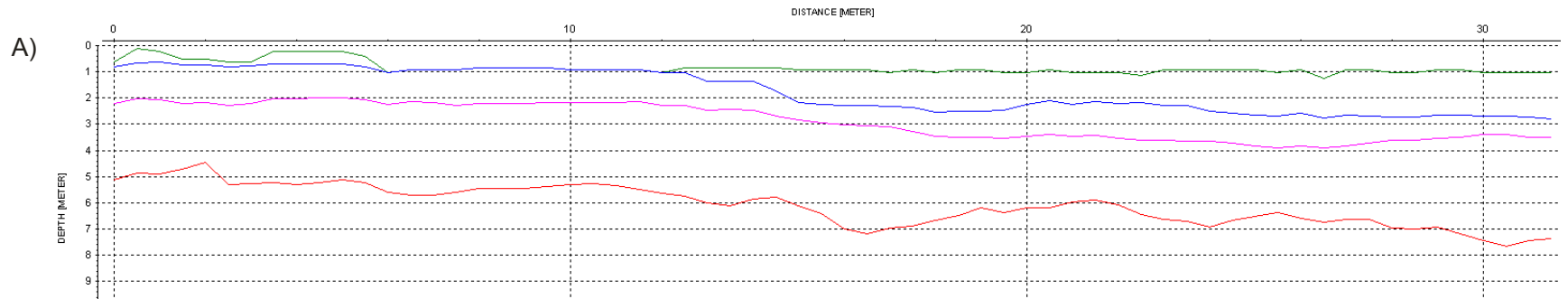
- Dry sandy soil with pebbles (Bottom)
- Water saturated soil, with sand and pebbles (Bottom)
- Linear stratified clay (Bottom)
- Glacial Outwash (Bottom)

Quilcayhuanca - Q8



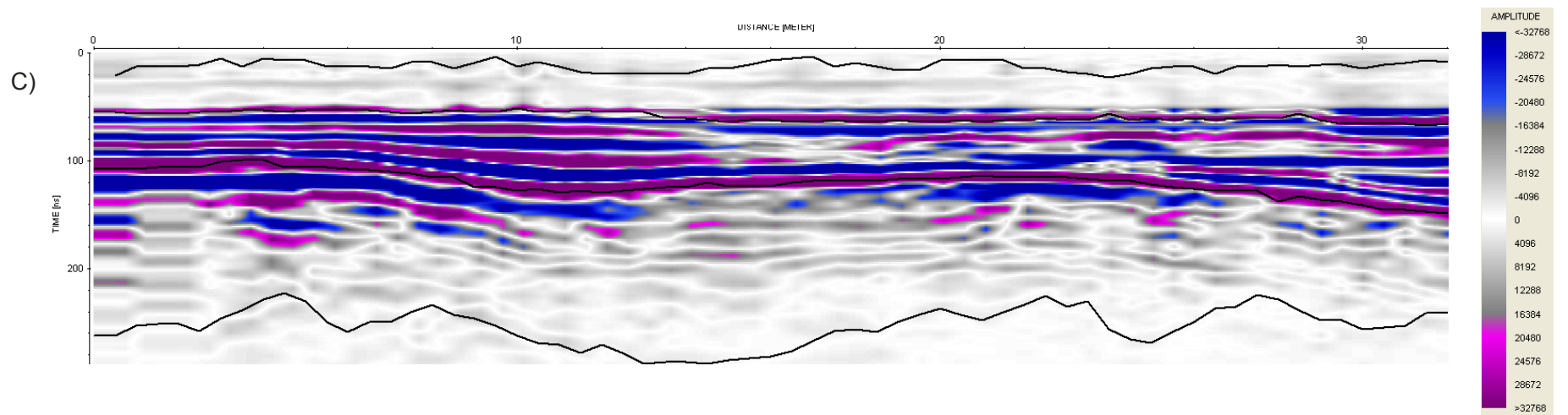
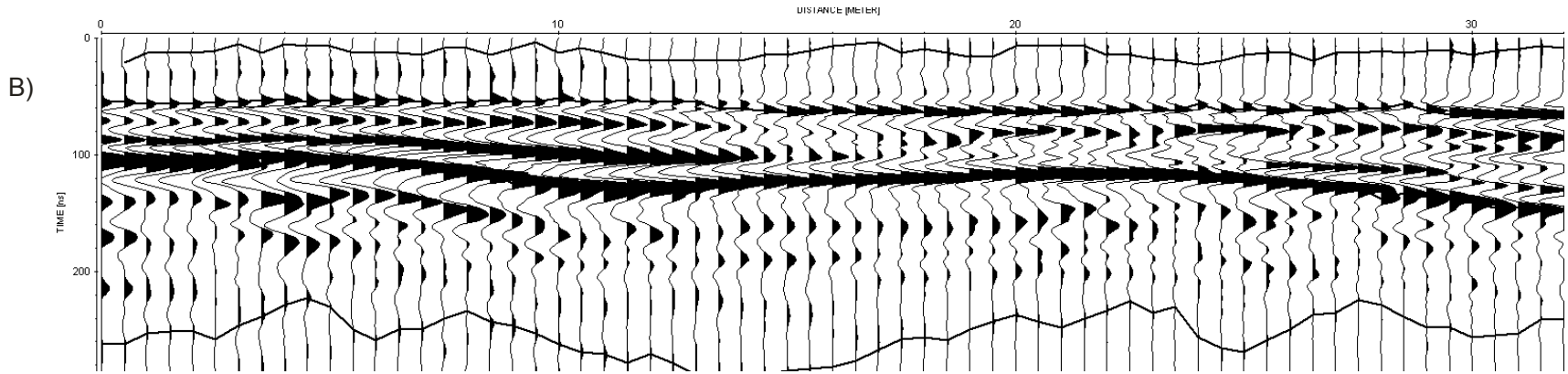
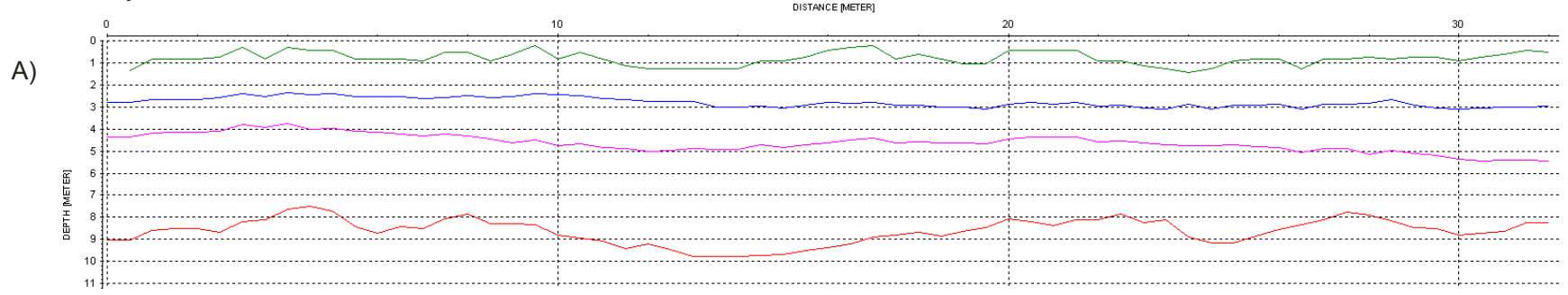
- Dry sandy soil with pebbles (Bottom)
- Water saturated soil, with sand and pebbles (Bottom)
- Linear stratified clay (Bottom)
- Glacial Outwash (Bottom)

Quilcayhuanca - Q9



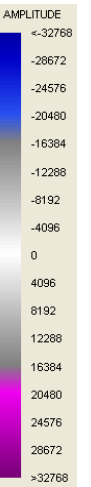
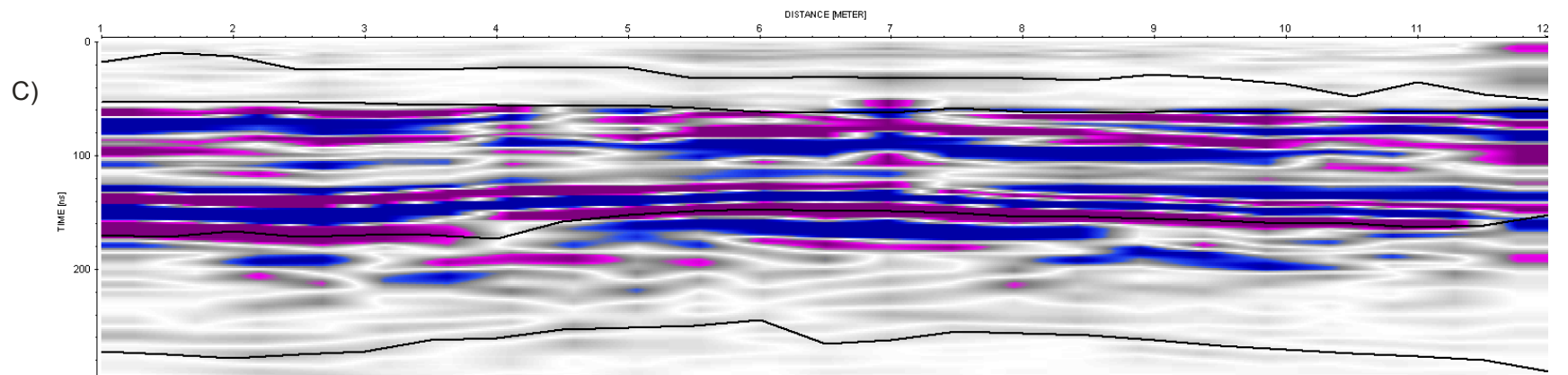
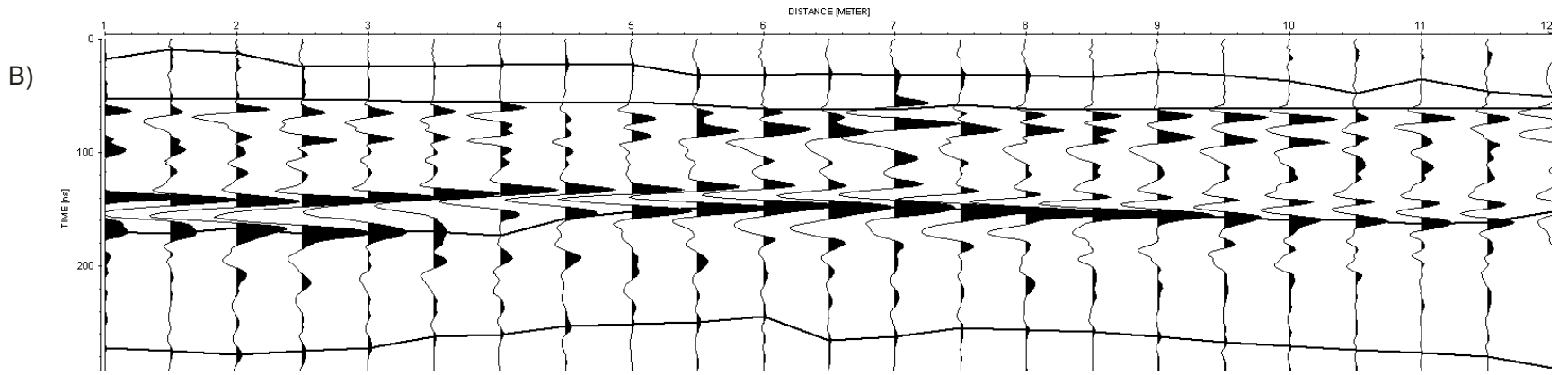
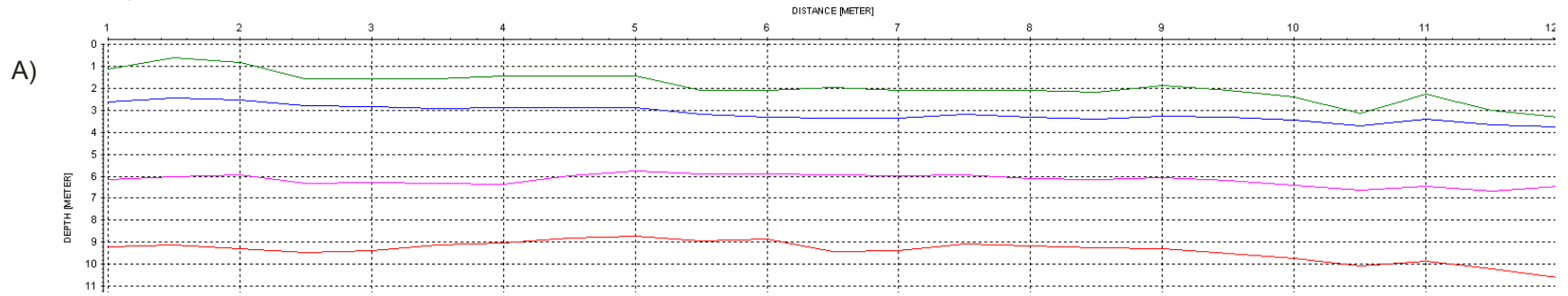
- Dry sandy soil with pebbles (Bottom)
- Water saturated soil, with sand and pebbles (Bottom)
- Linear stratified clay (Bottom)
- Glacial Outwash (Bottom)

Quilcayhuanca - Q10



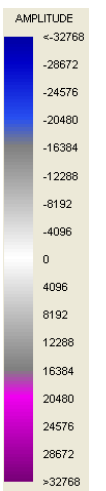
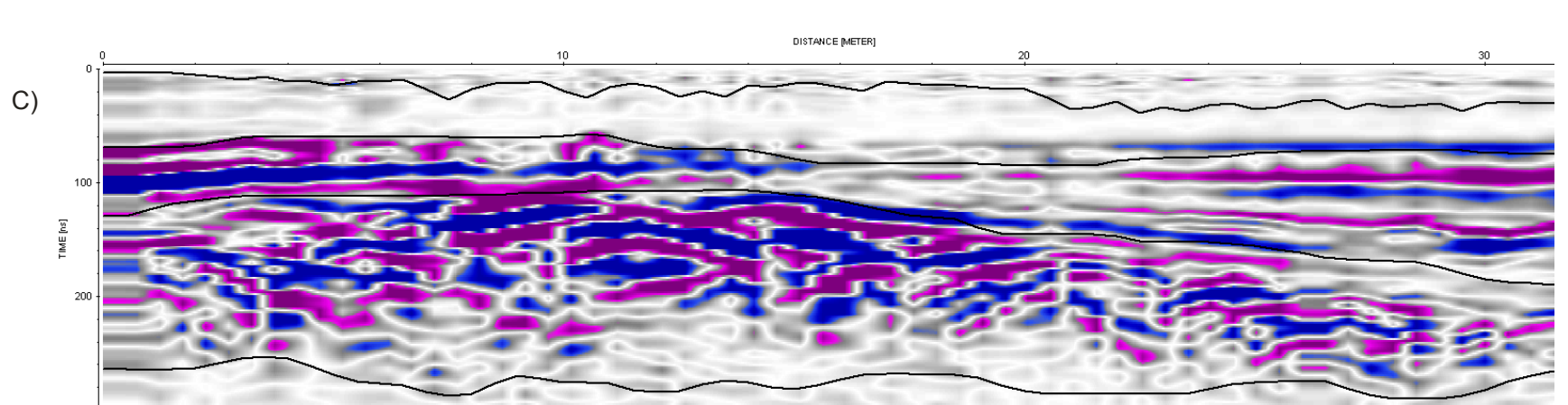
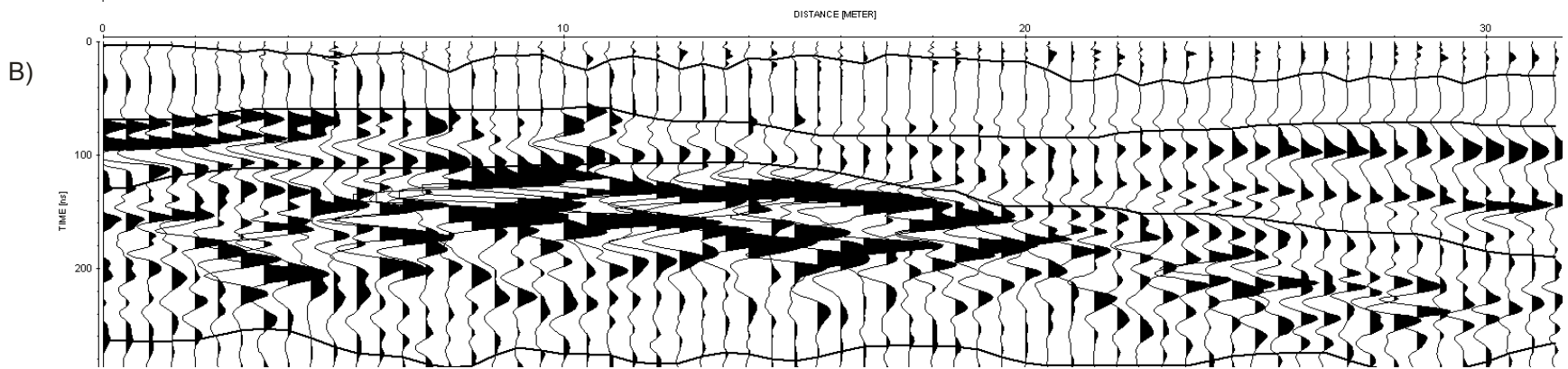
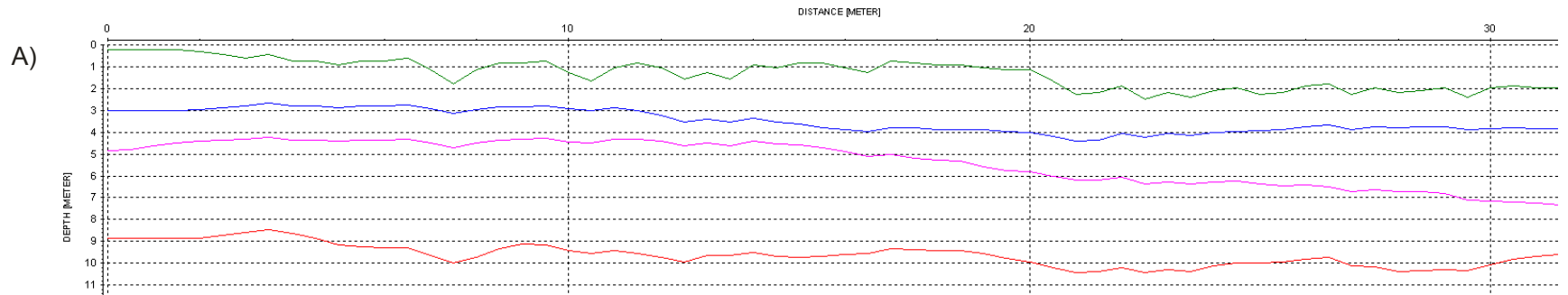
- Dry sandy soil with pebbles (Bottom)
- Water saturated soil, with sand and pebbles (Bottom)
- Linear stratified clay (Bottom)
- Glacial Outwash (Bottom)

Quilcayhuanca - Q11



- Dry sandy soil with pebbles (Bottom)
- Water saturated soil, with sand and pebbles (Bottom)
- Linear stratified clay (Bottom)
- Glacial Outwash (Bottom)

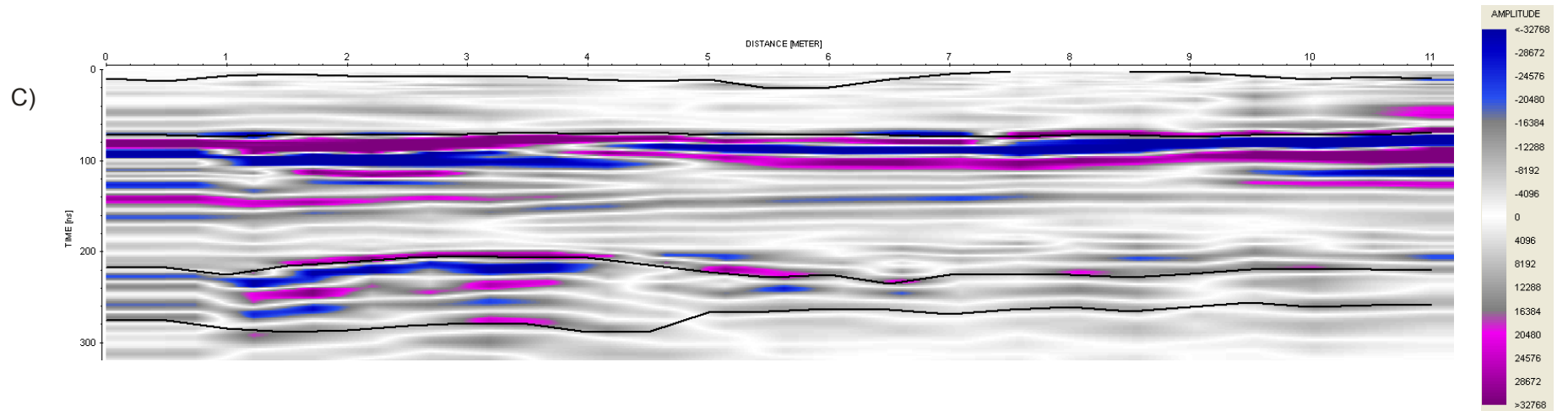
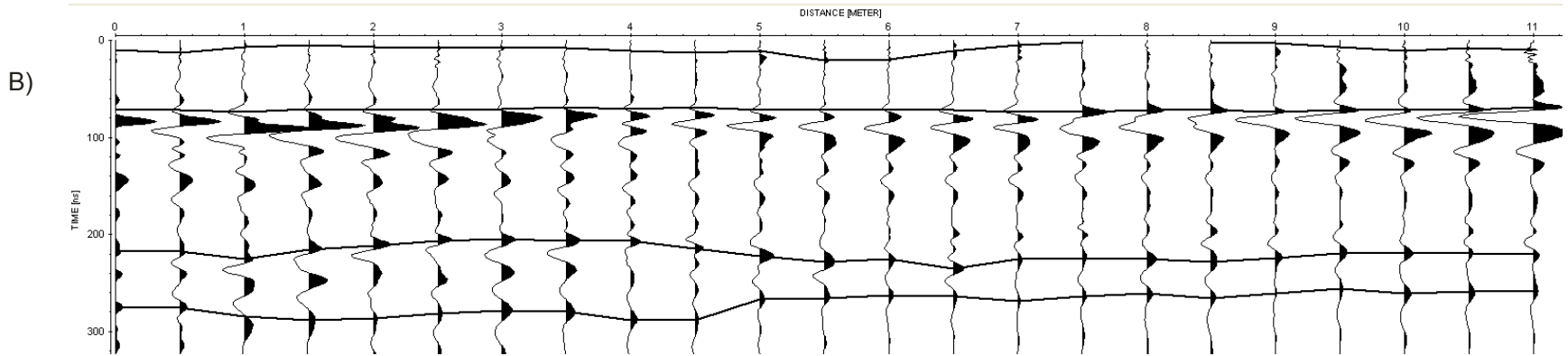
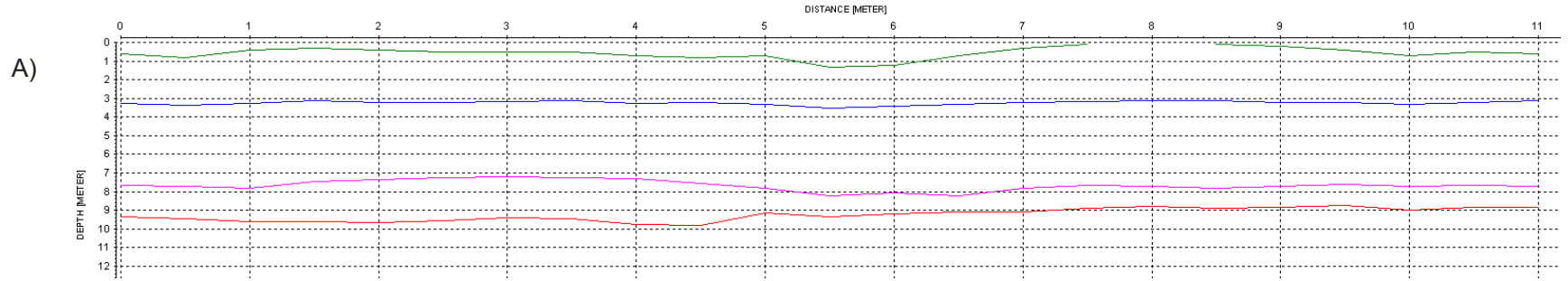
Quilcayhuanca - Q14





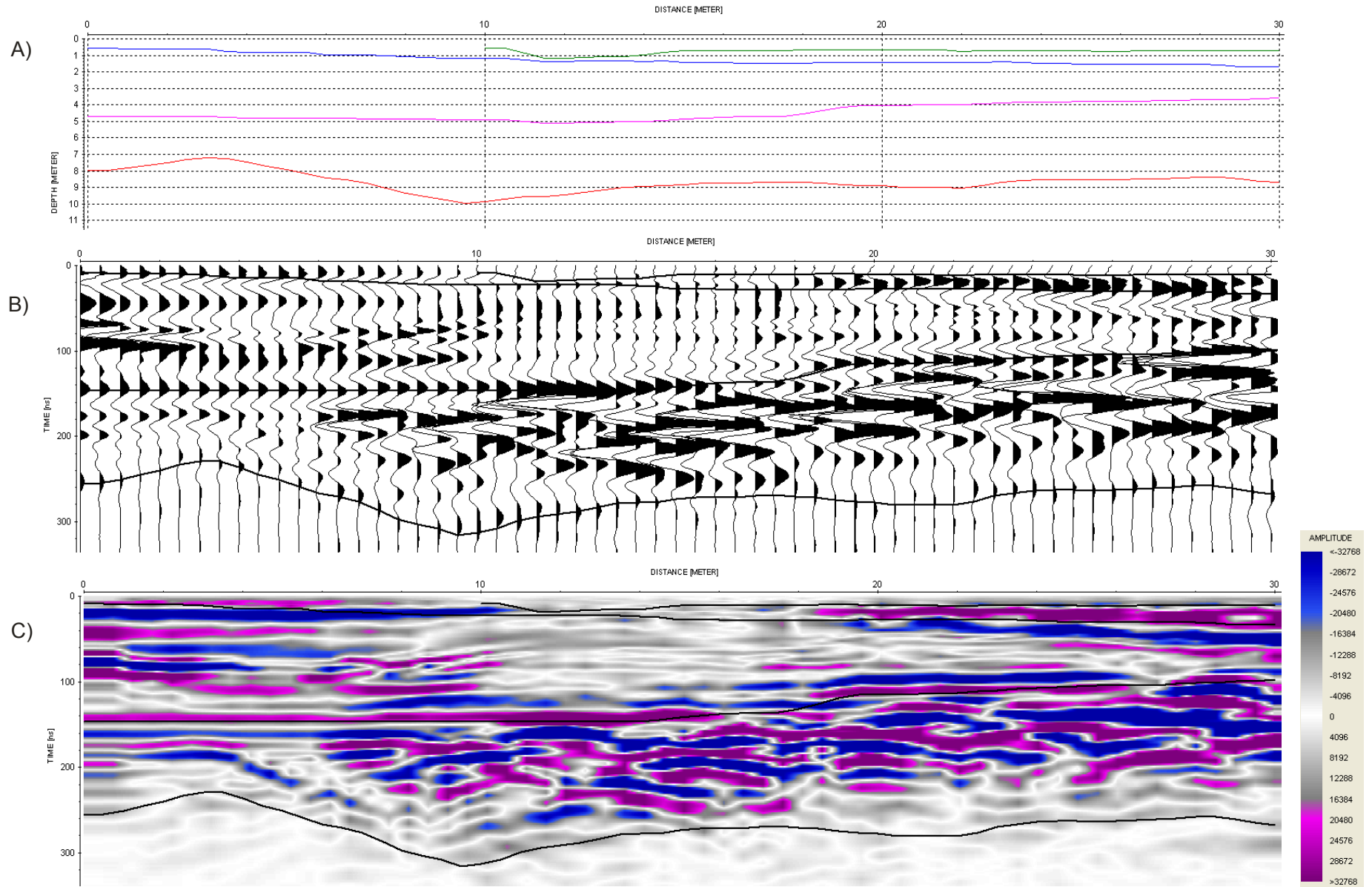
- Dry sandy soil with pebbles (Bottom)
- Water saturated soil, with sand and pebbles (Bottom)
- Linear stratified clay (Bottom)
- Glacial Outwash (Bottom)

Quilcayhuanca - Q22



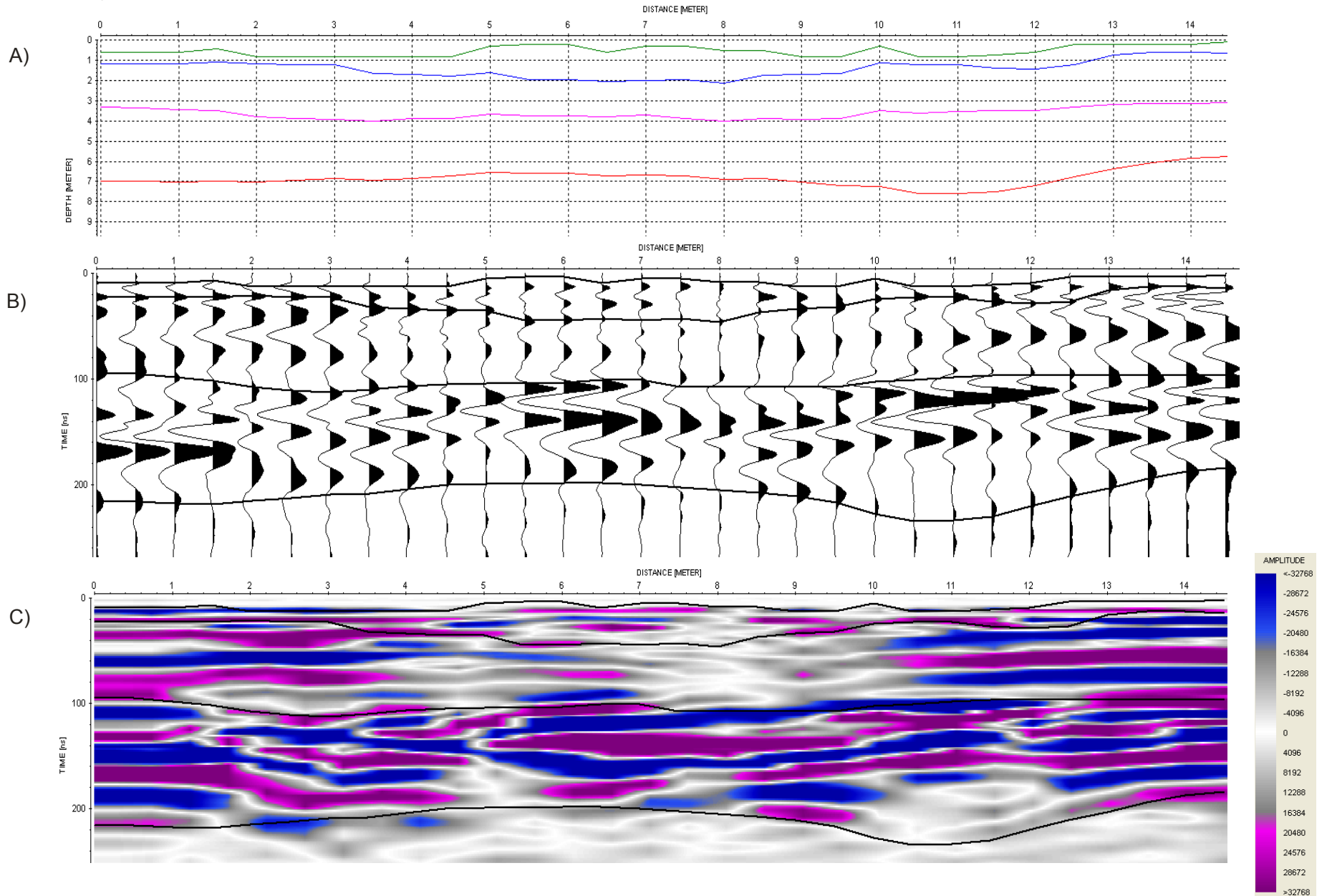
- Dry sandy soil with pebbles (Bottom)
- Water saturated soil, with sand and pebbles (Bottom)
- Linear stratified clay (Bottom)
- Glacial Outwash (Bottom)

Quilcayhuanca - Q23



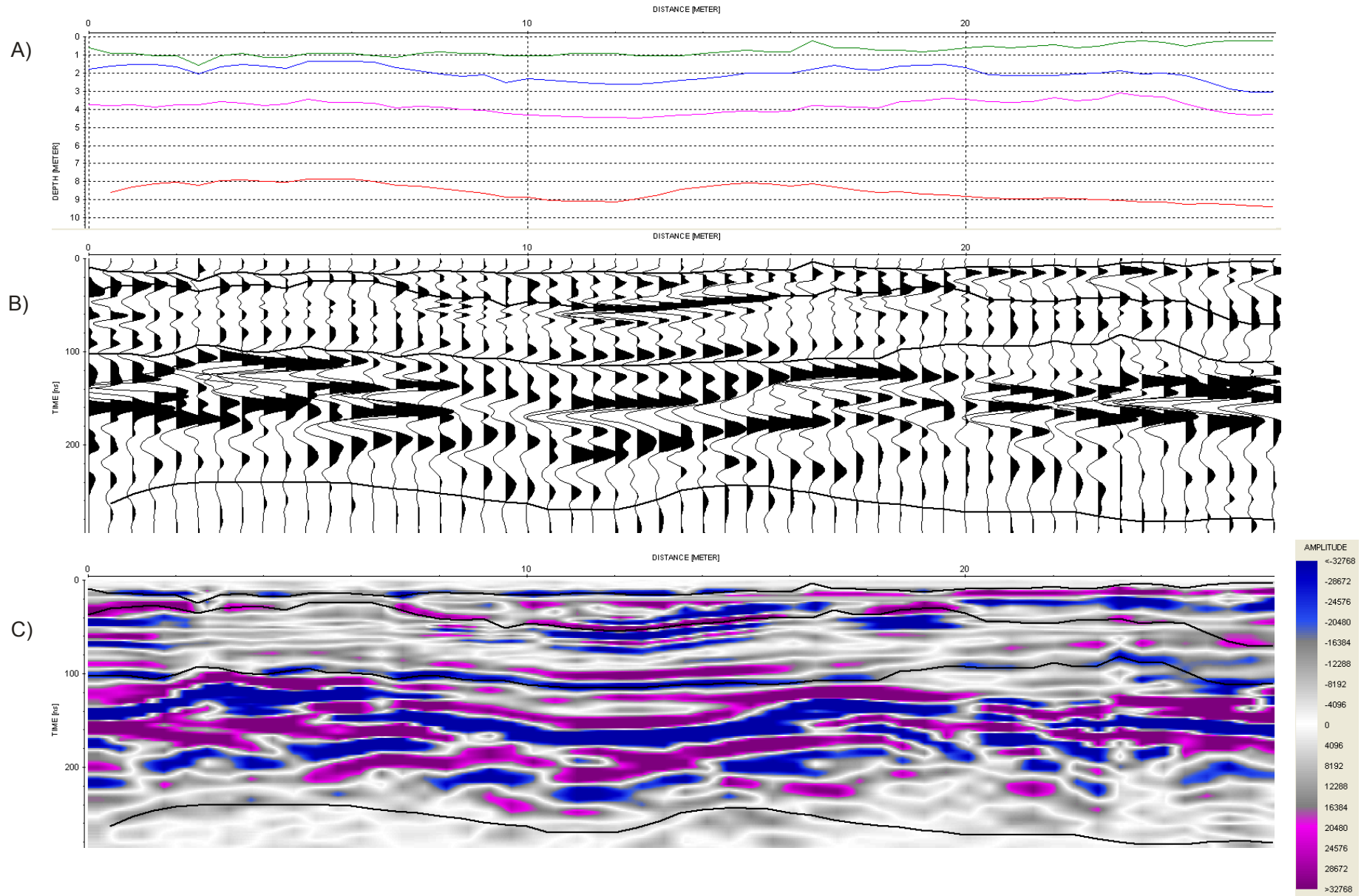
- Dry sandy soil with pebbles (Bottom)
- Water saturated soil, with sand and pebbles (Bottom)
- Linear stratified clay (Bottom)
- Glacial Outwash (Bottom)

Quilcayhuanca - Q24



- Dry sandy soil with pebbles (Bottom)
- Water saturated soil, with sand and pebbles (Bottom)
- Linear stratified clay (Bottom)
- Glacial Outwash (Bottom)

Quilcayhuanca - Q30



Appendix 2 – Yanamarey GPR results. The location of these profiles can be seen in Figure 2.

A) A true depth profile, which delineates the three stratigraphic units and the perched watertable. They are plotted with velocities obtained from CMP surveys and Baker et al., 2007.

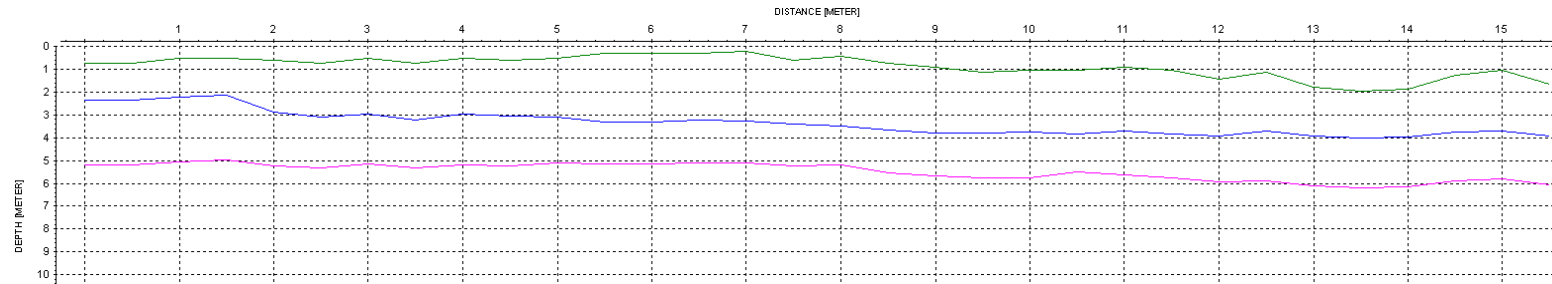
B) The wigglemode GPR profile, which highlights the strongest reflections.

C) The point mode GPR profile shows continuous groundwater surface reflections and the laterally continuous clay layer.

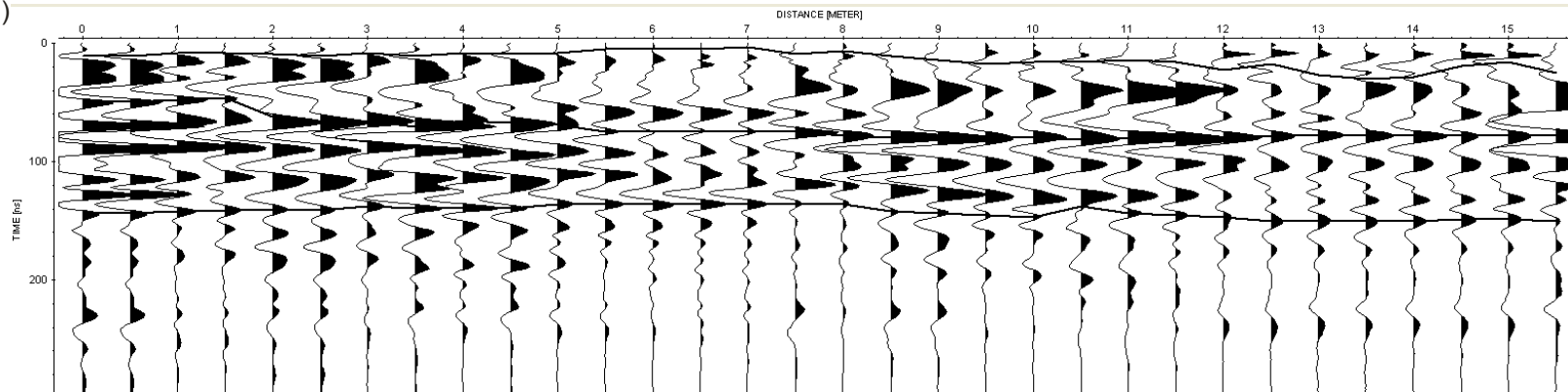
Yanamarey - 98-2

- Dry sandy soil with pebbles (Bottom)
- Water saturated soil, with sand and pebbles (Bottom)
- Linear stratified clay (Bottom)

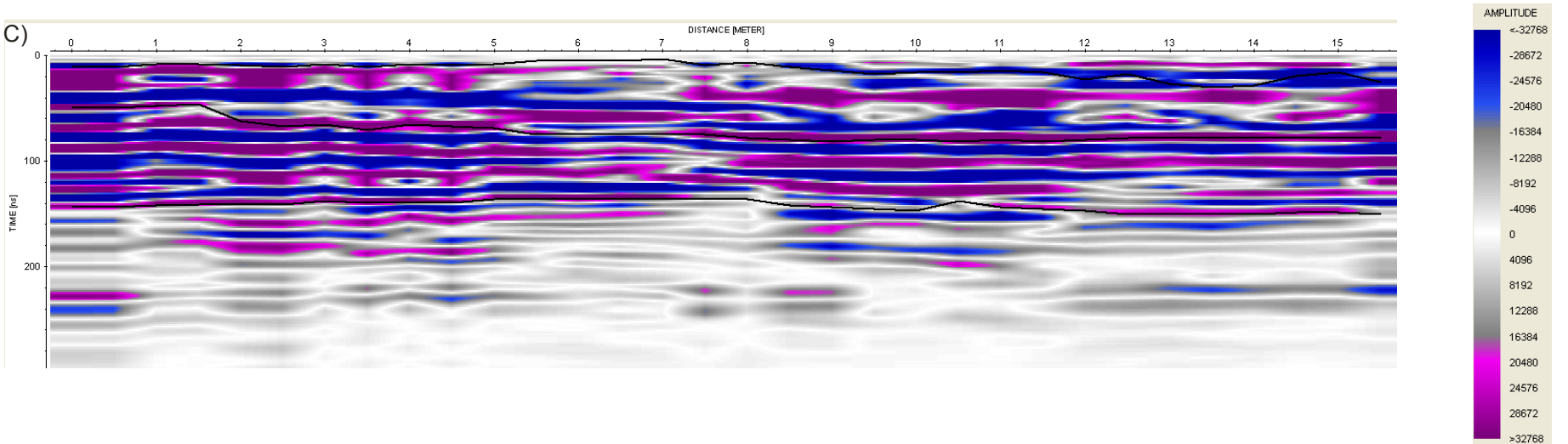
A)



B)

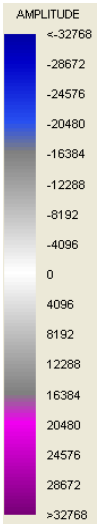
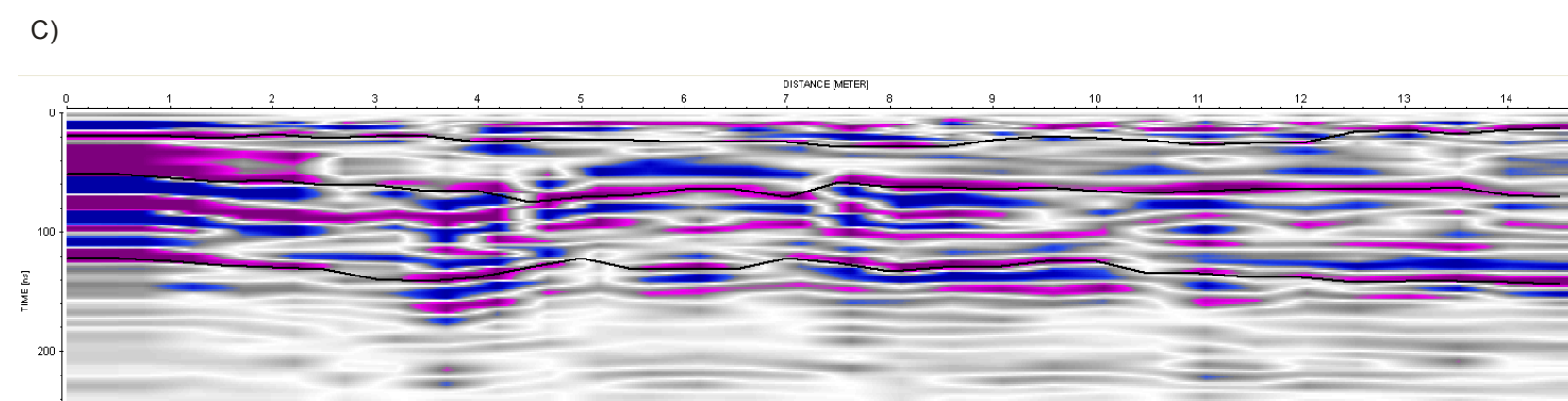
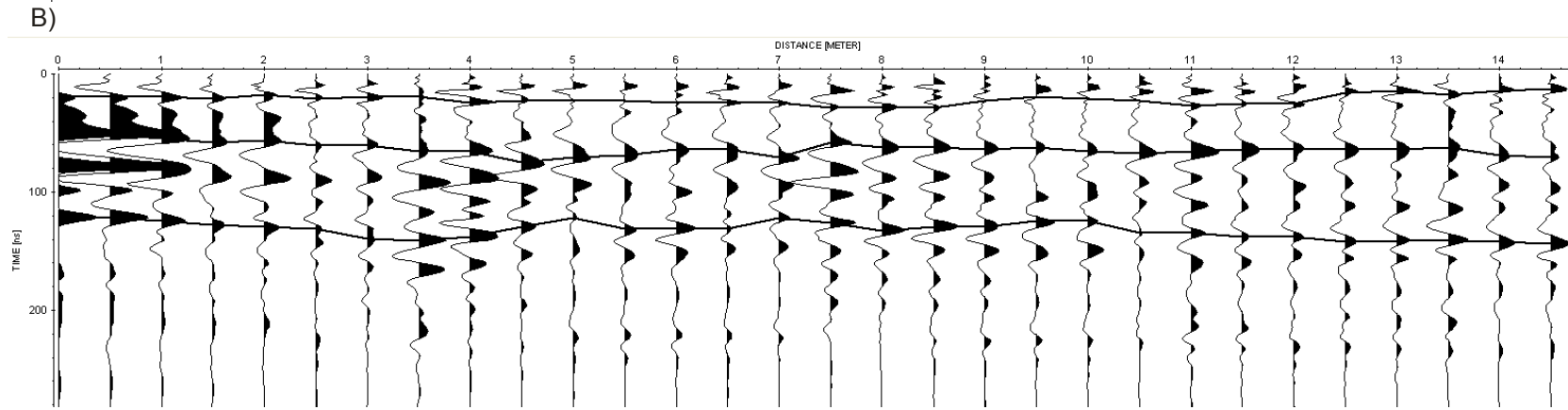
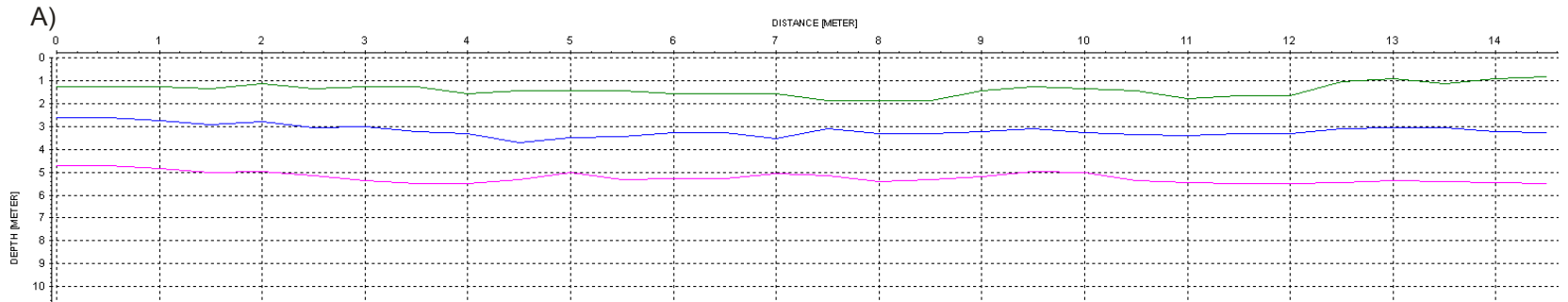


C)



Yanamarey - 98-3

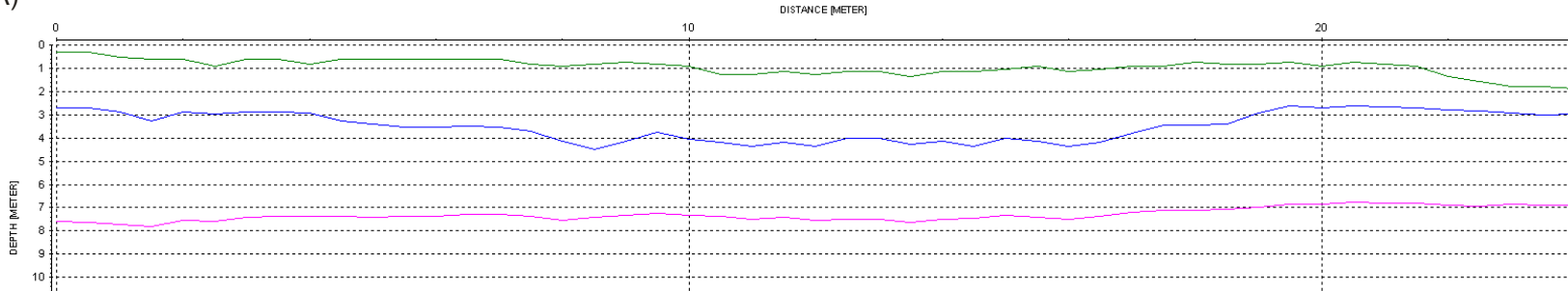
- Dry sandy soil with pebbles (Bottom)
- Water saturated soil, with sand and pebbles (Bottom)
- Linear stratified clay (Bottom)



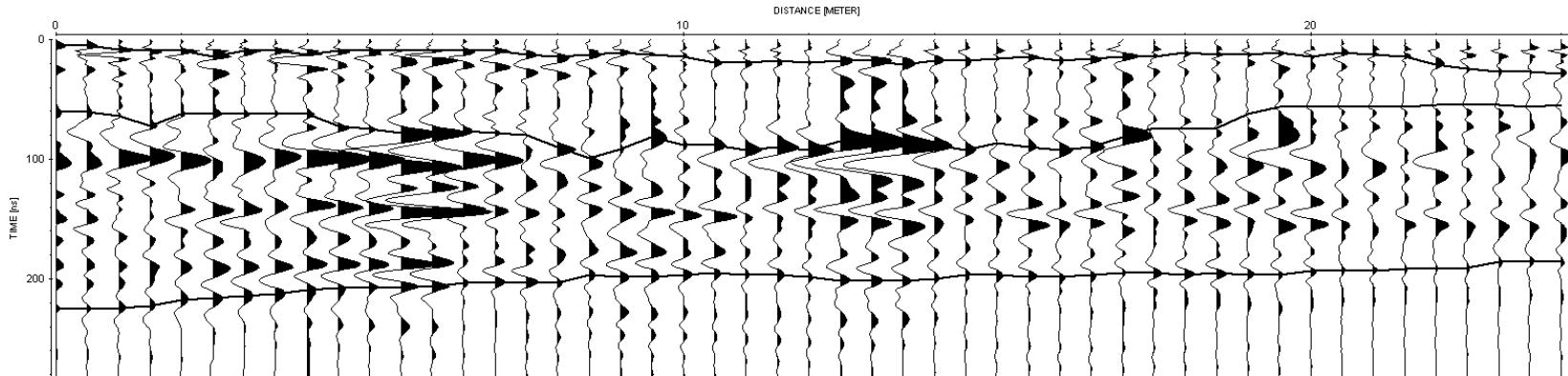
Yanamarey - 98-5

- Dry sandy soil with pebbles (Bottom)
- Water saturated soil, with sand and pebbles (Bottom)
- Linear stratified clay (Bottom)

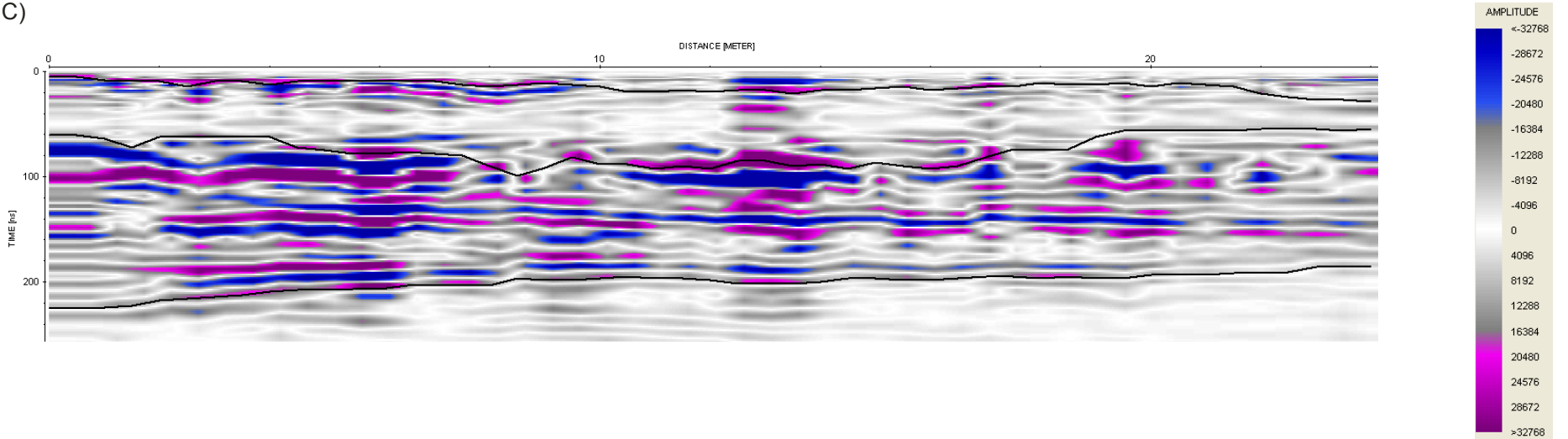
A)



B)



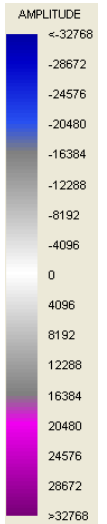
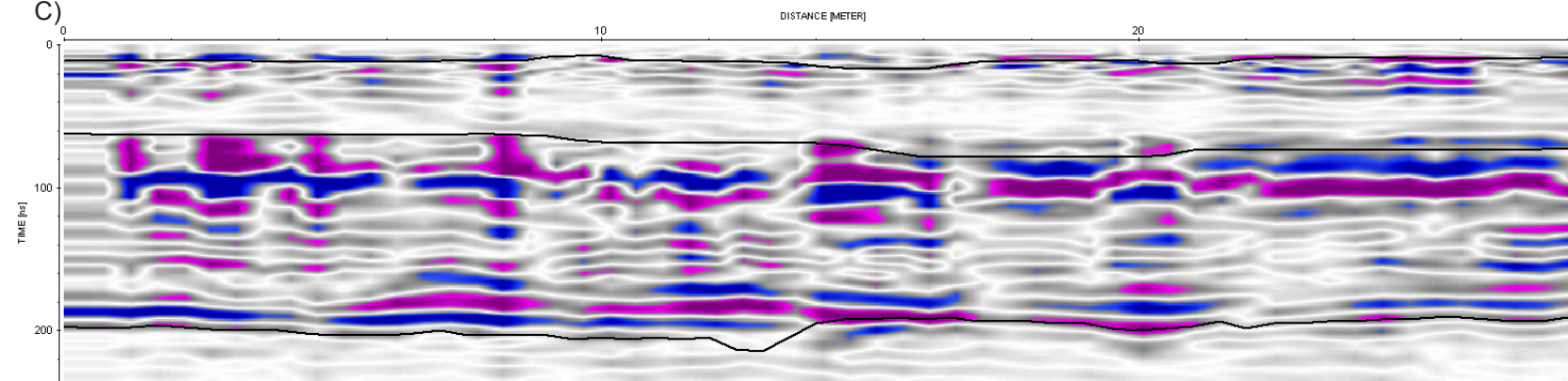
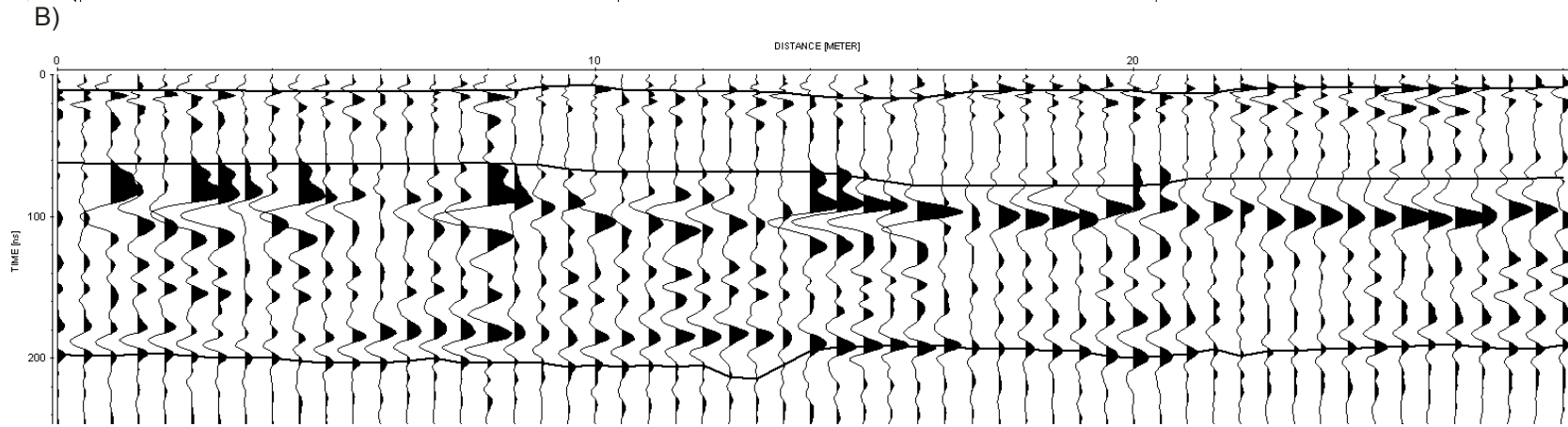
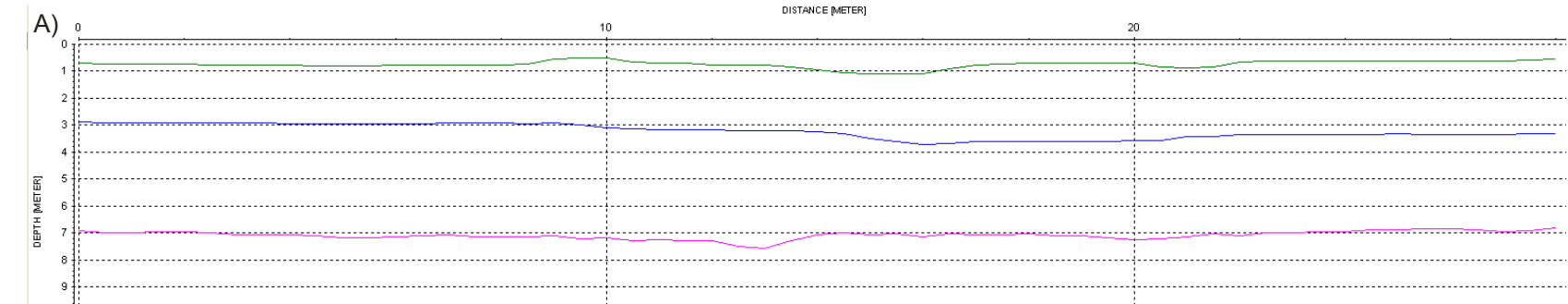
C)





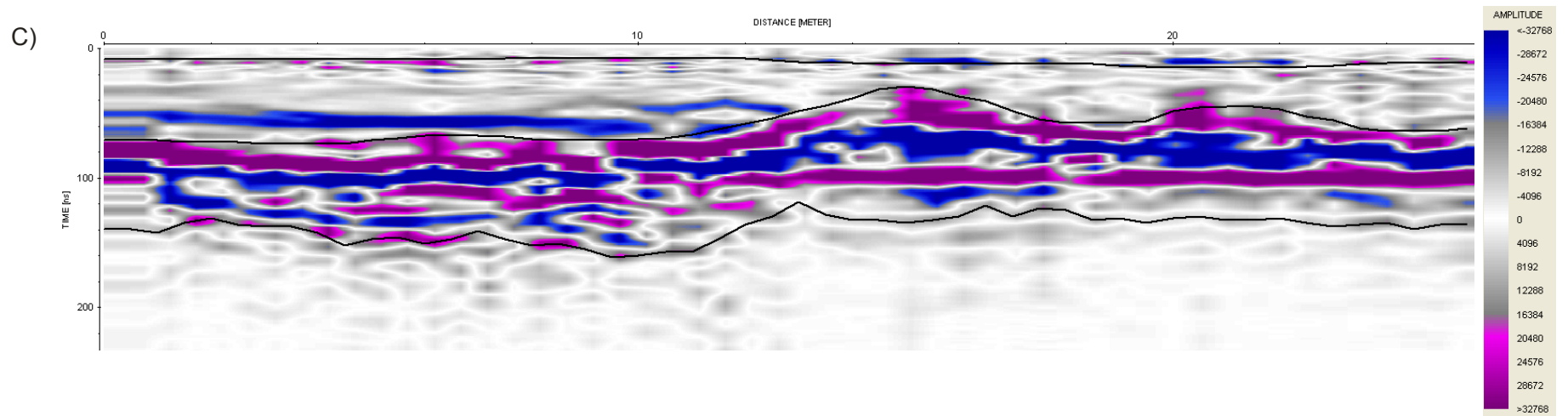
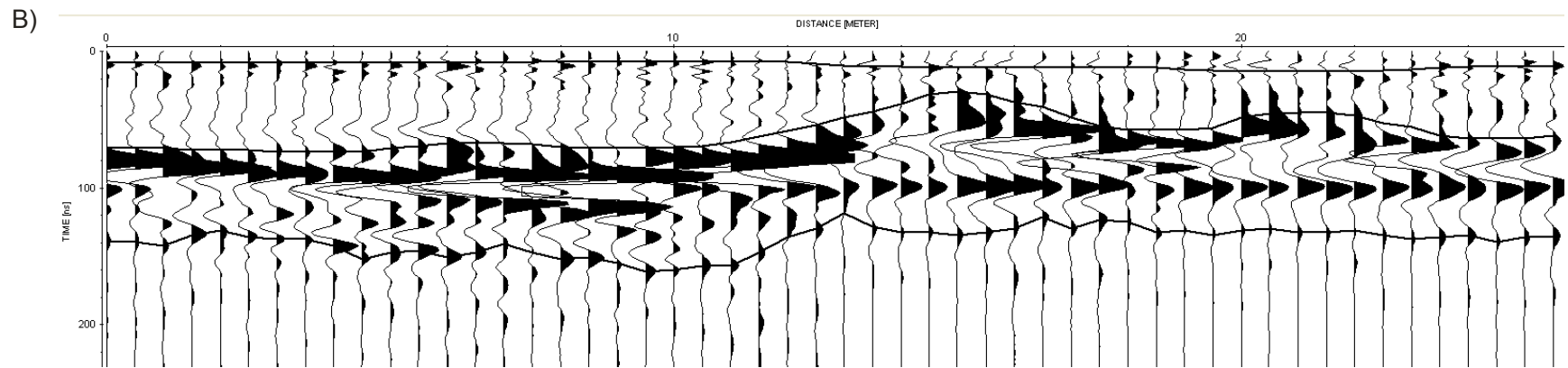
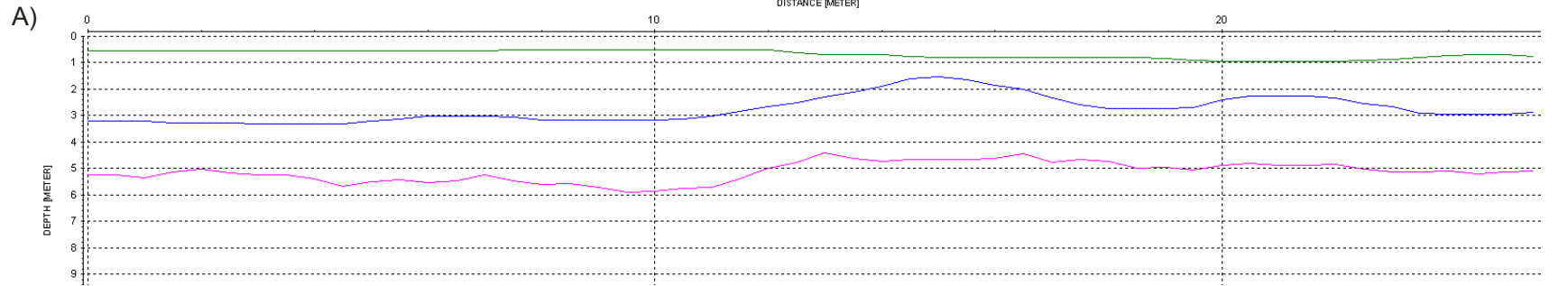
Yanamarey - 98-6

- Dry sandy soil with pebbles (Bottom)
- Water saturated soil, with sand and pebbles (Bottom)
- Linear stratified clay (Bottom)



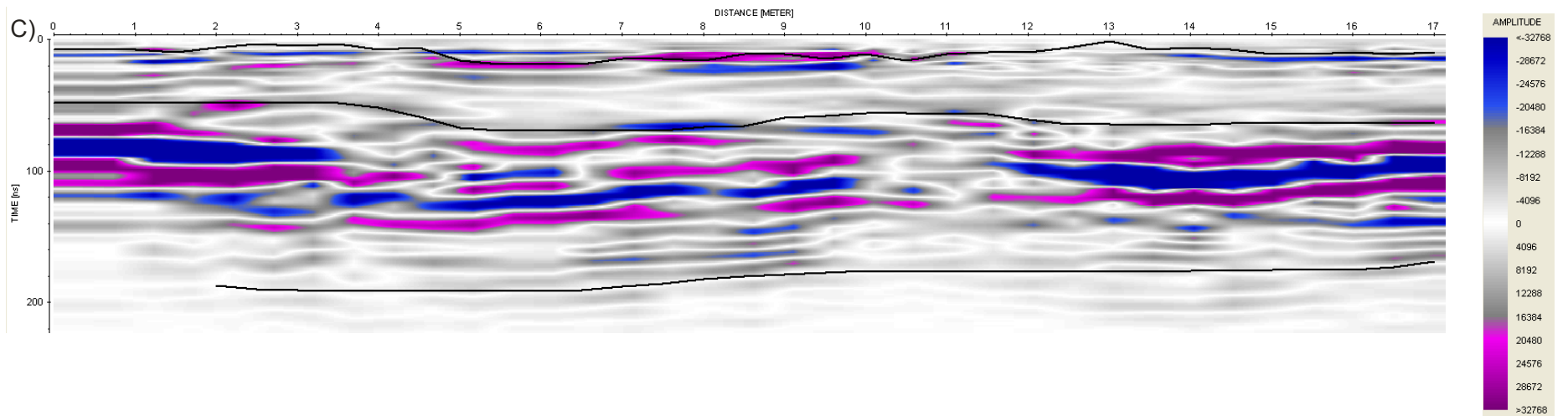
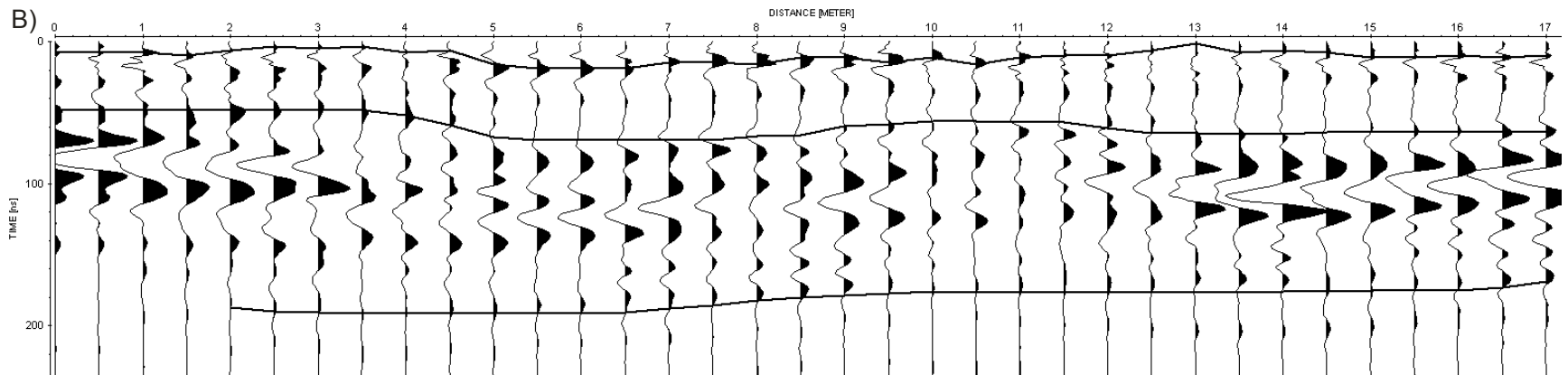
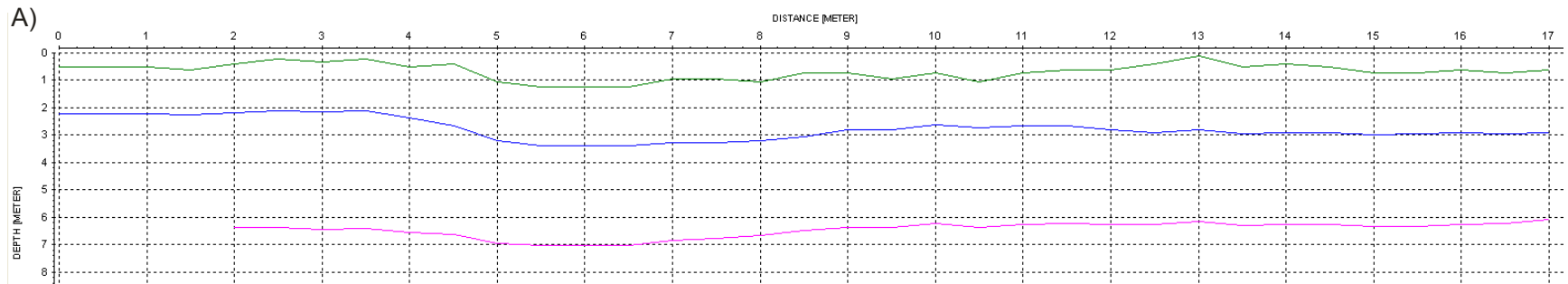
- Dry sandy soil with pebbles (Bottom)
- Water saturated soil, with sand and pebbles (Bottom)
- Linear stratified clay (Bottom)

Yanamarey - 99-2



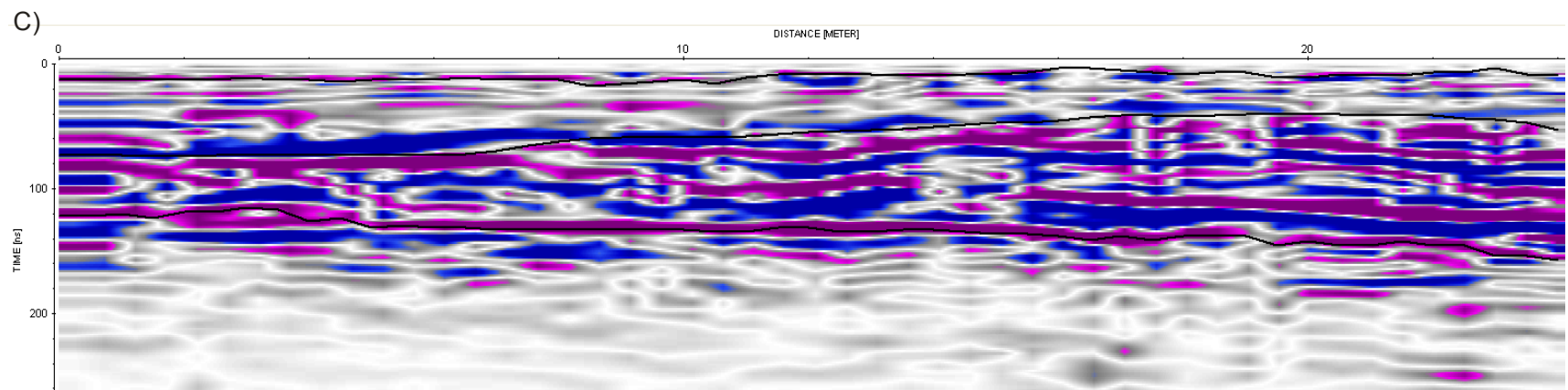
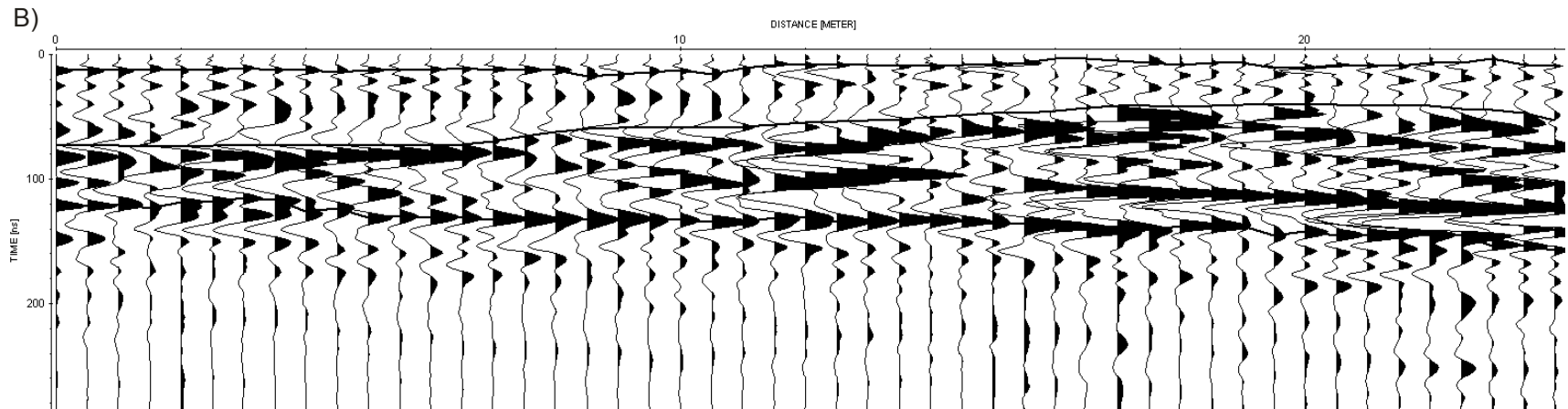
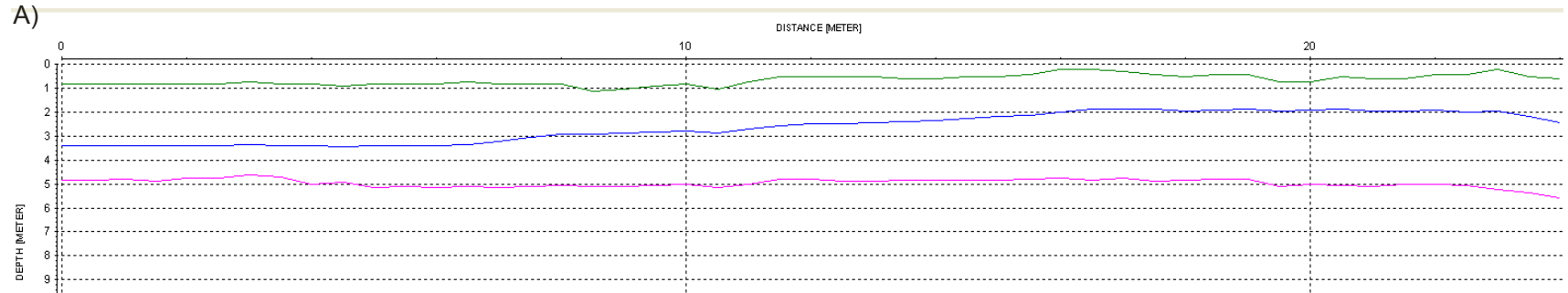
Yanamarey - 99-3

- Dry sandy soil with pebbles (Bottom)
- Water saturated soil, with sand and pebbles (Bottom)
- Linear stratified clay (Bottom)



Yanamarey - 99-4

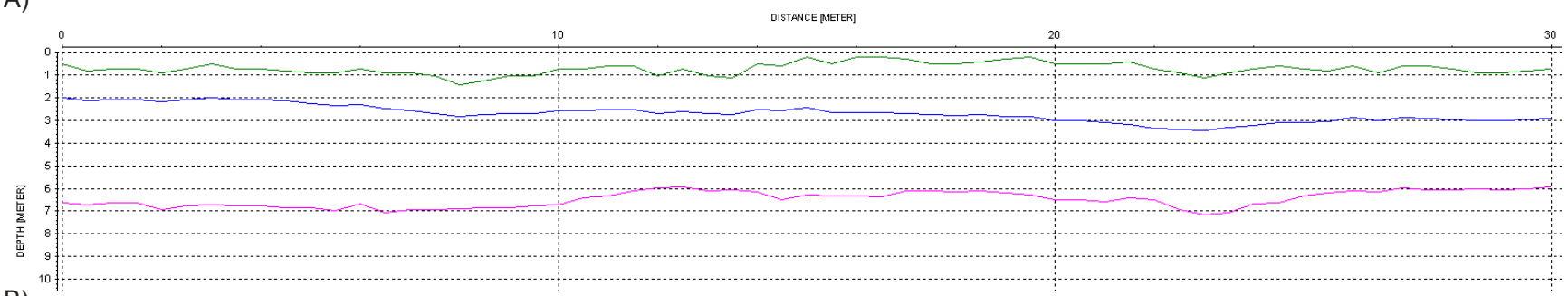
- Dry sandy soil with pebbles (Bottom)
- Water saturated soil, with sand and pebbles (Bottom)
- Linear stratified clay (Bottom)



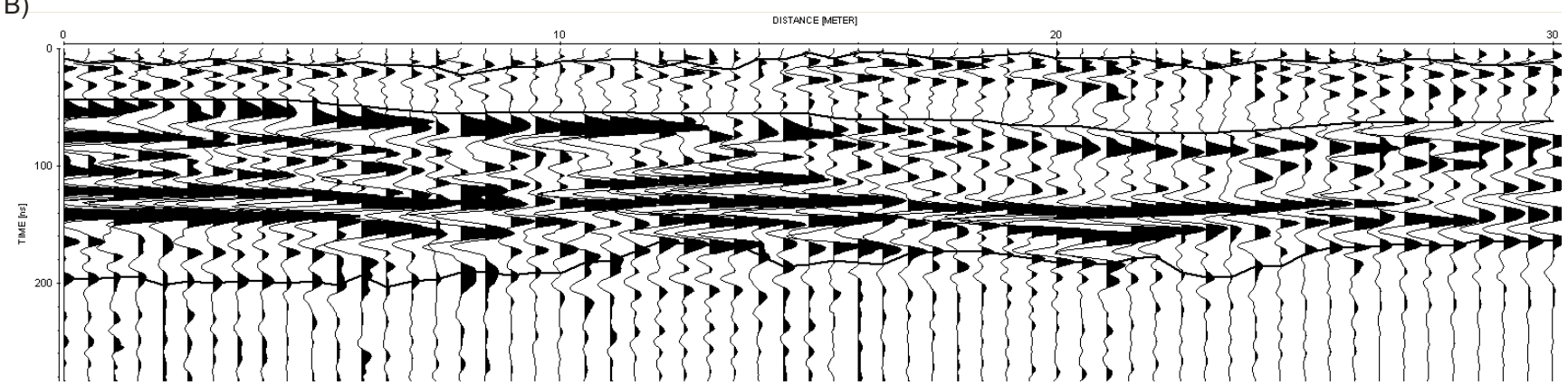
- Dry sandy soil with pebbles (Bottom)
- Water saturated soil, with sand and pebbles (Bottom)
- Linear stratified clay (Bottom)

Yanamarey - 99-5

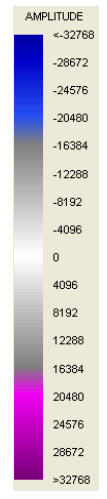
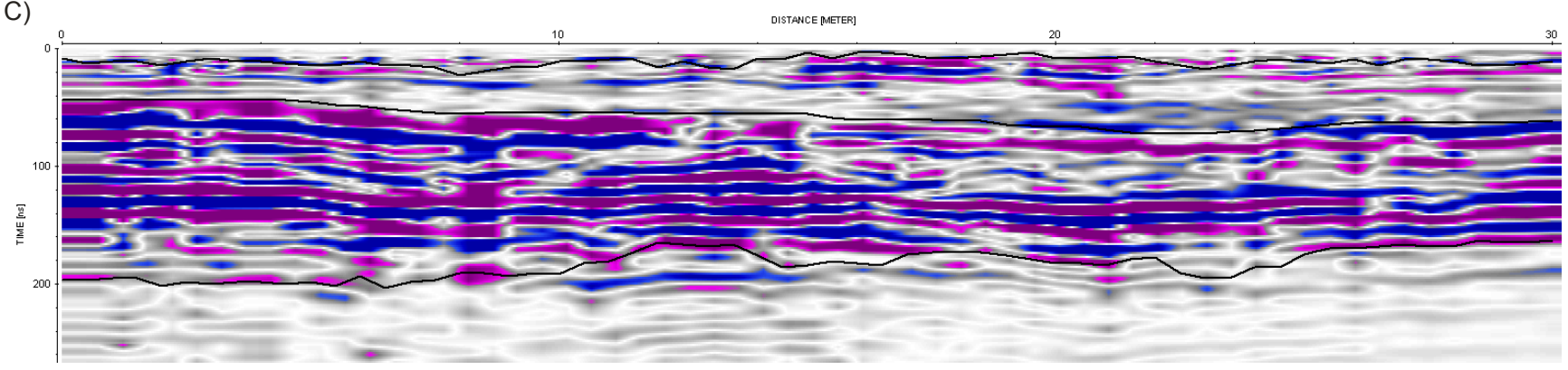
A)



B)



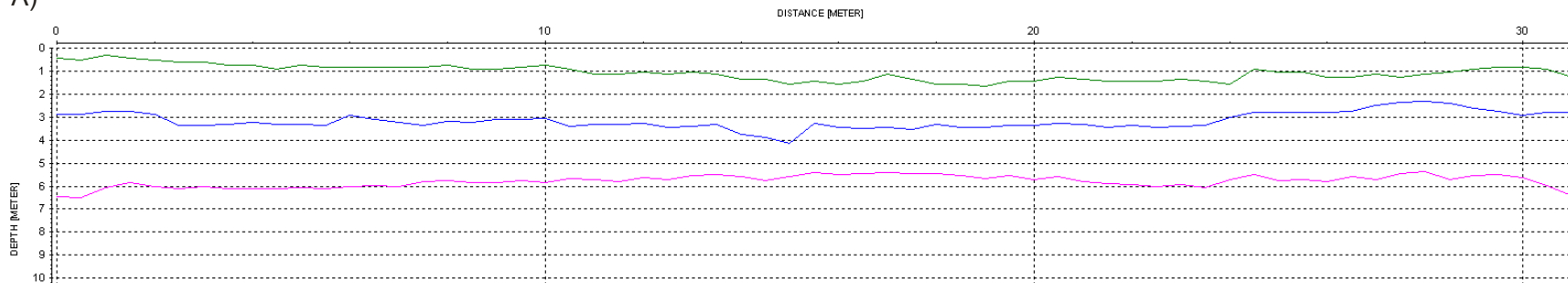
C)



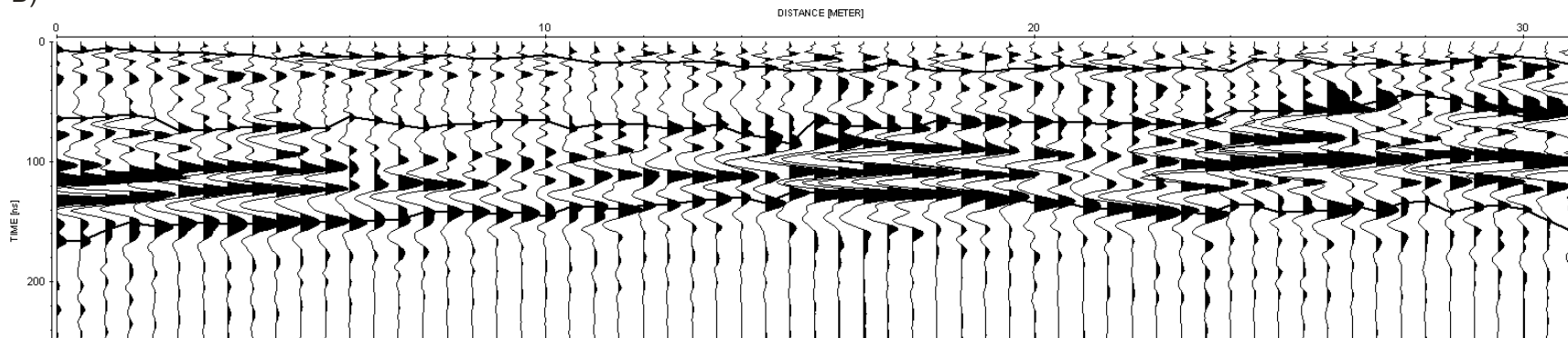
Yanamarey - 99-7

- Dry sandy soil with pebbles (Bottom)
- Water saturated soil, with sand and pebbles (Bottom)
- Linear stratified clay (Bottom)

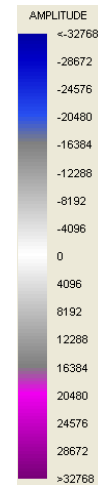
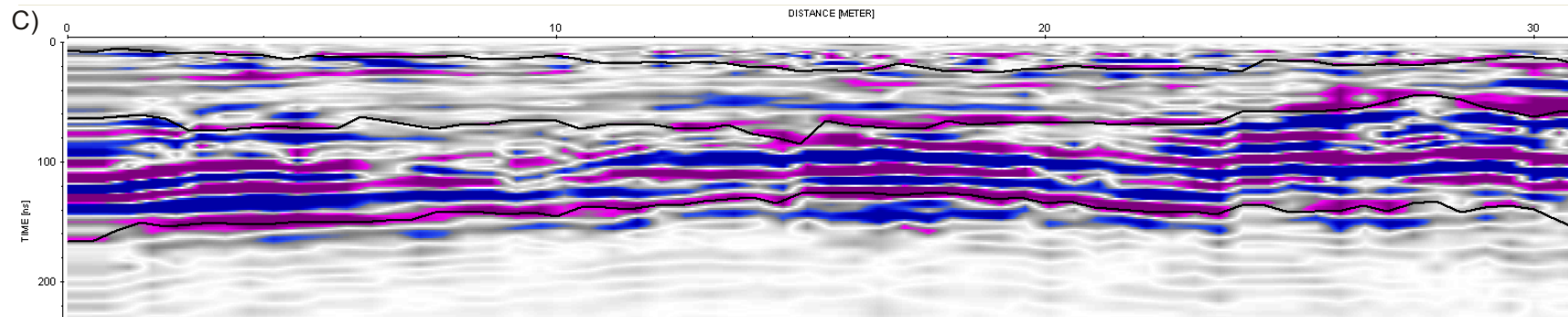
A)



B)

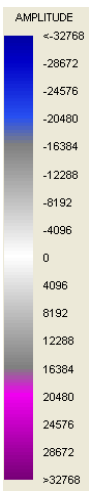
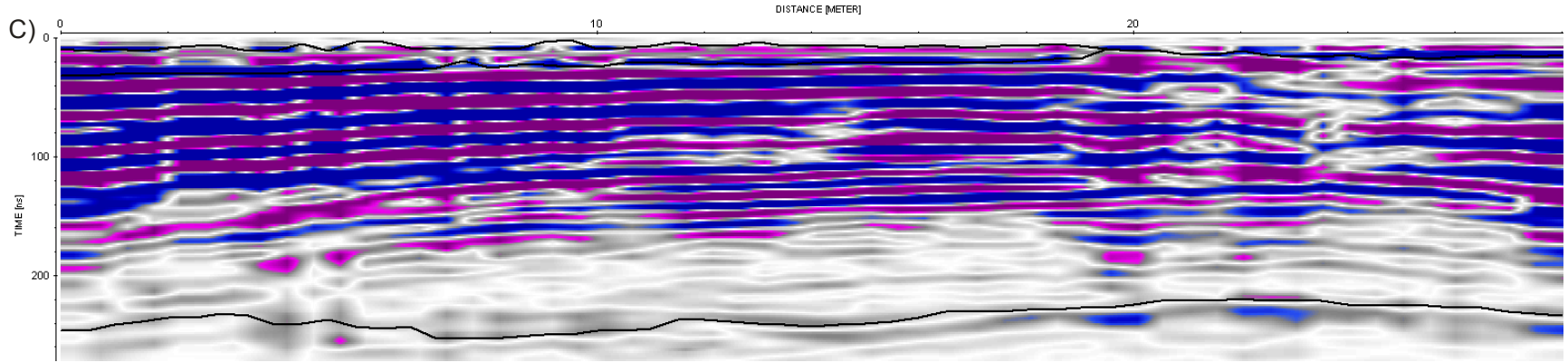
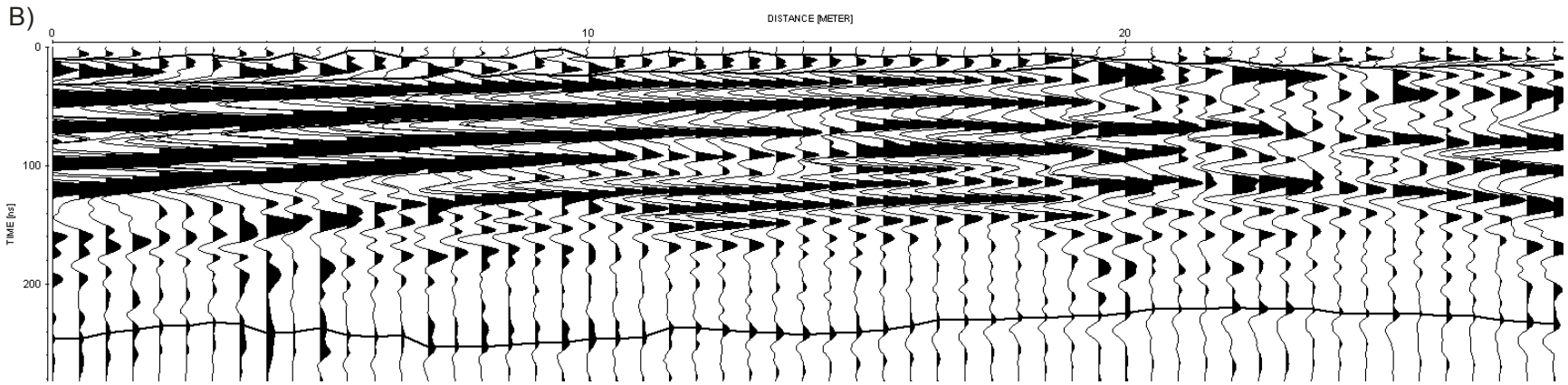
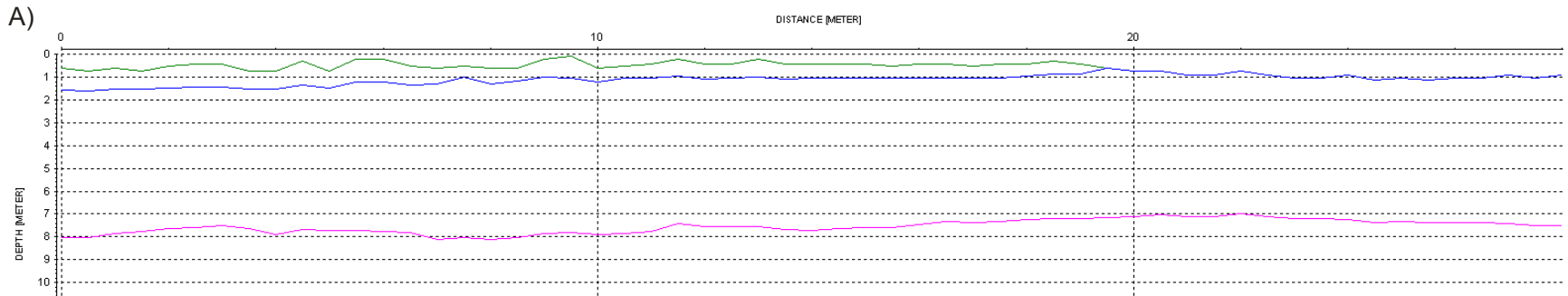


C)



- Dry sandy soil with pebbles (Bottom)
- Water saturated soil, with sand and pebbles (Bottom)
- Linear stratified clay (Bottom)

Yanamarey - 99-10



Appendix 3 –Required streambed velocity parameters and collected data for the ten day data temperature sensors. Physical parameters were based on published literature values for systems with similar sedimentology (Farouki, 1981 and Hatch, 2006). Locations of the temperature sensors can be seen in Figure 3.



**Required Input Parameters for the  
One Year Data**

Parameter	Symbol	Units	One Year Data (A – C)
Temperature	T	Degrees Celsius	The Maximum and Minimum Temperature for ibuttons A, C and E (see appendix A)
Period	P	Hours	24
Depth	z	Meters	0.15m – 0.1164m (due to erosion)
Effective Thermal Conductivity	K	Cal/s-cm-C)	0.00500
Effective Porosity	$n_e$	Unitless	0.08
Total Porosity	$n_t$	Unitless	0.3
Volumetric Heat Capacity of Water	$C_w$	Cal/s-cm <sup>3</sup> -C)	1.00000
Volumetric Heat Capacity of Sediments	$C_s$	Cal/s-cm <sup>3</sup> -C)	0.55000

**Required Parameters  
10 Day Data – Location 1**

Parameter	Symbol	Units	Notes
Temperature	T	Degrees Celsius	The Maximum and Minimum Temperature for two ibuttons B1, B2, B3 and B4 (see Appendix B)
Period	P	Hours	24
Depth	z	Meters	Varies between ibuttons
Effective Thermal Conductivity	K	Cal/s-cm-C)	0.00400
Effective Porosity	$n_e$	Unitless	0.4
Total Porosity	$n_t$	Unitless	0.6
Volumetric Heat Capacity of Water	$C_w$	Cal/s-cm <sup>3</sup> -C)	1.00000
Volumetric Heat Capacity of Sediments	$C_s$	Cal/s-cm <sup>3</sup> -C)	0.6500

**Required Parameters  
10 Day Data – Location 2**

Parameter	Symbol	Units	Notes
Temperature	T	Degrees Celsius	The Maximum and Minimum Temperature for two ibuttons B5, B7 and B8 (see Appendix C)
Period	P	Hours	24
Depth	z	Meters	Varies between ibuttons
Effective Thermal Conductivity	K	Cal/s-cm-C)	0.00500
Effective Porosity	n <sub>e</sub>	Unitless	0.08
Total Porosity	n <sub>t</sub>	Unitless	0.3
Volumetric Heat Capacity of Water	C <sub>w</sub>	Cal/s-cm <sup>3</sup> -C)	1.00000
Volumetric Heat Capacity of Sediments	C <sub>s</sub>	Cal/s-cm <sup>3</sup> -C)	0.5500

**Required Parameters  
10 Day Data – Location 3**

Parameter	Symbol	Units	Notes
Temperature	T	Degrees Celsius	The Maximum and Minimum Temperature for two ibuttons B11 and B12 (see Appendix D)
Period	P	Hours	24
Depth	z	Meters	Varies between ibuttons
Effective Thermal Conductivity	K	Cal/s-cm-C)	0.00400
Effective Porosity	n <sub>e</sub>	Unitless	0.6
Total Porosity	n <sub>t</sub>	Unitless	0.6
Volumetric Heat Capacity of Water	C <sub>w</sub>	Cal/s-cm <sup>3</sup> -C)	1.00000
Volumetric Heat Capacity of Sediments		Cal/s-cm <sup>3</sup> -C)	0.5000

### One Year Temperature Sensors

<b>Date</b>	July 16, 2006 - June 17, 2007		
<b>iButtons</b>	A	C	E
<b>Depth</b>	In Stream	15cm	35cm
<b>Location</b>	9°40.679 S, 77°17.561 W		
<b>Elevation</b>	4316m		
<b>Material</b>	Unconsolidated Mineral Clay		

\*iButton B was damaged

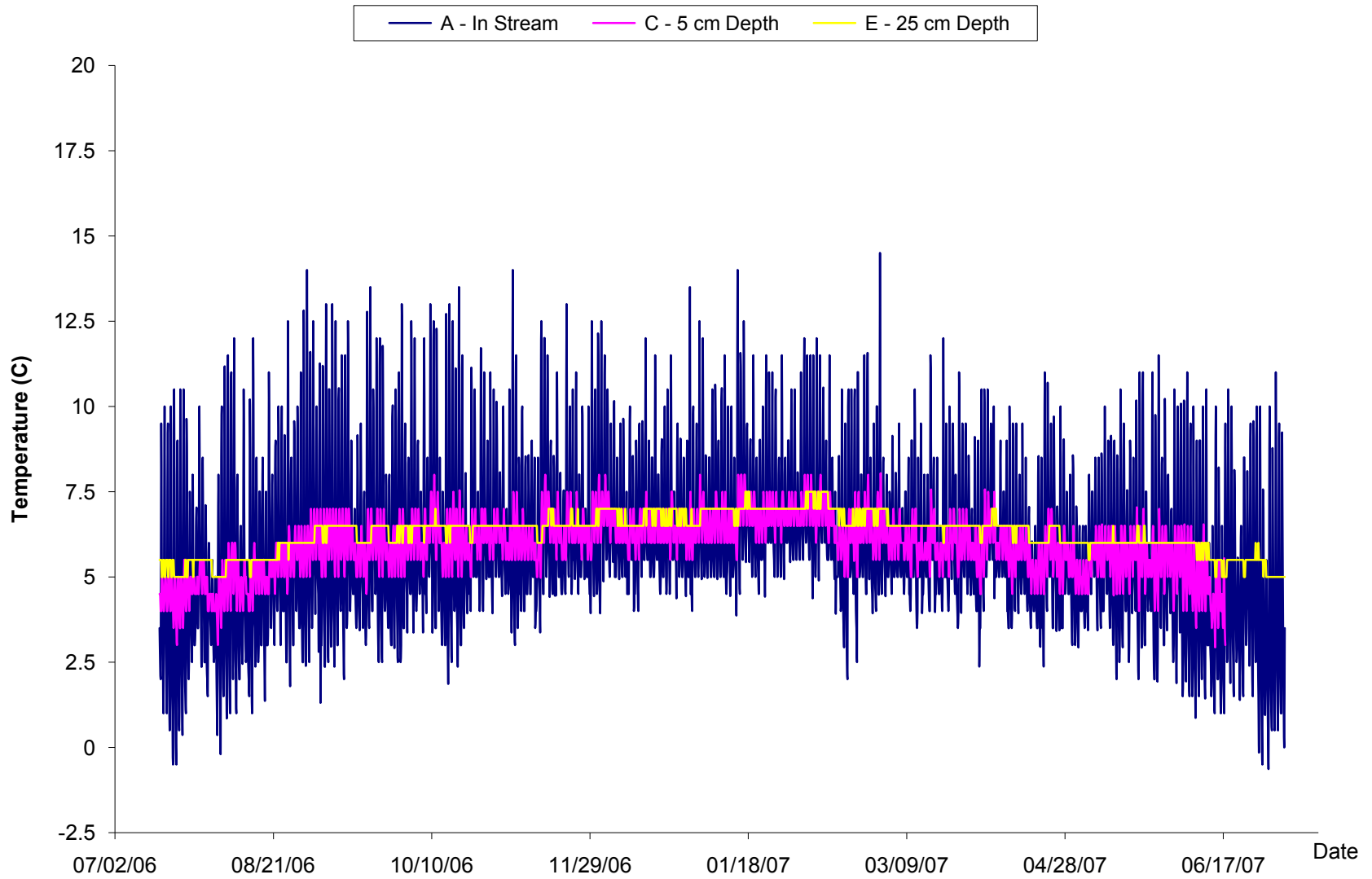
### 10 Day Temperature Sensors

<b>Dates</b>	July 8th - July 17, 2007			
<b>iButtons</b>	B1-B4	B5-B8	B9-B12	B13-B16
<b>Location</b>	9 40.559 S	9 40. 673 S	9 40.721 S	9 40.775 S
	77 17.503 W	77 17.563 W	77 17. 585 W	77 17.620 W
<b>Elevation</b>	4330 m	4312 m	4309m	4305m
<b>Material</b>	Pebbles in Stream	Unconsolidated Mineral Clay	Rocky Stream	N/A

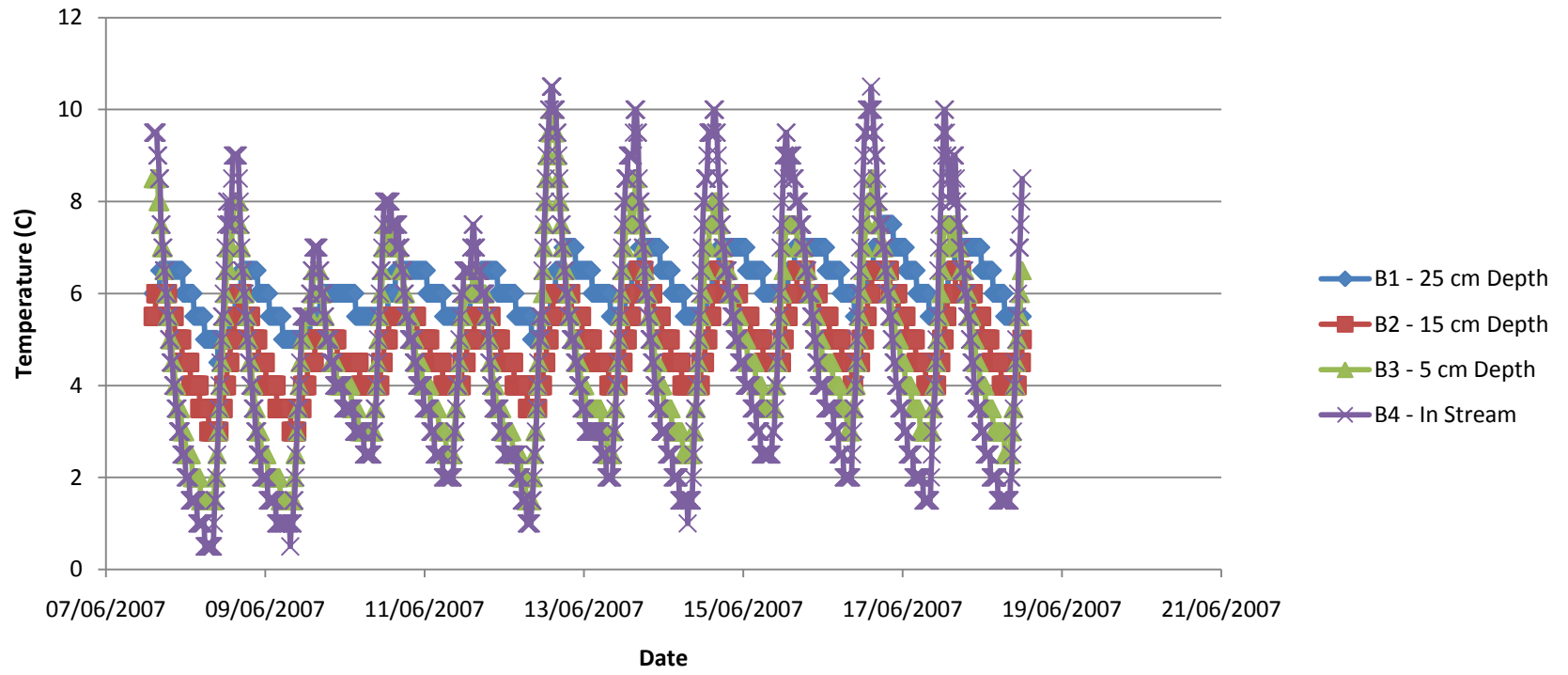
	Stick 1	Stick 2	Stick 3	Stick 4	Depth (cm)
Top (Stream)	B4	B8	B12	B16	
	B3	B7	B11	B15*	5
	B2	B6*	B10*	B14*	15
Bottom	B1	B5	B9*	B13*	25

\*Damaged

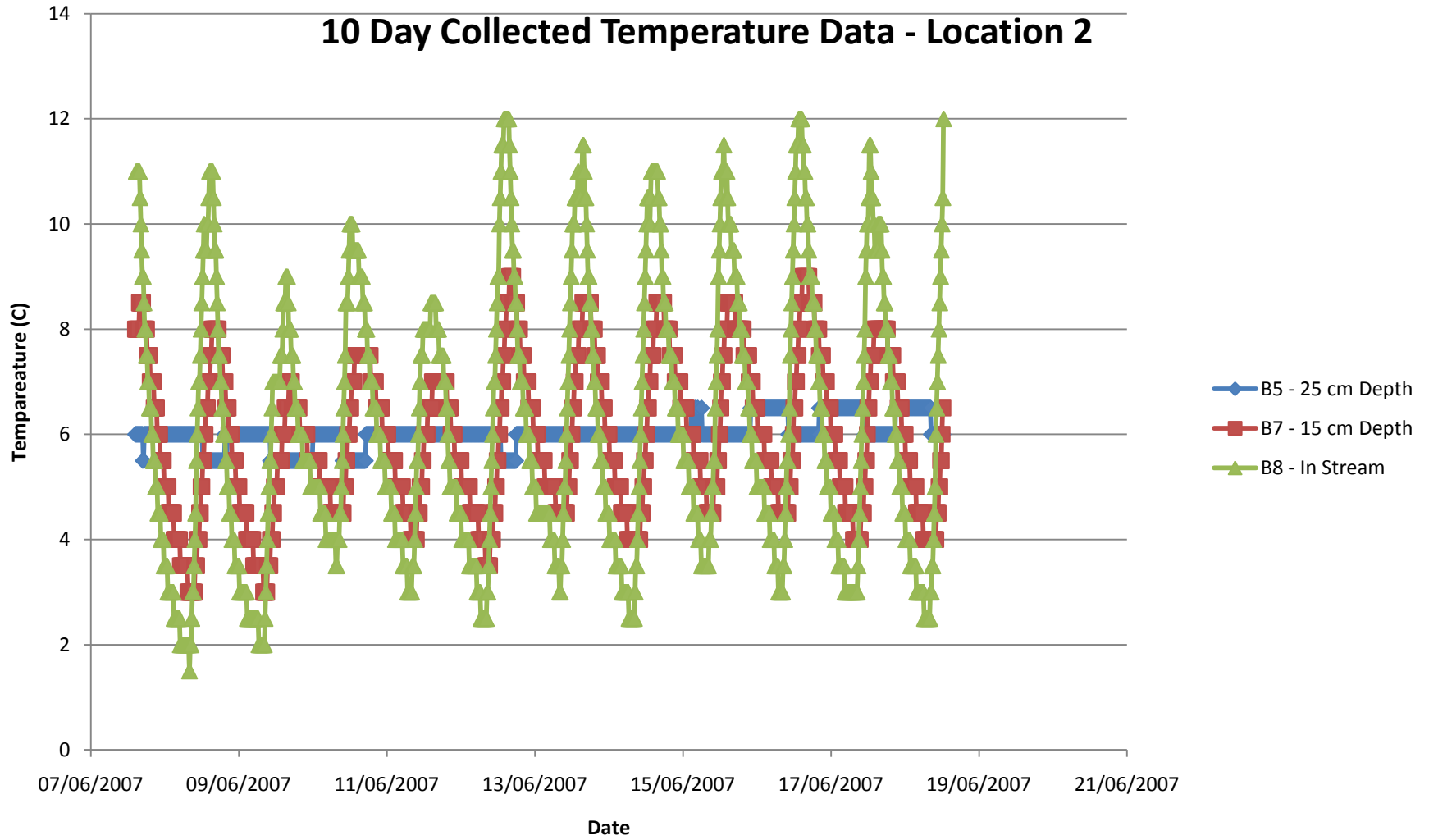
### One Year Collected Temperature Data



### 10 Day Collected Temperature Data - Location 1



# 10 Day Collected Temperature Data - Location 2



### 10 Day Collected Temperature Data - Location 3

